

Reply to Referee #1

(Interactive comment on Atmos. Chem. Phys. Discuss., <https://doi.org/10.5194/acp-2019-534>)

We would like to thank the reviewer for her or his time and the beneficial comments, which will help to improve the manuscript. Please find the replies to the referee comments below. The page and line numbers given by the referee relate to the manuscript in discussion, the numbers in our reply to the revised manuscript.

Referee comments are highlighted in **bold**, *changes* in the manuscript in *italic*.

Main criticisms of this paper:

- 1) **Additional referencing of the literature is needed to put the paper into context and understand what is novel in this work.**
- 2) **An uncertainty analysis is needed.**
- 3) **Some of the writing is confusing and needs to be edited for clarity.**
- 4) **There are gaps in the descriptions of the measurements and methods that make the work difficult to understand or reproduce.**

These points are discussed in the detailed comments below.

Title: The title should be reworded. Perhaps something like, “Cloud radiative forcing at the Arctic springtime marginal sea ice zone derived using low-level airborne observations.”

The title proposed by the reviewer would implicate that we analyze/characterize the CRF during the ALOUD campaign and analyze e.g. its dependence on surface and cloud properties. However this is not the primary intension of the manuscript and will be done in more details in an upcoming paper. Instead, the manuscript aims to discuss and refine the methods used to derive the CRF. In particular, we show the importance of the clear sky albedo estimate for the estimate of CRF, for which in fact we need observations to show the impact. However, we acknowledge that the focus of the work was not made clear. We changed the title to:

“Reassessment of shortwave surface cloud radiative forcing in the Arctic: Consideration of surface albedo-cloud interactions”

Language (overall): The authors should go through the paper and make sure every paragraph makes a single, clear point. They should also go through each sentence and make sure that it is correct, comprehensible, and stated as simply as possible. I suggest asking a colleague to read the paper and then working with them on how to clarify anything that they do not understand.

We apologize that our writing was confusing and restated/edited a couple of sections. Please see the marked-up manuscript for details.

Abstract lines 1 and 2: “warming or cooling effect . . . on the radiative energy budget.”Clouds do not cool the energy budget. Please restate.

We have changed the first two sentences in the abstract accordingly to:

“The concept of cloud radiative forcing (CRF) is commonly applied to quantify the impact of clouds on the surface radiative energy budget (REB). In the Arctic, radiative interactions between microphysical and macrophysical properties of clouds and the surface modify the warming or cooling effect of clouds, complicating the estimate of CRF obtained from observations or models.”

First paragraph of the introduction: This paragraph is difficult to understand, has a lot of unnecessarily detail, and only provides general motivation. I think a few sentences can explain that clouds are important for the Arctic. What is really needed prior to the second paragraph is more specific motivation for this work, including why estimates of CRF and REB are important and how they are used and calculated in the literature (discussed more below).

We agree, that the focus of the introduction did not fit perfectly the motivation of the study. Therefore, we changed the introduction to be more specific on the general estimate of CRF. In addition, we added a literature overview in the new section 3.1 “Common approaches” describing the state of the art methods to calculate the CRF.

Furthermore we restated the sentence about the cloud feedback (more specifically cloud radiative feedback) to (p.2 l.2):

“One prominent example is the cloud radiative feedback, which includes the effects of an increasing cloud amount in the Arctic, balancing between potential increase of both longwave downward radiation (positive) and cloud top reflectivity (negative).”

Page 2 lines 18-22: these sentences are a distraction from the rest of the paragraph, which focuses on SZA and albedo.

We completely changed this section. (See marked-up manuscript)

When the words heterogeneous or heterogeneity are used, the authors need to state what is varying – for heterogeneous sea ice is it type of ice? Or ice fraction? What is meant by heterogeneous albedo?

The reviewer is right, we should have been more specific. We intended to say “fluctuations of albedo in space scale”, or “heterogeneous albedo fields”. This heterogeneity is caused by sea ice concentration, patches of snow on bare sea ice etc. We reworded the sections, where it was unclear or misleading and used the two extended phrases “fluctuations of albedo”, or “albedo fields”.

Abstract and Introduction: Is the most important result the application of the parametrization of Gardner and Sharp (2010) to measurements? If this is the case, this should be clear in the abstract and introduction. For example, the authors state in the introduction that, “Both processes have been parametrized, for example by Gardner and Sharp (2010) based on simulations, however, their impact on estimates of the CRF in the Arctic have not yet been evaluated.” They should go on to state in the following paragraph that they apply these parametrizations in this work.

The reviewer is right that we should have emphasized the importance of the Gardner and Sharp (2010) parameterization more clearly, which enables to reproduce the clear sky albedo from the cloudy observations. We added in the abstract:

“A method to consider this surface albedo effect by continuously retrieving the cloud-free surface albedo from observations under cloudy conditions is proposed, using an available snow and ice albedo parameterization.”

As well we modified the last paragraph in the introduction to make the outcome/structure of the study more clear:

“In section 4 a method is introduced to retrieve the shortwave surface albedo in the hypothetical cloud-free atmosphere from measurements under cloudy conditions, by using an available snow and ice albedo

parameterization from Gardner and Sharp (2010) and a shortwave transmissivity-based retrieval of cloud liquid water path (Appendix A)."

Introduction: Although the paper has a long reference list, missing are examples from the literature of calculations of CRF and radiative fluxes based on observations in the Arctic. Context of the literature is also needed to show what ideas or parametrizations are novel here. For example, if Eqs (7) and (8) are novel, please make that clear in the introduction as well as in Sect. 3, as well as how they relate to calculations of CRF in the literature. The authors should explain how CRF is used in such studies, what are the shortcomings, and how their work addresses these shortcomings.

We extended the introduction by a section discussing the general conclusions from available studies (p.2 l.14).

"Long-term ground-based observations of CRF in the Arctic (Walsh and Chapman, 1998; Shupe and Intrieri, 2004; Dong et al., 2010; Miller et al., 2015) showed that in the longwave wavelength range clouds tend to warm the surface. The magnitude of the warming is influenced by macrophysical and microphysical cloud properties (e.g., Shupe and Intrieri, 2004) and by regional characteristics (Miller et al., 2015) and climate change (Cox et al., 2015). In the solar spectral range, clouds rather cool, whereby the strength and timing over the year is determined, besides cloud microphysical properties, by the solar zenith angle (SZA) and the seasonal cycle of surface albedo (e.g., Intrieri et al., 2002; Dong et al., 2010; Miller et al., 2015). However, the required cloud-free reference ($F_{net;cf}$) poses a serious problem to all observations in the cloudy Arctic (Shupe et al., 2011), as the unknown thermodynamic and surface albedo conditions in cloud-free environments is modified by the presence of clouds itself."

In addition, we added a more detailed literature overview in the new section 3.1 "Common approaches", where a discussion of the available approaches is given (please see the new manuscript). This section aims to identify shortcomings of the common approaches such as the representations of cloud-free albedo.

Measurements: More information is needed about the measurements. What wavelengths are used? Presumably the aircraft had both up-looking and down-looking pyrgeometer and pyranometers?

In section 2.2 we referred to two papers Wendisch et al. (2019) and Ehrlich et al. (2019b). These papers give a detailed overview of the campaign (Wendisch et al., 2019) and instrumentation (Ehrlich et al., 2019b), where all required information is provided. They extensively describe the campaign, the flights, the instrumentation, wing-by-wing comparison and necessary processing. However, to make it easier for the reader we added some general specifications of the broadband radiometer in the revised manuscript (p.4 l.3).

"In this paper, shortwave and longwave, upward and downward broadband irradiance have been analyzed from measurements with a frequency of 20 Hz obtained from two sets of Pyranometer (0.2-3.6 μm) and Pyrgeometer (4.5-42 μm). From 5 these irradiance data the net irradiance and surface albedo have been derived."

(Also, please use "longwave" and "shortwave" instead of "terrestrial" and "solar.")

We have changed the wording, equations, subscripts and labels in the figures.

The text refers to the cloudy ABL, but I think data are only used where the cloud was above the aircraft? (E.g. all upwelling flux measurements were for clear skies). Please clarify this.

We apologize if the definition of CRF in the introduction with “cloudy” was misleading and we changed it to “all-sky”. However, as stated in Ramanathan et al. (1989), “cloudy” is not equal to overcast conditions. The low level section are not filtered for overcast conditions. All data, from overcast, broken cloud fields, and clear-sky conditions are included, as can be seen in the CRF distributions shown in Fig. 10b,c (clear-sky values around 0).

As described in section 3.2 the upward longwave fluxes cancel in the CRF equation assuming the instantaneous approach. The upward shortwave fluxes or the surface albedo are obtain in all-sky conditions and are corrected by the method described in section 4 to represent the cloud-free albedo.

How did you ensure that there was no cloud around or below the aircraft?

The average flight altitude for the low-level section was 80m, and often even below 60m. Therefore, the low-level section were always below the lowest cloud base. There have been cases with precipitation, but precipitation does influence the radiative fluxes only little. To confirm the cloud-free conditions below the aircraft, we used cameras installed in the aircraft, participated in the flights or checked the Nevzorov Probe (LWC,TWC) data (if available) for cloud particles in flight altitude. (Dataset available: <https://doi.org/10.1594/PANGAEA.906658>)

Please also provide more detail about measurements of atmospheric thermodynamics, and a table showing the various measurements (with time and location) as context.

During the ACLOUD campaign we obtained hundreds of in situ profiles covering the 6 weeks with 2 aircraft and dropsondes in a region north-west of Svalbard (see Fig. 1), which were merged with radiosoundings from Ny-Alesund and from the (partly moving) research vessel Polarstern during the PASCAL campaign, described in section 2.2 and 2.3. Therefore, it is hard to give a comprise overview of these data in a single table. In general, the airborne in situ profiles are distributed similar to the flight pattern shown in Fig. 1 (descending/ascending before/after each low-level section from/to lower/higher altitude). We added (p.4 l. 10):

“The local atmospheric thermodynamic state, including air temperature and relative humidity was determined by dropsondes (Ehrlich et al.,2019) and aircraft in situ observations (Hartmann et al.,_2019) during ascents and descents in the vicinity of the low-level flight sections.”

All details (e.g. cruise track of Polarstern) can be accessed from the cited papers Wendisch et al. (2019) and Ehrlich et al. (2019). The datasets are all available on the PANGAEA database (see data availability). Time series of vertical profiles from radiosoundings during ACLOUD/PASCAL are shown in Knudsen et al. (2018).

Finally, Page 2, line 11 implies that this work uses all-sky minus clear-sky (other definitions of CRF use cloudy-sky minus clear sky). Were all downwelling flux measurements of cloudy sky?

See reply three comments above. We used all scenes during the flight sections including overcast, broken cloud fields and clear sky.

Radiative transfer simulations: Sufficient information is needed here that the results are reproducible. What was the vertical resolution? How were the measurements (dropsonde, radiosonde, and surface) merged? What was used for concentrations of other trace gases (most notably for the longwave calculations, CO2). It would be helpful to specify which flux and albedo terms were calculated with the various models (longwave, shortwave and 2D vs. 3D). What are the uncertainties for the radiative

transfer calculations?

We apologize that we did not fully described these technical details, which are in fact important for the reproducibility. We extended the section 2.3 to fulfill all points:

“The radiative transfer simulations for the cloud-free conditions were performed with the libRadtran package (Emde et al., 2016) using the one-dimensional, plane-parallel discrete ordinate radiative transfer solver DISORT (Stamnes et al., 1988) and the molecular absorption parameterization from Kato et al. (1999) for the shortwave spectral range (0.28–4 μm), and from Gasteiger et al. (2014) for the longwave wavelengths range (4–100 μm).”

“Hence, profiles from in situ measurements of temperature and relative humidity on board of both aircraft and, if available, dropsonde measurements from the Polar 5 aircraft were used to replace the radiosounding layers by the local atmospheric profiles.”

“The atmospheric levels below flight altitude were linearly interpolated to the surface temperature observed by the KT-19 assuming an emissivity of unity. The assumption of the black-body emissivity is justified by the high spectral emissivity for nadir observations in this wavelength range (Hori et al., 2006).”

“The sub-Arctic summer profile (Anderson et al., 1986) was used to complete the profiles including gas concentrations up to 120 km altitude.”

“The high vertical resolution of the in situ observations was reduced for the radiative transfer simulations to 30m below 1000m and stepwise increases to 5km at 120km altitude. The surface albedo is obtained from upward and downward looking pyranometers and a method described in section 4.”

In the last paragraph of section 2.3 we clarify which radiative transfer model is used for which purpose (p.5 l18):

“Spectral surface albedo values for the sensitivity study in section 3.5 were simulated using the spectral Two-streAm Radiative TransfEr in Snow model (TARTES) (Libois et al., 2013). 3D radiative transfer simulations for the albedo smoothing kernels applied in section 3.4 and the appendix A were performed with the open-source Monte Carlo Atmospheric Radiative Transfer Simulator (MCARaTS) (Iwabuchi, 2006; Iwabuchi and Kobayashi, 2008).”

Regarding the uncertainties of radiative transfer simulations we referred to Randels et al. (2013). We added in section 3.4.1 (p.12 l.14-16):

“In addition to measurement uncertainties of the used broadband radiometer (<3 %, (Ehrlich et al., 2019b)), the radiative transfer modelling can induce a bias (<2 %) in the shortwave wavelength ranges (Randles et al., 2013).”

Section 3.2: A lot of work has been done on the longwave CRF that is relevant here. For example, Cox et al 2015 (listed above) examines temperature and humidity.

We are sorry, if the focus of this section was not made clear. This study should show, how important it is to track thermodynamic profile changes during large scale processes like warm air intrusions or cold air outbreaks, because they significantly influence the local estimate of CRF and how these processes impact

the local energy budget. We did not intend to generally explain how temperature and humidity changes downward irradiance.

We changed some sentences in this section and added specific citations to make the focus of the section more clear:

(p. 8 l. 30-31)

“As was shown by Tjernström et al. (2015, 2019) such events might significantly impact the local energy budget along the trajectory.”

(p.10 l. 4-6)

“Especially for air mass transformation like warm air intrusions and cold air outbreaks in the Arctic (Pithan et al., 2018), this is a relevant issue, and requires a precise representation of air mass transformations by models or local in situ observations along the trajectory.”

Uncertainty analysis: A variety of assumptions are made in this work and the calculations and measurements all have associated errors and uncertainties. An uncertainty analysis is needed.

In the following we try to give a realistic estimate of uncertainties based on the presented workflow, which consisted of uncertainties in the observed broadband radiation and surface albedo, the simulated radiation, the LWP equivalent retrieval and the retrieved cloud-free albedo and cloud-free net fluxes. A detailed discussion of this uncertainty analysis would blow up the manuscript significantly and distract from the main conclusions. We, therefore, did not put all the calculations in the revised manuscript but added the uncertainty estimate where it was needed.

Uncertainties in the LWP equivalent retrieval:

To keep the uncertainties in a realistic range, we applied an deviation between the observed and simulated downward solar irradiance of 1.2 %, based on the results from the cloud-free flux closure study in section 3.4 (Figure 4 and deviations in the text). The albedo uncertainties result in 2.4 %. In Figure 1 (this document) the estimated absolute and relative uncertainties are given over ice and open ocean as a function of LWP and for a solar zenith angle of 60° (representative for ALOUD). The theoretical observations and lookup tables for the “observed” conditions are combined in worst case scenario.

We added in the appendix (p. 23 l. 16-17):

“The relative uncertainty range of this retrieval for homogeneous clouds and surface can be expected between 15 % and 35 % over open ocean and sea ice respectively.”

Uncertainties in the retrieval of cloud-free albedo:

In Fig. 2 (this document) synthetic distributions of LWP and Albedo are applied to the lookup tables generated using the parameterization from Gardner and Sharp (2010). The major contribution to the

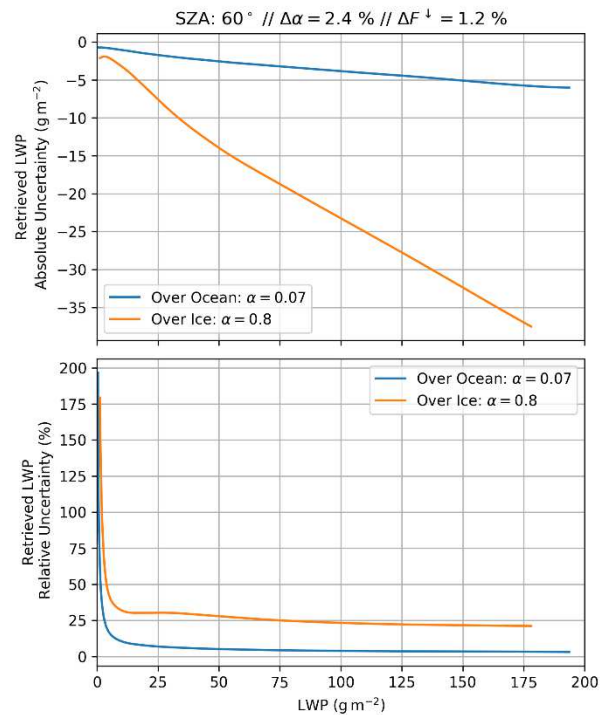


Figure 1 Absolute and relative retrieval uncertainties of equivalent LWP as a function of cloud LWP and for two surface albedos above open ocean (0.07) and sea ice/snow (0.8).

uncertainties of the retrieved cloud-free albedo stems from the observed broadband albedo itself. Uncertainties from the LWP retrieval contribute only minor to errors in the cloud-free albedo. Given the uncertainty of the observed albedo of 2.4 % and the error in simulated shortwave F_{down} of (2 %), we conclude that the relative uncertainty of solar net fluxes ($F_{down_cf} - \alpha_{cf} * F_{down_cf}$) is below 20 % above ice and lower above the open ocean and added in section 4.1.1 (p. 18 l. 32 – p.19 l.2):

“The uncertainties in the estimate α_{cf} and the shortwave $F_{net,cf}$ depend mainly on the observed α_{all} , as was investigated by applying synthetic albedo and LWP distributions to the lookup tables. Due to the non-linear increase of α_{all} with LWP the potential error induced by uncertainties in the retrieved LWP is larger for lower LWP and additionally depends on the prevailing surface types. The overall uncertainty in the cloud-free shortwave net fluxes using the retrieved α_{cf} can be expected below 20% above high surface albedos, decreasing with decreasing surface albedo.”

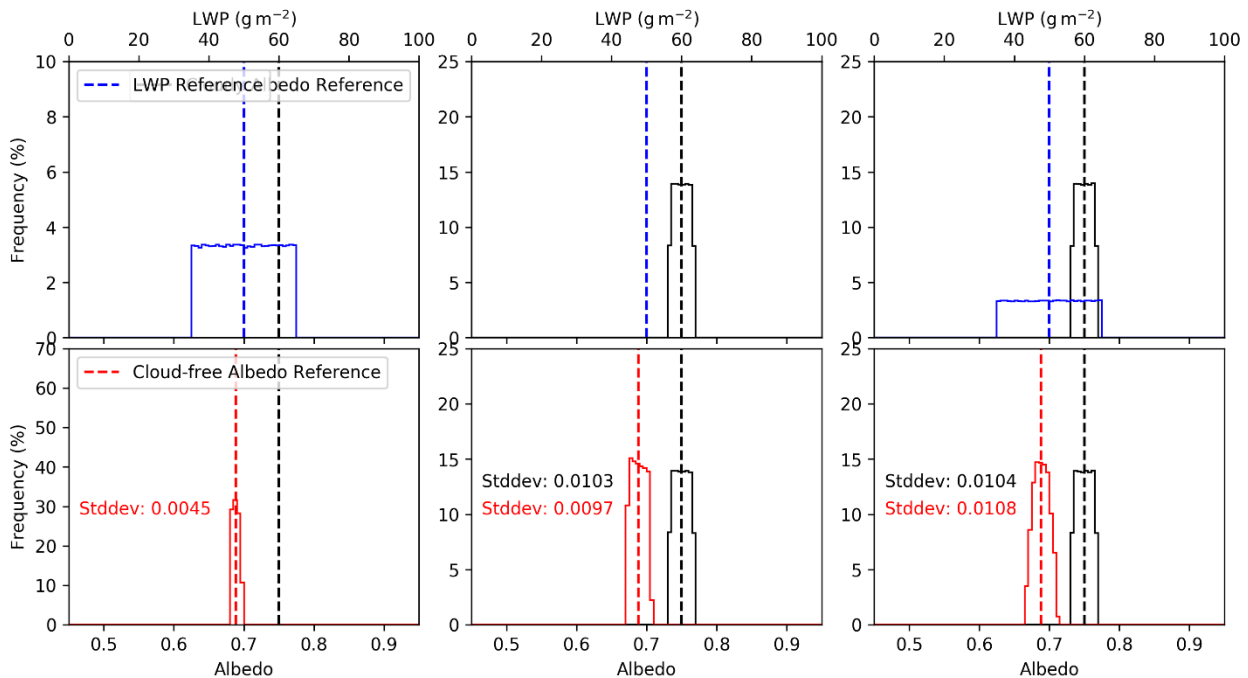


Figure 2 Upper Panels: Input for the cloud-free albedo retrieval. Lower Panels: Output of cloud-free albedo (red distribution). Albedo input in black as reference. Left panels: Only LWP uncertainty applied. Middle panels: Only albedo uncertainties applied. Right panel: LWP and Albedo uncertainties combined.

Technical details:

- I_f needs to be defined before the first time it is used.
We corrected it for the first appearance in section 2.1.

Additional changes:

We changed a typo on page 16 l.27-18 (manuscript in discussion):
The average SZA during the low level flights over sea ice under cloudy conditions was 61° not 59°.

“These values hold for the ACLOUD observations with an average LWP during cloudy conditions over sea ice of 58 gm⁻² and a SZA of 61°.”

We corrected a wrong statement on p.16 l. 22-24 (manuscript in discussion):

“The non-linearity in the functional dependence of surface albedo and LWP spreads the frequency distribution, while the mode for cloud-free conditions is not affected. “

In section 4.1 we reduced the paragraph covering the ice fraction dependent scaling of the Gardner and Sharp (2010) parameterization, because only homogeneous sea ice distributions are discussed/showed with respect to the surface albedo-cloud interaction and the required introduction of the equation, which would distract from the section (p. 19 l.5-7):

“However, making use of the cosine weighted sea ice fraction I_f and its linear relation to the albedo, changes due to the surface albedo-cloud interaction can be scaled to the prevailing I_f by assuming diffuse radiative transfer (Lambertian albedo) (not shown in this study).”

Reply to Referee #2

(Interactive comment on Atmos. Chem. Phys. Discuss., <https://doi.org/10.5194/acp-2019-534>)

We would like to thank the reviewer for her or his time and the beneficial comments, which will help to improve the manuscript. Please find the replies to the referee comments below. The page and line numbers given by the referee relate to the manuscript in discussion, the numbers in our reply to the revised manuscript.

Referee comments are highlighted in **bold**, *changes* in the manuscript in *italic*.

General comments In summary, I think this is interesting work, but it needs a more solid foundation and a discussion about the why's and the how's, and less details on ALOUD; maybe do a separate but more extensive paper on CREs during ALOUD, referencing this paper.

See third comment.

Maybe I'm nitpicking, but the terminology has been changed by the climate community, from Cloud Radiative Forcing, or CRF, to Cloud Radiative Effect, or CRE, quite a while ago.

As was noted by reviewer 3, there are inconsistencies in the definition of CRF and CRE. These parameters represent different definitions, as described in Cox et al. (2015). We derive the instantaneous CRF and, therefore, kept CRF in the revised manuscript. To make the definition of CRF more precise, we added this sentence in section 3.2 (p.71.10):

"As was stated by Cox et al. (2015) the CRF definition refers to net irradiances, while the cloud radiative effect (CRE) characterizes only changes in the downward irradiance."

The title is also in my personal opinion too long and clunky; try something shorter. Maybe "Interactions between surface albedo and clouds for Arctic cloud radiative effect estimation".

We changed the title to:

"Reassessment of shortwave surface cloud radiative forcing in the Arctic: Consideration of surface albedo-cloud interactions"

The content in the study balances along many borders and as a consequence it doesn't quite fulfill any of the topics it crosses well enough. It is unclear if this is a theoretical study that uses ALOUD data just because it's good and convenient or if it is a contribution to ALOUD as such. I already hear the authors say "can't it be both?" and my response is it would be a better radiation interaction paper if ALOUD was tuned down and a better ALOUD paper if the radiation stuff was more background and the actual results were more detailed. Typically to be a good paper on both aspects it would have to be longer – which is not good. There is also a lot taken for granted on the readers; not everyone is a radiative transfer modeling expert. So choices must be made.

We tried to reduce the ALOUD topic as much as possible, but the study needs to be based on observations to show the impact of the investigated physical processes in real conditions. A study completely based on theoretically constructed scenarios would raise the question how relevant these results are in reality. The

results shown are not meant to specifically characterize the clouds observed during ACLOUD. ACLOUD data is more a test base to apply the new approach and contributes in the end with (see abstract):

“Applying ACLOUD data it is shown that the estimated average shortwave cooling effect by clouds almost doubles over snow and ice covered surfaces (-62Wm^{-2} instead of -32Wm^{-2}), if surface albedo-cloud interactions are considered.”

However, these observations require an introduction, especially because it is a new dataset with challenges discussed in this paper. We totally agree that unfortunately these sections partly distract from the main aspect of the paper. On the other hand, observations like the one from ACLOUD enables to quantify the dependence of surface albedo with cloud LWP (Fig. 9) from observations, a process that represents the major motivation for this study. Regarding “**can’t it be both?**”, we have the opinion it must be both. By using synthetic radiative transfer simulation the manuscript shows, why surface albedo-cloud interactions matter for the estimate of CRF. The solution of this problem depends on the application on real data when the cloud-free albedo needs to be estimated from cloudy sky observations, a problem reported by different studies in literature. Only with help of the ACLOUD data, we can show that the proposed approach does lead to an improvement of the CRF estimates.

Furthermore, we keep the ACLOUD specific interpretation of the cloud properties as short as possible. We do not interpret the obtained CRF in detail, simply the relevant sign of the distributions and magnitude of changes related to surface albedo-cloud interactions (main aspect of this manuscript) are highlighted. The interpretation of CRF during ACLOUD will be treated in an upcoming paper.

Besides the use of an old terminology (CRF instead of CRE) there needs to be a much more in-depth and philosophical background.

See reply to comment 2.

Why are we interested in CRE (or CRF) and how does that impact how we do these calculations? The question “How does the clouds affect the surface energy budget” is not the same as the question “How would the surface energy budget look if the clouds were not present?”. As an example, the authors argue both that changes in surface broadband albedo between cloudy and clear states must be considered, and that the details in thermodynamic are important. However, we know that the thermodynamic profiles for clear and cloudy cases are very different. The presence of clouds depends on the vertical profiles, but the clouds themselves also modify the profiles by their presence. Yet the authors argue that we change the surface albedo to how would be without the clouds, but keep the thermodynamic profiles as they are; only remove the cloud water. I think that the answers depend on what we want to use this metric for. Ideally the answer to my second question above would have us examine the conditions in clear and cloudy conditions separately, not modifying cloudy cases by removing the condensed water. However, the Arctic is a very cloudy place and there are not enough clear cases to make this possible. Therefore, I think this paper needs a much more detailed introduction and background to what we are trying to do and why.

We agree, that the motivation and definition of the CRF is not well given in the manuscript. Therefore, in the revised manuscript, a new section is added. In the new section 3.1 the available approaches applied in literature to derive CRF are discussed. We adjusted the introduction to explain what is changing between

the cloudy and cloud-free atmospheric state in the Arctic and how it affects the estimate of CRF by the approaches listed in Section 3.1.

For the longwave CRF we are totally aware of changing thermodynamics between the cloudy and clear state. However, we aim to quantify an instantaneous effect, switching cloud on/off without changing the atmospheric profile. This is justified by putting the main focus on radiative effects caused by the shortwave CRF (see also changes in the title). To highlight which approach we use, we added “instantaneous” CRF at couple of sections, what should make clear, that we neglect the impact of changes of temperature and humidity.

1) Effects of proper thermodynamic profiles:

1) This is pretty obvious; of course one must use the profile from the same location as the CRE is considered. In this paper this is discussed in the context of aircraft observations covering an area, but the conclusion is also important for fixed-point observations. One question is, if a proper sounding at the location is not available, from how far away can it be used? This question of course has no answer other than “it depends.” But here one could also raise the issue of cloudy profiles being different from the corresponding clear case; in other words, if we could magically remove the cloud water so that the clouds vanish, what would that do to the thermodynamic profiles? Or, are the profiles found in clear conditions systematically different from those in cloudy conditions? From both modeling and observations in subtropical stratocumulus regions we know that the moist PBL is deeper and warmer when clouds are present; for the Arctic we don’t really know, but I would wager a bet that they are different!

We did not intend to discuss in general how the atmospheric thermodynamic profiles influence the estimate of CRF and that a local profiles are required, which is of course obvious. In this section the focus is mainly on the impact of air mass transformation, such as warm air intrusions or cold air outbreaks, which changes the thermodynamic state within relatively small horizontal scales. By citing the literature from Tjernström et al. (2015,2019) and Pithan et al. (2018) in this section our message should get more clear now. Regarding the thermodynamic states, see also new section 3.1.

“...from how far away can it be used?”

Yes, it depends on the scenario and where exactly a different air mass is located. We, therefore, do not try to give a general answer to this question and try to estimate the effect for our observations where we use the in situ profiles directly before and after each low level leg to replace the layers of the remote radiosoundings from Polarstern or Ny-Alesund.

“..., if we could magically remove the cloud water so that the clouds vanish, what would that do to the thermodynamic profiles?”

See comment above. We aim to quantify an instantaneous effect neglecting changes of the thermodynamic state and their impact on the terrestrial CRF. To clarify this we added the new section 3.1.

2) Effects of heterogeneous surfaces

2) That heterogeneous surfaces poses a problem for upwelling shortwave radiation is also pretty obvious. This is a main factor in the MIZ but also in the pack ice mainly due to melt ponds.

In this section we focus on the impact of surface heterogeneity on shortwave downward radiation by horizontal photon transport, not the obvious upwelling shortwave radiation, which is roughly a linear function of cosine weighted sea ice concentration.

This pa-per doesn’t even mention the effect of melt ponds, presumably because there weren’t any during ALOUD.

We mention melt ponds and discuss their effects in several sections in the paper, although we had only a low percentage during the ALOUD campaign as was shown by Jäkel et al. (2019). Of course we are aware

of their radiative effects in the summer melting season, which are part of the hypothesis Fig. 8 and discussed in section 3.5/3.51 as well as the conclusion.

So is this an ALOUD paper using advanced radiation methods or a radiation paper using ALOUD observations?

See our reply to the general comment above.

Moreover, to this reviewer it is not obvious that the downwelling radiation is dependent on surface albedo; in most NWP or climate models that I know this is not considered, but may be ignorant.

The downward radiation is affected by the surface albedo due to multiple scattering effects. With increasing surface albedo, the upward irradiance will increase. This increased upward irradiance is then scattered back by aerosol particles and atmospheric gases in cloud-free conditions (or clouds during cloudy conditions) back to the surface. This multiple scattering contributes to an increase of downward irradiance over highly reflective surface types like snow, compared to absorbing surfaces like water (see also reply next comment). This effect of course is considered in NWP models as it is simulated by any radiative transfer scheme.

What is not considered in NWP models is:

- Horizontal photon transport due to multiple scattering between neighboring grid cells (3D radiative transfer required, or the areal average albedo) (see section 3.4)
- A change of the surface albedo due to different illumination conditions (cloudy vs. cloud-free) and cloud optical thickness (see section 3.5/3.51). This effect is a major subject of the manuscript.

Either way, for a reader like me, this needs to be discussed in more detail. Commenting about “horizontal photon transport” is not sufficient.

In the revised manuscript, a short explanation of the horizontal photon transport in case of inhomogeneous surface conditions is given (p.8 l.2).

“For highly reflective surface types like snow the upward irradiance is significantly higher compared to over mostly absorbing surfaces like ocean water. A part of this upward irradiance is scattered back towards the surface (often referred to as multiple scattering), and thus, contributes to the downward irradiance. Consequently the multiple scattering between surface and atmosphere causes an increase of downward irradiance over snow and ice compared to open ocean. Photons reflected from a bright surface like an ice flow might scatter back to the surface increasing the downward radiation over dark areas like surrounding ocean water. For airborne observations in the MIZ, characterized by strong variability in surface albedo due to the variable sea ice cover, as well as ground based measurements in heterogeneous terrain, this, often referred to as, horizontal photon transport due to multiple scattering from the surrounding area to the actual point of observation is not negligible for the estimate of F_{down_sw} (Ricchiuzzi and Gautier, 1998; Kreuter et al., 2014).”

In addition we cite five papers distributed in the manuscript (Ricchiuzzi and Gautier, 1998; Kreuter et al., 2014; Weihs et al., 2001; Wendisch et al., 2004; Pirazzini and Raisanen, 2008), which specifically discuss this topic.

If this is a factor, how large is it?

The magnitude of the horizontal photon transport is quantified for the case study in Fig. 3. To make this more obvious, we added/reworded this section by (p.10 l. 22):

“However, due to horizontal photon transport from surrounding ice fields in reality the changes in $F_{sw,cf}$ are less pronounced. The quantitative impact of multiple scattering on $F_{sw,cf}$ is indicated by the gray shaded area in Fig. 3b with a maximum contribution of almost 40Wm^{-2} (relative to open ocean).”

What is it caused by? Are there differences between say the MIZ, with alternating ice and open water, pack ice with melt ponds, pack ice with open leads, or pack ice with many substantial pressure ridges? Or all of the above?

The 3D radiative effects due to horizontal photon transport in the MIZ are complex and depend on the given scenario (surface albedo map) as indicated by the reviewer.

The presented approach (smoothing the surface albedo using an appropriate filter shape, simulated using simplified scenes (see replies to the other reviewers)) can only give a rough estimate of the conditions during ALOUD, but on the other hand, it is still simple enough to be applied to observations. However, to address this issue, we added a short discussion in section 3.4 (p.12 l.2):

“This enables a more reliable estimate of the CRF in the heterogeneous MIZ and over the specific surface types, taking into account that the complexity of surface albedo fields in the MIZ can only be insufficiently represented by this simplified approach to estimate the areal averaged albedo.”

3) Effects of the clouds on the characteristics of the solar radiation.

3) Changes in the spectral composition from absorption in clouds is a real tangible effect that one can discuss if it is necessary to compensate for or not; see my discussion above.

The change of the spectral composition is not only due to absorption. The largest difference is the almost wavelength independent scattering by clouds (Mie regime) compared to the preferred scattering of short (blue) wavelength of atmospheric gases (Rayleigh regime). Clouds are white, the cloud-free sky is blue. In section 3.5/3.51 of the manuscript, we demonstrate why these spectral differences are of relevance and how a compensation affect the estimated CRF.

Changes due to the different distribution between direct and diffuse radiation is trickier. Also the cloud albedo is sensitive to solar zenith angle.

All these effects are considered and analyzed in the radiative transfer based study in section 3.5/3.51.

Finally, the language is mostly OK, but occasionally I stumble on unnecessarily difficult wording, for example “exemplarily” in the context it is used is an existing word but even the dictionary indicates it isn’t much used in modern English.

Thanks for this remark, we reworded the sections.

There are also past/present inconsistencies; what is done and presented in this paper is sometimes described in past tense and sometimes in present. Either is fine with me; just be consistent.

We apologize for these inconsistencies and corrected it.

Finally, final: among the data made available here, only a subset is actually really made available; the rest is just referenced.

During the submission of the manuscript, the publication process of the data in PANGAEA was not finalized and parts of the data might have been inaccessible. All basic data from the broadband radiometers, dropsondes, radiosondes, aircraft temperature and humidity measurements, and the camera images are available (Please see data availability). The publication of derived quantities such as LWP, cloud-free albedo and CRF is currently in progress. We wanted to wait for the reviews before publishing the data. The references will be added in the manuscript before publication. The just referenced data are dataset with a doi made fully available on the PANGAEA database.

Title is unnecessarily clunky

We changed the title, see reply third comment.

also here and throughout the paper, Cloud Radiative Forcing (CRF) should be replaced by Cloud Radiative Effect (CRE); even maybe surface CRE.

See first reply in this document.

Page 1, line 23: Comma after amplification.

Corrected.

Page 2, line 1-2: If this is the prime question, one can not use the cloud profile minus the cloud as representative for clear conditions; one must do the clear and the cloudy cases completely separately.

Thanks for this comment, which indicates, that our text might lead to a mix-up of the cloud feedback in the Arctic and the cloud radiative forcing. The former is obtained from climate model studies, the latter is a measure of how cloud influence the energy budget at a certain location and time. The manuscript only deals with the cloud radiative forcing. We changed the sentence to more clearly separate feedback and CRF (p.2 l.2).

“One prominent example is the cloud radiative feedback, which includes the effects of an increasing cloud amount in the Arctic, balancing between potential increase of both longwave downward radiation (positive) and cloud top reflectivity (negative).”

Page 2, line 3: It is not at all clear that clouds are cooling the surface in the Arctic in summer, so I would drop “dominates”. It depends on a lot of factors, some of which this paper deal with. A clear case when this statement is correct, perhaps the only one observed case, is for SHEBA; the only annual observations that exist and BTW where the CRE was calculated without any of the corrections discussed here. Suffice it to say that I’ve seen summer conditions with a lot of snow and almost no melt ponds at very high latitudes where surface temperatures plummets when the clouds dissipate.

The reviewer is totally right. See the changes in the previous comment. We furthermore added a more specific discussion of the CRE of Arctic clouds (in the introduction) (p.2 l.14):

“Long-term ground-based observations of CRF in the Arctic (Walsh and Chapman, 1998; Shupe and Intrieri, 2004; Dong et al., 2010; Miller et al., 2015) showed that in the longwave wavelength range clouds tend to warm the surface. The magnitude of the warming is influenced by macrophysical and microphysical cloud properties (e.g., Shupe and Intrieri, 2004) and by regional characteristics (Miller et al., 2015) and climate change (Cox et al., 2015). In the solar spectral range, clouds rather cool, whereby the strength and timing over the year is determined, besides cloud microphysical properties, by the solar zenith angle (SZA) and the seasonal cycle of surface albedo (e.g., Intrieri et al., 2002; Dong et al., 2010; Miller et al., 2015).”

Page 2, line 11: The cases are “clear” or “all-sky”, so I would swap places between “all-sky” and clear here. You can still define that as “cloudy” from her on, but it should be stated that the normal case is the existing clouds; not just when it is completely overcast.

Ramanathan et al. (1989) defines cloudy as not necessarily overcast, but to clarify the definition throughout the whole manuscript we changed it to “all-sky”.

Page 2, line 20: Here it is stipulated that surface albedo affects the incoming (downwelling) solar radiation for clear skies. To me that is not obvious, and even if it is obvious from multiple reflections in

clouds it is not obvious that it is important for clear-sky radiation. Do spend some more time on this please.

We discuss here multiple scattering in cloud-free conditions, not multiple scattering related to clouds.

This part was moved to section 3.2, where we state now (p. 8 l.1):

“The downward shortwave irradiance at the surface in cloud-free conditions ($F_{dw_sw_cf}$) is modulated by the atmospheric profile parameters, but also by the surface albedo. For highly reflective surface types like snow the upward irradiance is significantly higher compared to over mostly absorbing surfaces like ocean water. A part of this upward irradiance is scattered back towards the surface (often referred to as multiple scattering), and thus, contributes to the downward irradiance. Consequently the multiple scattering between surface and atmosphere causes an increase of downward irradiance over snow and ice compared to open ocean. Photons reflected from a bright surfaces like an ice flow might scatter back to the surface increasing the downward radiation over dark areas like surrounding ocean water. For airborne observations in the MIZ, characterized by strong variability in surface albedo due to the variable sea ice cover, as well as ground based measurements in heterogeneous terrain, this, often referred to as, horizontal photon transport due to multiple scattering from the surrounding area to the actual point of observation is not negligible for the estimate of F_{dw_sw} (Ricchiuzzi and Gautier, 1998; Kreuter et al., 2014).”

Page 2, line 14-15: “. . . observations of . . . conditions and of atmospheric thermodynamic state.”

This sentence was removed from the introduction.

Page 2, line 26: Is shape the right word here? Isn't it the magnitudes; not just the shape?

Yes the reviewer is right, we intended to say spectral albedo type not shape. This sentence was removed from the introduction and the topic is covered now in section 3.5.1.

Page 2, line 28: Comma after “albedo”.

This sentence was removed from the introduction.

Page 3, line 17-18: Here's an example of tense mismatch: “. . . were investigated in this paper” and “. . . aircraft is displayed . . .”. Later on same page the dataset “is” merged and on line 3-4 on the next page “. . . concentration was calculated . . .”.

We checked the whole manuscript for tense mismatch. Thanks for this eye-opener.

Paragraph starting on Page 6, line 29: How do you handle the observed surface albedo when calculating CRE (or surface $\bar{i}A_D \sim F$)? The text says that the clear-sky albedo is set to 80% and the zenith angle to 80°; presumably those were not the observed conditions?

Only for this sensitivity study in section 3.3 the albedo and SZA was fixed. For all simulations used to derive the CRF based on observations (section 4), the cloud-free albedo estimated from the measured are applied. To clarify that it is only applied for this sensitivity study, and why we did this, we added (p.9 l.7):

“The surface albedo and SZA is fixed for this sensitivity study to 0.8 and 60° respectively, similar to the observed conditions over sea ice during that flight, in order to avoid any effects induced by changing SZA or surface albedo.”

Section 3.3: Spend some time explaining why albedo affects downward solar radiation.

See reply on comment on Page 2, line 20.

Also, explain the choice of albedo filter; is there any theoretical consideration here or was it “trial and error”?

There is no analytic theoretical basis for the filter. However, we based our choice on 3D radiative transfer simulations of the downward irradiance in case of a typical lead, which are presented here in Fig. 1 (this document). The simulations indicate, that the shape of a La-Place distribution (with the shape parameter as defined now on in the section) is required/suitable to obtain the observed weighting of albedo information in the near-field of the aircraft. Yes it is “trial and error”.

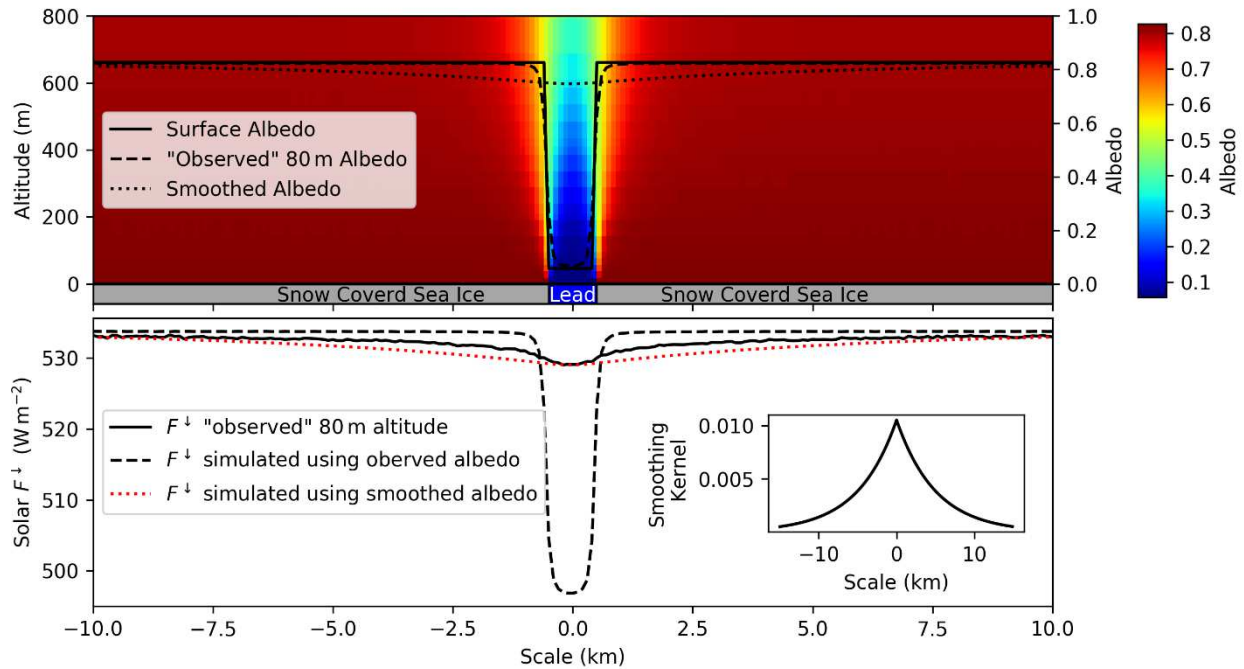


Figure 1 Broadband shortwave 3D radiative transfer simulations in clear-sky conditions of a 1 km lead embedded in homogeneous sea as shown in the lower bound of the upper panel. Upper panel: Vertical distribution of albedo. Comparison between surface albedo, albedo as observed by an aircraft in 80 m flight altitude and the smoothed albedo using the filter embedded in the lower panel. Lower panel: Comparison between 3D downward irradiance perpendicular to the lead as it would be observed in 80 m altitude (solid), 1D simulations using the observed albedo as input and the final product 1D simulations using the smoothed albedo. SZA is set to 60°.

Although the match (red dashed to solid black) is not perfect, by comparing it with the approach using simply the observed albedo (dashed black) it becomes clear that a certain smoothing is required. We tried different filter shapes and found that the La Place filter gives the appropriate weighting of the near and far-field albedo for this specific scene also for different lead sizes. It should be stated as well, that this smoothing depends on the atmospheric profile (here simply subarctic summer standard profile), albedo distribution etc. and can only give a rough estimate of the observed conditions during ACLOUD.

Paragraph starting at Page 9, line 14: It seems to me this is a test comparing calculated results to observed results from a clear day; correct? If so, maybe this should not be reported under this heading? And maybe the term CRF (or rather CRE) should not be used when there are no clouds and the CRE is expected to be zero?

Yes, this is correct, here we look at cloud-free conditions. Ideally, the CRF should be zero. However, we still think, that we need to use CRF in this section as well. The idea of the histogram is to give an uncertainty estimate for the CRF and not for, e.g., the downward irradiance. This approach is similar to Shupe and Intrieri (2004). The calculations use the same method as described in 3.3 to estimate the CRE. Differences

from zero indicate the uncertainties related to non-cloud effects. In the revised manuscript, we separate this comparison by using a subsection 3.4.1:

“Uncertainty estimate in cloud-free conditions”

In addition, we give the average and standard deviation of downward irradiance between simulations and observations in the text.

Page 10, line 6: Explain SSA.

SAA is a measure of the snow grain size. To make this link more clear, we added *“a measure of snow grain size”* to the introduction of SSA and added a citation of Gardner and Sharp (2010), where it is nicely introduced (p.13 l.4).

“Different snow packs with a density of 300 kgm⁻² are specified with various values of snow geometric thickness and specific surface area (SSA, a measure of snow grain size) (Gardner and Sharp, 2010), and located above a layer representing bare sea ice with a wavelength constant broadband albedo of 0.5.”

Page 10, line 9: I don't think you could find a case with 1 cm snow thickness in reality. That would be > 1cm at some location and no snow at other.

The purpose of these three snow packs is to represent a typical spectral albedo not necessarily “one of the real” snow packs in the Arctic. It is more relevant to show the spectral features related with the onset of melting. Of course, on small spatial scales, the snow depth can vary and be zero. However, the albedo used in the simulations should represent the spatial average of a representative area where snow covered and bare ice are mixed. As the TARTES model is not made for slush or melt-ponds, the snow thickness is a scaling factor for the shorter wavelengths to roughly represent snow or white ice in the summertime Arctic.

An example of 2-4cm of snow above sea ice can be found in Fig. 4 in Zatko and Warren (2015), where nicely the impact on the shorter wavelength is shown in reality.

Zatko, M., & Warren, S. (2015). East Antarctic sea ice in spring: Spectral albedo of snow, nilas, frost flowers and slush, and light-absorbing impurities in snow. *Annals of Glaciology*, 56(69), 53-64. doi:10.3189/2015AoG69A574

Paragraph starting at Page 10, last line: This should come before the calculation specific. First explain why and then how.

In the revised manuscript, these effects are already introduced in the introduction (p.2 l.31):

“Besides temperature and humidity changes, clouds modify the illumination and reflection of the surface. For highly reflecting snow surfaces, radiative transfer simulations show that two processes are crucial: (i) A cloud-induced weighting of the transmitted downward irradiance to smaller wavelengths, causing an increase of shortwave surface albedo, and (ii) a shift from mainly direct to rather diffuse irradiance in cloudy conditions, which decreases the shortwave albedo (Warren, 1982). Observations have shown that, in general, there is a tendency that the surface albedo is larger in cloudy, compared to cloud-free conditions (e.g., Grenfell and Perovich, 2008), and was demonstrated for a seasonal cycle by Walsh and Chapman (1998) for highly reflecting surface types.”

Page 11, line 3-4: Why is diffuse radiation coming in at a zenith angle of _50_? When the cloud is thick enough that where the sun is in the sky can no longer be determined, is there a zenith angle at all? I thought, but may be wrong, that diffuse mean precisely that the radiation was equally strong in all directions.

It is correct, that the radiation field below clouds is diffuse and the Sun is not visible. The 50° represent an “effective” solar zenith angle for which the surface albedo of pure direct illumination is similar to diffuse illumination. The angular weighted incoming diffuse irradiance has an “effective” (average) incoming angle of 50°, for details we refer to Warren (1982) or Gardner and Sharp (2010).

In the manuscript we write (p.13 l.19):

“... clouds decrease the averaged incoming (effective) angle of the mainly diffuse irradiance to approximately 50° above snow (Warren, 1982).”

Page 11, line 18: Drop “the”.

Corrected.

Page 12, line 17: “. . . with increasing LWP is not, or only poorly, parameterized. . .”

Corrected.

Page 12, line 18: Unclear past tense in “have been used”. Previously, or did you do this work now. In the previous case, give reference; in the latter, present tense should be used.

Corrected.

Figure 8: The SHEBA albedo line includes melt ponds and eventually even a lead. The drop in albedo starting at the beginning of June is due to this; as there were no melt ponds I ACLOUD(?), your comparing apples and pears here. ; as there were no melt ponds I ACLOUD(?)

As ACLOUD is limited in time, the aim of this section is to transfer the results estimated for the albedo-cloud interaction to the seasonal cycle in the Arctic. The SHEBA data, even when influenced by melt ponds, is the only comparable data set available. Therefore, the comparison does not aim to have a perfect match between ACLOUD and SHEBA. As was shown by Intrieri et al. 2002 with the onset of melt pond formation and the related strong drop in the albedo, the total CRF shifts to a cooling effect. ⇔ For ACLOUD we had higher albedo values, but we still find the transition to a total cooling in the end of the campaign caused by the surface albedo-cloud interaction (which is not represented in the study from Intrieri et al. (2002)). That is why we state in the last sentence of section 4.2 that the transition to the cooling might start earlier in the year, simply by accounting for surface albedo cloud interaction and represents a reassessment of shortwave CRF in the Arctic.

To make this clearer, we extended this sentence in the conclusion (p.21 l.17):

“Hence, the observed albedo trend during the campaign (Fig. 8) induces a transition in CRF from a warming to a cooling already for snow covered surface types, and thus, earlier in the season as reported during SHEBA.”

For the SZA calculations, did you take into account that SHEBA moved northward during the year?

As stated in the figure description: “Computed daily averaged SZA for 80° N in dashed black.” it is fixed and only serves as a reference in which range of Figure 7 the underestimation/overestimation might take place. As shown in Fig. 1, 80° N is representative for ACLOUD and for the last months of SHEBA.

Another idea would be to redo the SHEBA Intrieri et al. CRE study with this new information. Maybe a bit more work than anticipated for now, but it would be interesting.

That’s true but out of the scope of this study. The interpretation of the SHEBA CRF with the new knowledge is exactly why we made this hypothetical sketch. However, we do not have yet the radiative transfer model to represent the melt pond properties and, therefore, the SHEBA CRF was not revised. Additionally, we wrote in the conclusion that further effort is required to fully understand the seasonal cycle of solar CRF

in the Arctic by application of a similar approach to long-term observations like SHEBA or the upcoming MOSAIC. In general this approach using the parameterization from Gardner and Sharp (2010) is easy to apply to common ground based stations in the Arctic with cloud microphysical remote sensing instrumentation providing high quality LWP values, however a snow and ice dominated surface is required (no slush, melt ponds,... etc.). We added to the conclusion (p.21 l. 26):

“The proposed method to estimate the surface albedo in cloud-free conditions using the parameterization from Gardner and Sharp (2010) can be easily applied to common Arctic long-term observations above snow and ice surface types, especially if high quality LWP measurements are available.”

Page 13, line 2 & 3: Again, two examples of past-tense confusion. When was this done; for this paper or by an earlier investigator.

Corrected.

Page 13, line 10: Using both “indicate” and “might” in the same sentence almost obliterates the conclusion.

We removed “might” from the sentence.

Page 14, line 4: Can’t find any red line in Figure 8.

We changed it to: “red scatter points” in the figure description and in the given line.

Page 17, line 5: “indispensable” is a strong word. Since it is impossible to know the cloud-free state with any accuracy, I would mellow the language here. If something indispensable is also im-possible, then why even try?

We reworded the sentence (p.20 l. 11):

“To estimate the warming or cooling effect of clouds on the surface REB in the Arctic from observations or models, a precise characterization of the cloud-free state is required.”

Page 17, line 11: If by “local” you mean in one single specified point, then I’m confused. The lo-cal albedo is what it is; it is different at a different locale when the sea ice is variable; I still get hung up on this concept. If you are referring to the effects on the cloud free downwelling radiation, that I wanted to have elaborated on, the at least write “local cloud-free albedo”.

The reviewer is right, the word “local” is confusing in this sentence and was removed.

Page 18: lines 27-31: Only part of the data is available, a large chunk is only cited. Why? Appendix A: OK; but, why don’t show that this works, using aircraft passages over Polarstern, where you have both transmissivity and LWP?

All primarily measured data are made available on the PANGEA database. DOI-links, where the specific dataset can be downloaded are given in the references. The publication of derived quantities such as LWP, cloud-free albedo and CRF is currently in progress. We wanted to wait for the reviews before publishing the data. The references will be added in the manuscript before publication.

We would have very much liked to validate the method using PASCAL data. Unfortunately this was not possible for different reasons. For the PASCAL campaign unfortunately no broadband albedo measurements are available from the ship. Without the information of broadband albedo, transmissivity cannot be interpreted or linked to cloud microphysics, due to multiple scattering.

In order to validate this retrieval we compared different observations during the ALOUD/PASCAL campaign with our estimate of LWP. In Fig. 2 (this document) a comparison of LWP for the 2 June 2017

flight is shown. In situ observations of the Nevzorov probe (dataset on PANGAEA: <https://doi.pangaea.de/10.1594/PANGAEA.906658>) during ascents and descents before and after low-level section (orange scatter in Fig. 2) are used to derive the LWC profiles, which have been vertically integrated to obtain the LWP. During that flight only low-level clouds have been present. In addition to our transmissivity based retrieval (blue scatter) the MODIS overpass (0945 UTC) is shown in red scatter points collocated to the aircraft low-level flight sections. For the flight section close to Polarstern (last flight section), the HATPRO microwave retrieval of LWP on Polarstern is shown for the times where the aircraft was close by (dataset on PANGAEA: <https://doi.pangaea.de/10.1594/PANGAEA.899898> or “Cloudnet” LWC data <https://doi.pangaea.de/10.1594/PANGAEA.900106>).

In general, the two first flight section have been over open ocean close to the MIZ. The third section is over the MIZ, while the last long section is in the vicinity of Polarstern, where a “staircase pattern” was flow.

In general, the transmissivity based retrieval shows a good agreement with the MODIS observations as well as the cloud microphysical in situ observations on the same aircraft. Unfortunately, the microwave radiometer retrieval shows significantly lower LWP values, which cannot be explain easily. From the good agreement with in situ and satellite observations we conclude, that our LWP retrieval fulfills the required accuracy to estimate the surface albedo in cloud-free conditions.

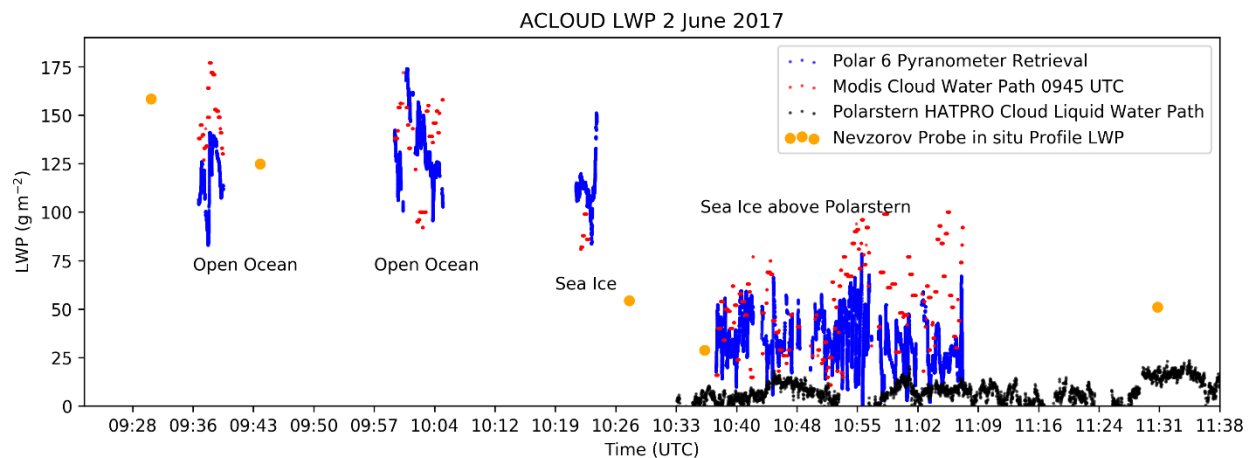


Figure 2 Time series of different LWP retrieval during the 2 June 2017 ACloud flight. The blue scatter represent the transmissivity based retrieval presented in this study, the scatter points collocated MODIS cloud water path retrieval. In orange scatter points the vertically integrated in situ profiles from the Nevzorov probe (measuring LWC) on Polar 6 is shown during descents and ascents before and after the low-level flight sections through the clouds. In black scatter the “Cloudnet” retrieval of LWP from the Polarstern research vessel for the time period where the aircraft was close by.

Reply to Referee #3

(Interactive comment on Atmos. Chem. Phys. Discuss., <https://doi.org/10.5194/acp-2019-534>)

We would like to thank the reviewer for her or his time and the beneficial comments, which will help to improve the manuscript. Please find the replies to the referee comments below. The page and line numbers given by the referee relate to the manuscript in discussion, the numbers in our reply to the revised manuscript.

Referee comments are highlighted in **bold**, *changes* in the manuscript in *italic*.

The manuscript “Reassessment of the common concept to derive the surface cloud radiative forcing in the Arctic: Consideration of surface albedo – cloud interactions” by Stapf et al. describes the calculation of cloud radiative forcing (CRF) from measurements collected from aircraft over the MIZ in the eastern Arctic near Svalbard during the ALOUD campaign in June 2017. The authors leverage the spatial nature of their measurements over the heterogeneous surface albedo that is characteristic of the MIZ to identify and correct biases in calculations of CRF under such conditions. The targeted biases are specifically those associated with cloud-surface albedo interactions when the estimates of the shortwave clear-sky surrogates used in the CRF calculation are derived using radiative transfer models. The authors focus on a relevant problem that is suitable for ACP and this problem has received less direct attention from previous studies than analogous problems in the infrared. However, I respectfully disagree that this as a “reassessment” of CRF calculations, as the influence of surface albedo on CRF has been acknowledged previously and managed in various ways.

Please find the discussion after the first major comment.

The focus on albedo is warranted here because the observational platform and environmental conditions discussed make the present work particularly sensitive in that regard but I think the advancement promised by the title is overstated. I would be more comfortable with the paper being presented in either of the following ways:

(a) As calculations of CRF in the MIZ during ALOUD with the albedo work being an important, though incidental component. In this case more work or more detailed explanations of the longwave calculations are needed (see comments below).

(b) If the authors wish to focus on the shortwave, they should drop the longwave data altogether and pitch the study as a proposed methodology for calculations of shortwave CRF in the MIZ where treatment of clear-sky shortwave fluxes requires special attention. In either case, the study needs to be more carefully contextualized and motivated by referencing previous work.

I also suggest a thorough copy editing for grammar, typos, missing words or letters, etc., of which there are many to be found.

Major Comments:

(1) The introduction and study motivations need substantial improvement. Some portions of the introduction actually belong in the Methods section. More troubling is that the study promises to improve upon (indeed, to “reassess”) surface-based observations of CRF without actually referencing a single example of previous work on this subject, which has developed for several decades in the Arctic. I suggest rewriting the introduction to more clearly contextualize the present work in the existing literature. I have included some (not exhaustive) useful references throughout this review.

The reviewer is right, we should have made more clear, that we focus on the shortwave estimate of CRF. Therefore, we changed the title to:

“Reassessment of shortwave surface cloud radiative forcing in the Arctic: Consideration of surface albedo-cloud interactions”

However, after including a literature overview of the common approaches to derive the CRF from the last two decades (section 3.1), an introduction focusing on the estimate of CRF and the conclusion part from section 3.5, we come to the conclusion, that the general knowledge of the seasonal cycle of shortwave CRF in the Arctic is based on simplified assumptions.

Neither available observational, nor model studies represent the discussed process (surface albedo-cloud interaction, see section 3.5) sufficiently. Climate models will not even rudimentarily represent this effect. However, these kind of models are used to estimate the cloud radiative feedback. Therefore, we want to point out the importance of reconsidering the described processes with respect to the estimate of the solar CRF. We added also in the conclusion (p.21 l.34):

“The shortwave net irradiances depend not alone on cloud transmissivity and surface albedo, moreover the interaction between both needs to be represented. ”

To draw the attention also to the modelling community.

Another also quite important aspect is the homogenization of CRF estimates from different available studies/datasets. For the shortwave CRF, we provide an approach for snow surface types, which can be easily applied to long-term and high quality ground-based observations. As an example, the three important studies from Shupe and Intrieri (2004) during SHEBA, Dong et al. (2010) for Barrow/Alaska and Miller et al. (2015) for Greenland used different approaches for their CRF estimates.

We discuss the different approaches in the new section 3.1 and why a comparison of the CRF values of specific studies might be error-prone and misleading.

In section 3.5 we give reasons to estimate the shortwave CRF using the cloud-free albedo, but we also want to make clear, why our approach should give a better estimate of shortwave CRF.

There are two approaches available deriving the shortwave CRF specifically with a cloud-free albedo estimate.

The first one is from Miller et al. (2015), where the cloud-free observations are linearly fitted as a function of SZA. In Gardner and Sharp (2010) (Fig. 10b) it is shown that the albedo is a non-linear function of SZA, which is further affected by the snow grain size. In Fig. 2 from Miller et al. (2015) this fit is shown and shows significant deviations from the applied fit, potentially induced by snow grain size on the Greenland ice sheet. Neglecting these fluctuations can easily cause deviations in the shortwave net flux, and thus, also in the shortwave CRF for the specific prevailing conditions. For example assuming a downward irradiance of 550 Wm^{-2} for an SZA of 60° and applying a cloud-free albedo data point of 0.79 and 0.87 in the study from Miller et al. will cause deviations of up to 44 Wm^{-2} in the CRF. These albedo induced fluctuations in CRF are concealed in the obtained time series and might be related to precipitation events, warm or cold periods, or the seasonal cycle.

For the cloud-free albedo or upward shortwave estimate from the climatological approach in Dong et al. (2010) it is stated:

“The clear-sky SW-up flux is estimated using the technique described in the study by Long [2005], where the clear-sky solar zenith angle dependence of the surface albedo is taken into account, and the clear-sky SW-up flux is estimated by the clear-sky albedo and SW-down flux.”

However, if we look at Long (2005) it is noted that only the observed albedo (cloudy) can reproduce significant changes in the surface albedo (like precipitation events) during longer cloudy periods (nicely shown in Fig. 1 in Long (2005)).

Although an albedo change like the presented one in the Southern Great Plains will not occur in the Arctic snow grain size can quickly change the surface albedo. That demonstrates that during longer cloudy periods, which are common in the Arctic, the cloud-free surface albedo estimate by this approach will induce significant uncertainties.

That is why we state in section 3.1 (p.6 l.27):

“An application of the climatological approach is primarily limited by the high cloud fraction commonly observed in the Arctic (Shupe et al., 2011). It causes large uncertainties in the estimated cloud-free irradiance, as reported by Intrieri et al. (2002), preventing an application to long-term observations with reported high cloud fractions (e.g., Sedlar et al., 2011).”

Also in the following sentence:

“Although the climatological approach will produce a more realistic estimate of CRF (especially longwave) with reduced uncertainties and representation of humidity changes (Dong et al., 2006), it remains unclear how representative a monthly average of cloud-free irradiance with a monthly averaged cloud fractions often well above 90% can be.”

For the longwave range, we state now in the introduction (p.2 l.28):

“As demonstrated by Walsh and Chapman (1998), the surface temperature change accompanied by the transitions from cloudy to clear skies is not an instantaneous effect; it rather occurs in the range of hours to days and potentially only advanced boundary layer models might be able to predict the transition between the two states after a given time.”

While the terrestrial instantaneous CRF studies from Shupe and Intrieri (2004), Sedlar et al. (2011) and Miller et al. (2015) can be nicely compared for saturation effects with increasing LWP, the estimate from Dong et al. (2010) appears unique as compiled by Miller et al. (2015). However, we know that the climatological approach with a colder surface temperature in cloud-free conditions should cause a weaker warming effect in the longwave CRF compared to the instantaneous approach. On the other hand, the cloud-free surface temperature response to changes in the cloud cover is a function of time as demonstrate by Walsh and Chapman (1998) and other surface fluxes. This circumstance raises the question, which time span after a dissipation of clouds is representative for longwave cloud-free fluxes estimated by the climatological approach, 5 minutes or 1 day? In the shortwave instead, we see an instantaneous response of surface albedo and shortwave net fluxes.

Another issue is added by the study from de Boer et al. (2011).

de Boer, G., Collins, W. D., Menon, S., and Long, C. N.: Using surface remote sensors to derive radiative characteristics of Mixed-Phase Clouds: an example from M-PACE, Atmos. Chem. Phys., 11, 11937-11949, <https://doi.org/10.5194/acp-11-11937-2011>, 2011.

There the temperature inversion caused by cloud top cooling is removed for the radiative transfer simulations by linearly interpolating between the surface and atmosphere above the cloud induced inversion, while keeping the surface temperature the same, and thus, mixing both approaches.

In the end, we have a lot of different estimates of CRF in the Arctic, and we conclude in section 3.1 (p. 6 l. 34):

“By comparing the available studies, using different approaches to estimate the CRF, it becomes evident that the variety of strategies and the handling of physical processes involved in the CRF in the Arctic limits the comparability of the individual studies and our understanding of CRF in the Arctic.”

(2) The title indicates a focus on shortwave processes. In my opinion is a fair representation of main the scope of the work, yet there are sections devoted entirely to the longwave and total CRF. There are complications in CRF calculations that are specific to the longwave (Allan et al. 2003) which are analogous to the issues affecting the shortwave; e.g., lapse rate and surface temperature responses to clearing skies (Long and Turner 2008) and systematic differences in water vapor between skies that are clear and those that are cloudy (“water vapor CRF”, e.g., Dong et al. 2006). These issues are ignored and consequently the longwave and total CRF parts of the manuscript are somewhat confusing and do not serve a clear purpose. There is quite a lot packed into this study already. I think the study would be much clearer if only shortwave data were included, in keeping with the advertised focus of the work.

Obviously, the original title was misleading. We adjusted it to make the overall focus more clear.

“Reassessment of shortwave surface cloud radiative forcing in the Arctic: Consideration of surface albedo – cloud interactions”

“...there are sections devoted entirely to the longwave and total CRF...”:

In section 3.3 we also show the shortwave CRF. To quantify the total CRF in the Arctic and answer the question if a cloud is warming or cooling the surface, the longwave contributions needs to be included in this study, even when only the instantaneous effect is considered here.

We revised the manuscript in a couple of sections to make clear, that we simply derive the instantaneous longwave CRF, so the discussion about the longwave effects are not relevant at this point (besides the conclusion).

From section 4.2 and the conclusion we see a shift from a mainly warming effect of clouds during ACLOUD to a cooling one in the end of the campaign simply by accounting for surface albedo- cloud interactions. Furthermore we added in the conclusion (p.21 l.19):

“In addition, the instantaneous longwave CRF approach might additionally induce an overestimate of the warming effect potentially shifting the total CRF further to cooling.”

(3) Ehrlich et al. (2019b) (P3L30) is in review and the DOI provided is unreachable.

We apologize for that, but in our submitted manuscript the DOI works, unfortunately after the processing of ACP (discussion version) it does not work anymore. However it is an open access journal (ESSD) and can also be found without <https://doi>.

Thus, I cannot evaluate the processing of the radiometric data, which is central to this study. Indeed, I don't even know what equipment was used.

In section 3.2 we referenced two papers, which fully describe the campaign, the used instrumentation, the processing, also in Wendisch et al. (2019).

I wish to know more in particular because radiometric data from airborne platforms requires additional processing, though I am aware that the authors are familiar with some of these complexities (e.g., Ehrlich and Wendisch 2015). In addition to the instrument response corrections of the aforementioned work, how did you correct for tilt in the pyranometer?

The inertia correction is applied by the approach from Ehrlich and Wendisch (2015). In cloud-free conditions we applied the approach from Bannehr and Schwiesow (1993) and Boers et al. (1998) as described in Ehrlich et al. (2019b) to correct for the tilt/attitude of the sensor. In cloudy conditions an attitude correction cannot be applied as the irradiance is mainly diffuse, also the upward solar fluxes (assumed mainly diffuse) were not corrected out of this reason. Further details are given in Ehrlich et al. (2019b).

How did you correct the pyrgeometer data (measured at altitude) to represent the value that would be observed at the surface? (I think the answer is you did not [P7L9]).

Yes we did not correct the CRF to represent values at the surface, because the impact is of minor importance.

In the next sentence we made clear that we are not analyzing single irradiance quantities, which are definitely influenced by the flight altitude. In the sentence the reviewer refers to, we argue that the vertical gradient of longwave irradiance remains the same, if we remove the cloud in radiative transfer simulation from the atmosphere (instantaneous approach). We clarified this sentence (p.10 l.8):

“Due to the fact that the vertical gradient dF_{lw}/dz and dF_{lw}/dz below clouds remains almost the same with or without a cloud in the radiative transfer simulations (for atmospheric profiles as observed during ALOUD), the observed CRF in flight altitude can be related to surface CRF values causing uncertainties below $\pm 5 \text{ Wm}^{-2}$.”

To show that the average flight altitude of 80 m has only a minor impact on the CRF estimate, we simulated two observed thermodynamic states during the ALOUD campaign and implemented simplified vertical homogenous clouds. In Fig. 1 (in this document) it can be clearly seen that the vertical gradient between cloudy and cloud-free single flux directions changes only slightly. Consequently, also the vertical profile of CRF (right panels) changes only slightly (see values for flight altitude of 80m and the surface embedded). We have the opinion that “...can be related to the surface CRF...” is correct regarding the other potential uncertainties of radiative transfer modelling and observations. But we added an uncertainty of $\pm 5 \text{ Wm}^{-2}$ (conservative estimate) to account for this effect. The surface based inversion was a clear-sky profile observed by a dropsonde over water, of course the assumed cloud is kind of sketchy, but only serves as a test case for a stable atmosphere.

I have a similar question about the KT-19, which does not observe thermodynamic temperature of the surface, but rather a brightness temperature relative to the FOV and dependent on the path to the target. Is there any reason to similarly correct the shortwave data for altitude given that such details are the focus of the present work?

The flight altitude (average 80 m) does hardly affect the KT19 observations. We are aware of the study from Haggerty et al. (2003), which is cited in Ehrlich et al. (2019b). The applied corrections for flight altitude are necessary due to higher flight altitudes compared to the low-level observations during ALOUD. Regarding the assumed surface emissivity for the KT19 wavelength range we use the results from Hori et al. (2006), which indicate an emissivity in this wavelength range and for the nadir viewing angle close to unity. As the values are only used for a linear interpolation of the temperature profile (required for the radiative transfer simulations) from in average 80 m to the surface, an influence on the simulated downward irradiance can be excluded. We added in the specific sentence (p.5 l.9):

“The atmospheric levels below flight altitude were linearly interpolated to the surface temperature observed by the KT-19 assuming an emissivity of unity. The assumption of the black-body emissivity is justified by the high spectral emissivity for nadir observations in this wavelength range (Hori et al., 2006).”

The impact of flight altitude on the estimate of shortwave CRF can also be seen in the specific panels of Fig. 1 (in this document) and is minor important.

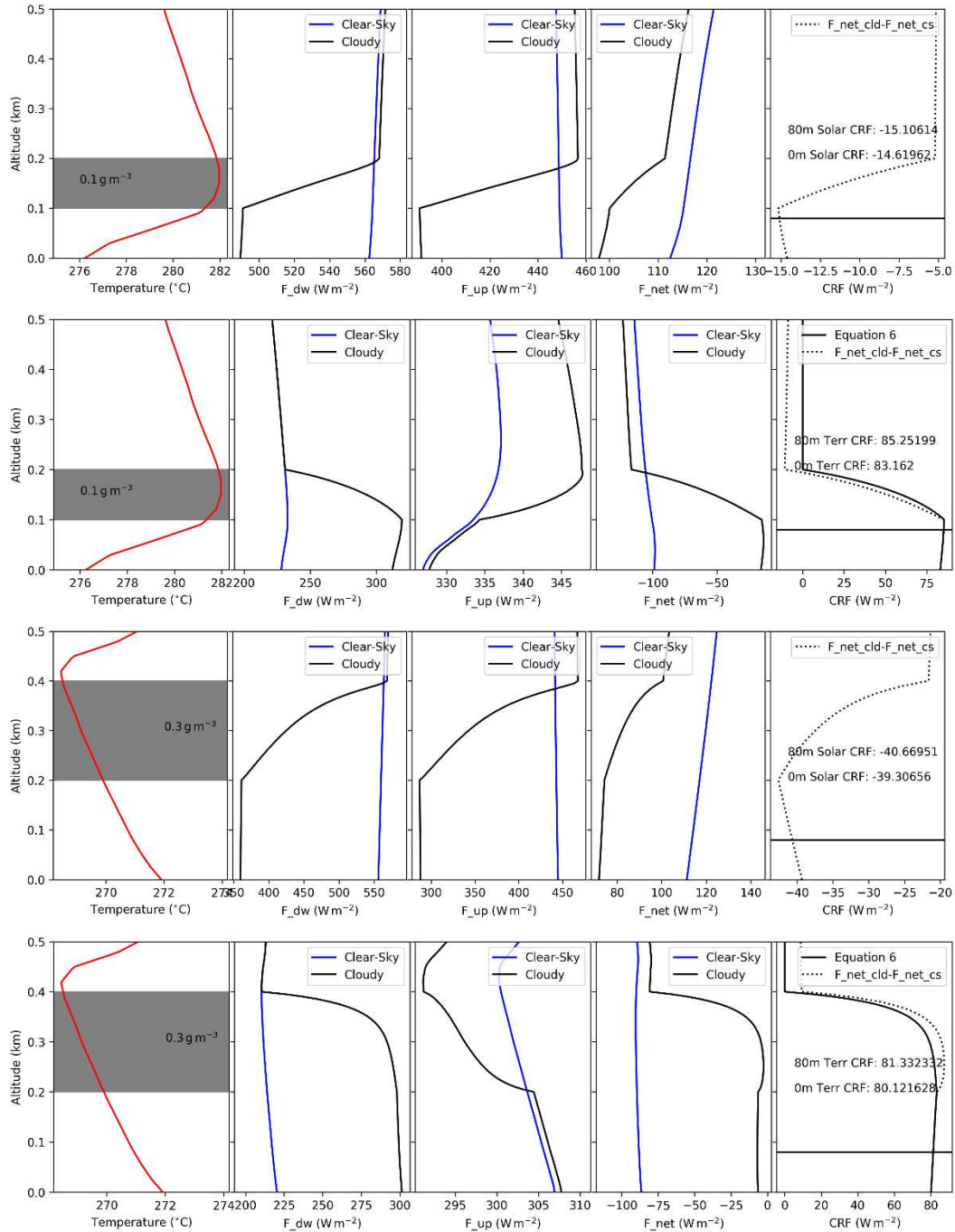


Figure 1 Simulated thermodynamic profiles during ALOUD with a rarely found surface based inversion and a typical profile over sea ice with a lifted inversion at 400m. Cloud extent and assumed homogeneous LWC is shown in the grey box together with the temperature profile (left panel). First row: Shortwave fluxes and CRF. Second row: Longwave fluxes and forcing. Third row: Shortwave fluxes. Forth row: Longwave fluxes. Fluxes are always given for cloudy and cloud-free (removed cloud) case. The surface emissivity is set to 0.99, the surface albedo 0.8 and the SZA 60° .

(4) Unless I misunderstand something, I believe there are errors in the presentation of the CRF equations. This is simple to correct if it is merely a typo in the subscripts, but if the equations were applied as stated the study's results could be impacted. Specifically, be careful how you use the terms "all sky" and "cloudy sky" because they are not equivalent in CRF nomenclature. CRF may be defined as either (all – clear) or as CF(cloudy – clear) where CF is the cloud fractional occurrence and the other terms refer to net radiative fluxes for "all" (clear and cloudy sky conditions together), "cloudy" (only times when clouds are present) and "clear" (clear skies). Ramanathan et al. discuss both definitions. Admittedly, they are confusing on the nomenclature themselves in using the term "cloudy" early on in discussing their Eqs (1) and (2), but their meaning becomes clear when they introduce Eq. (4). Your Eq. (2) is therefore incorrectly stated; it shows the maximum CRF (e.g., Intrieri et al. 2002). The "cld" subscript needs to be "all" or the entire right side of the equation needs to be multiplied by the cloud fraction. For your purposes, and for the Arctic in general, I suggest the former. This comment applies to equations throughout the text.

The reviewer is right that definition was kind of confusion, although cloudy is not equal to overcast (Ramanathan et al.). To avoid any issues with the cloud fraction definition, we replaced "cld" with "all" in the whole manuscript.

(5) P7L9: I do not agree that this is a good assumption. About 70% of the downwelling longwave at the surface originates from atmosphere below the altitude of your aircraft (Ohmura 2001). Your assumption is plausibly (not certainly) valid if the atmosphere is isothermal between surface and the base of the cloud. While this condition could be met, in your case studies (Fig. 2), it is not. Your observations of flux at the altitude of the aircraft should be corrected to represent the surface.

From our personal point of view the statement **"70% of the downwelling longwave at the surface originates from atmosphere below the altitude of your aircraft (Ohmura 2001)"** is kind of misleading and gives the impression that everything above does not matter, which is definitely not true. Please have a look on Fig. 1 (in this document). Even for single terrestrial flux directions the average flight altitude will cause a deviation well below 10 Wm⁻² (quite conservative estimate again), in the net fluxes even less, because of the same vertical gradient.

The atmosphere during ACLOUD was in the most cases not isothermal between surface and cloud base (during the low-level sections a least), which can be seen in Fig. 14 from Wendisch et al. (2019), where the distribution of the observed longwave net fluxes in the cloudy state shows always negative numbers indicating a colder "effective cloud base temperature" compared to the surface. The profile from the surface based inversion was during clear-sky conditions over open ocean and did not "affect" or observation during that day.

Nevertheless, the estimate of CRF is hardly influenced by the flight altitude. Please see also the answer to comment 3 together with Fig. 1 (in this document).

(6) P8L11-P9L7: The approach you suggest to achieve a downwelling clear-sky shortwave is intriguing, but more information is needed for future studies to adopt your method. As written, it is not reproducible and there is no information on the sensitivities of the estimation; for example, I would expect that a filter of constant width assumes that leads are randomly distributed and roughly of the same size. I would also like to know more about the justification for your choice of a Laplace distribution as the most appropriate filter for this application.

We added in section 3.4 the equation and settings of the estimated smoothing kernel to make it more reproducible. In addition we added (p.12 l.2):

“This enables a more reliable estimate of the CRF in the heterogeneous MIZ and over the specific surface types, taking into account that the complexity of surface albedo fields in the MIZ can only be insufficiently represented by this simplified approach to estimate the areal averaged albedo.”

Please see the next comment for further information about the simulations/estimate of filters.

Specific Comments

(1) Given that your upwelling shortwave is observed from an aircraft platform, the FOV covers and enormous area. I therefore do not understand why your albedo measurements (e.g., Fig 3a) are not implicitly area-averaged, even if observed from a relatively low altitude (e.g., Podgorny et al. 2018).

Thanks for bringing up this point. Yes, the albedo observed in the average flight altitude of 80 m is “already smoothed”. We did a mistake in estimating the smoothing kernel in the 3D simulation for the surface (0 m) and unfortunately neglected this altitude induced effect. So we revised the whole procedure and estimate the kernels for a representative flight altitude of 80 m.

In Fig. 2 (in this document) one of the clear-sky simulations is shown for a lead with 1 km width embedded in homogeneous sea ice similar to the study from Podgorny et al. (2018). In the upper panel the albedo is color coded as a function of scale and altitude. Also the comparison between surface albedo (0 m) and flight altitude (80 m) is shown, where the altitude induced smoothing effect can be seen, which is rather weak. The upward irradiance is cosine weighted so the alleged FOV is not really representative for the upward fluxes. In an average flight altitude of 80 m, 80 % of the signal is represented within a radius of 102 m below the aircraft. Even when we did not resolve the ground level, the smoothing effect is still in a small range, but of course the estimated filter width and shape changed accordingly (embedded in the lower panel).

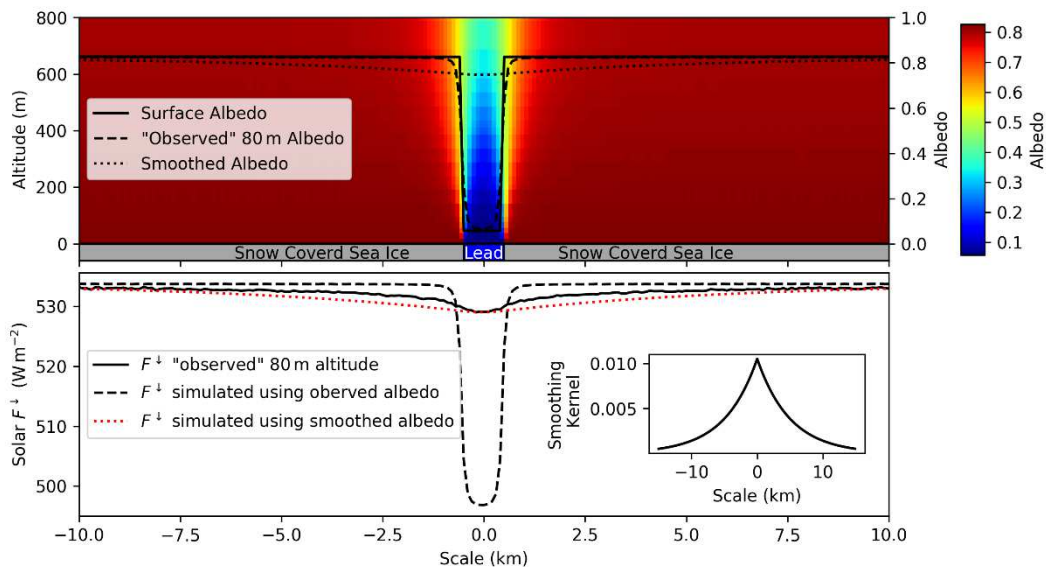


Figure 2 Broadband shortwave 3D radiative transfer simulations in clear-sky conditions of a 1 km lead embedded in homogeneous sea as shown in the lower bound of the upper panel. Upper panel: Vertical distribution of albedo. Comparison between surface albedo, albedo as observed by an aircraft in 80 m flight altitude and the smoothed albedo using the filter embedded in the lower panel. Lower panel: Comparison

between 3D downward irradiance perpendicular to the lead as it would be observed in 80 m altitude (solid), 1D simulations using the observed albedo as input and the final product 1D simulations using the smoothed albedo. SZA is set to 60°.

Also for the transmissivity based LWP retrieval, we recalculated the kernel and give the settings in the appendix to represent average flight altitude, as shown in Fig. 3 (this document).

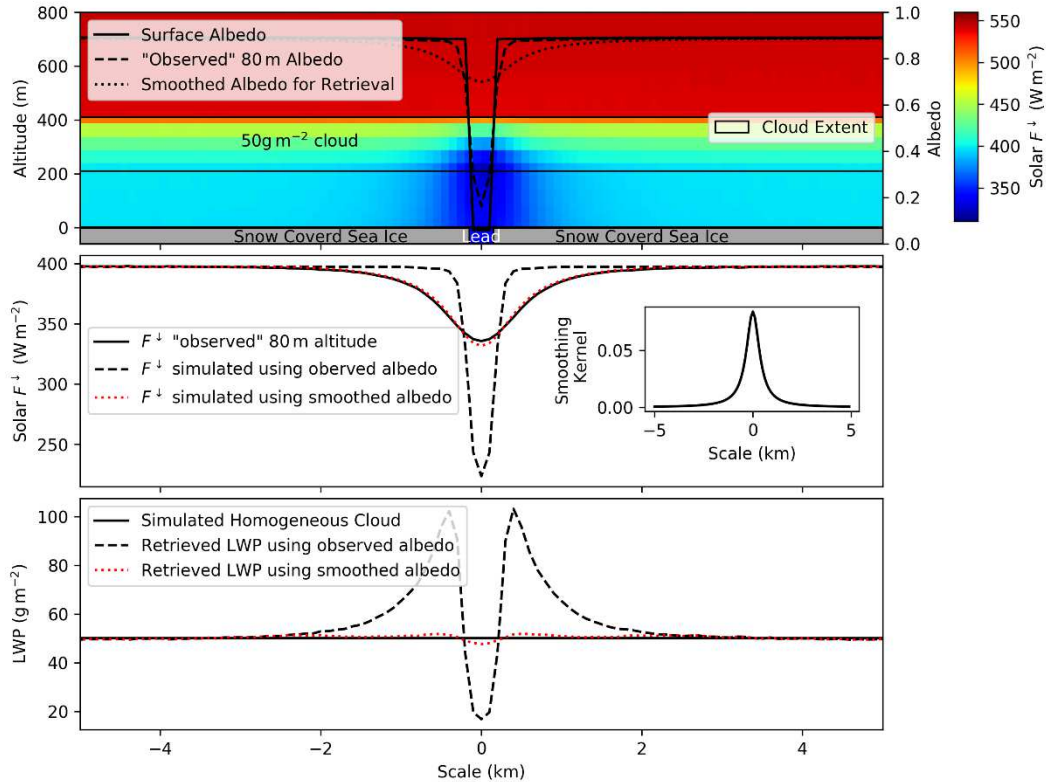


Figure 3 Broadband shortwave 3D radiative transfer simulations in homogeneous cloudy conditions with a constant LWP of 50 gm⁻² and a 300 m lead embedded in homogeneous sea, as shown in the lower bound of the upper panel. Upper panel: Vertical distribution of shortwave downward irradiance in the color code and comparison between surface albedo, albedo as observed by an aircraft in 80 m flight altitude and the smoothed albedo using the filter embedded in the middle panel. Middle panel: Comparison between 3D downward irradiance perpendicular to the lead as it would be observed in 80 m altitude (solid), 1D simulations using the observed albedo as input and the final product 1D simulations using the smoothed albedo. Lower panel: Impact of smoothed albedo on the LWP retrieval for the homogeneous 50 gm⁻² cloud. SZA is set to 60°.

As we state in the appendix the variety of potential surface heterogeneity prevents a specific solution. These results should work out for ACloud, where we exactly observed these simulated surface / cloud scenes, which brings us back to **“I would also like to know more about the justification for your choice of a Laplace distribution as the most appropriate filter for this application.”**

It simply fits to our observations and simulated cases and enables us to make it applicable to our study. A general solution like the one from Pirazzini and Raisanen (2008) requires unfortunately surface albedo maps, which we do not have.

The changes due to the new smoothing kernels caused small changes in Fig. 3, 4, 9 and 10, and the related statistics (text section 4.2 and 3.4.1). Due to the shorter scale of the clear-sky kernel in Fig. 3 changes in the areal averaged albedo occurred accordingly, which do not change the general picture. Changes in the kernel for the LWP retrieval caused only small changes in strongly fluctuating albedo sections, but did not affect the obtained statistics or retrieval of cloud-free albedo.

However, we found that occasionally surface albedo values exceeded the range of Gardner and Sharp (2010) parameterization and filtered the specific values out and added (p. 18 l.23):

“Rarely occurring surface albedo values above/below the range of the parameterization from Gardner and Sharp (2010) have been filtered out.”

Hence, the average values of CRF and Albedo in Fig. 10 and the distribution in Fig 10a and 9 changed slightly accordingly, see also changes in the values given in the text, abstract (p.1 l.12):

“Applying ALOUD data it is shown that the estimated average shortwave cooling effect by clouds almost doubles over snow and ice covered surfaces (~~-63~~-62Wm⁻² instead of ~~-33~~-32Wm⁻²), if surface albedo-cloud interactions are considered.”

And conclusion (p.21 l.14):

“For the ALOUD campaign, characterized by snow on sea ice in the beginning melting season, the averaged shortwave CRF estimate over homogeneous sea ice of -32Wm⁻² (cooling) almost doubles to -62Wm⁻², when surface albedo-cloud interactions are taken into account.”

(2) P2L18: Consider using “L” for longwave instead of “t” for terrestrial to avoid confusion with the terrestrial surface. “S” would then represent “shortwave” rather than “solar”.

We adapted the subscripts and wording in the whole manuscript.

(3) P2L18: It is true that RT simulations are a common approach, but there are other approaches as well. Long and Ackerman (2000) present a method for estimating clearsky fluxes that implicitly accounts for the albedo dependencies on sky conditions. (Refer also to Dong et al. (2010) and Long (2005)). More in line with your study, Miller et al. (2015) parameterized clear-sky albedo for their RT simulations, though your situation is considerably more complex with regard to surface cover. Other studies have analyzed the dependencies. These studies do not necessarily detract from your work here and in some ways maybe motivate it, but either way really need to be referenced.

We included the different approaches in the new literature overview in section 3.1. (See also reply to the first comment in this document)

(4) P4L15 - P5L4: (1) I don’t understand how (or when) you combined the dropsondes and NYA radiosoundings.

Before or after most of the low-level section the aircraft descended or ascended from/to higher altitudes, and thus, in situ profiles of thermodynamic state were observed. In addition dropsonde data from P5 could be used. For each low-level section we need a representative local thermodynamic profile for the calculations of F_{dw} (impact was shown for example in Fig. 2 in the manuscript). Therefore, we replaced the layers from the radiosoundings (either from Ny-Alesund or Polarstern (the temporal and spatial closer one)) with the local profiles to obtain a merged representative profile.

(2) You do not say how you represent the atmosphere above the height of the soundings; this is necessary (even if estimated using a standard atmosphere) to a reasonable effective TOA (say, 60 km).

(3) You do not say how you represent atmospheric gases that are radiatively active in the infrared, but were not measured by the sounding (not notably, CO₂, but also O₃, methane, etc.).

Thanks for this remark. We agree with the reviewer, that these are important information to make the study/ RT simulations reproducible. We included all information in section 2.3.

(5) P5L14-16: I do not agree that the upward longwave between clear and cloudy conditions is equal, but I doubt that this is what you actually mean to say. I think you mean you defined them to be so because (a) you do not account for the response of the atmospheric lapse rate (and surface skin temperature) to changes in sky cover and your calculations for the longwave are therefore “instantaneous” CRF (e.g., Miller et al. 2015),

We apologize for this unclear definition. After the literature overview and the definitions section this should be clear now.

and (b) that you also neglect the influence of differences in the amount of longwave reflected from the surface between clear and cloudy skies. It is acceptable to make the first assumption (see Allan et al. 2003), but you should include the emissivity term and then proceed with your CRF calculation. See my next comment.

We slightly adjusted the longwave CRF definition (Eq. 3 - 6) and account now also for the reflected downward longwave irradiance. (See changes in the definition section). Accordingly also the average longwave CRF value in Fig. 10b,c and section 4.2 changed slightly. See also next reply.

(6) P4 Eq. (4): This variable is more frequently referred to as (longwave) “cloud radiative effect” (CRE) (e.g, McFarlane et al. 2013; Viudez-Mora 2015; Cox et al. 2015, 2016) and should be distinguished somehow from CRF. At the surface CRF and CRE are different, the former being the difference in the net fluxes and the latter being the difference in the incident fluxes. Confusion sometimes arises because the terms are frequently used interchangeably in satellite studies, being that the terms are equal against the backdrop of space.

Thanks a lot for this remark. We totally agree that a standardized nomenclature (and definition) is required in the literature and a difference should be made between CRF and CRE. We added (p. 7 l.10):

“As was stated by Cox et al. (2015) the CRF definition refers to net fluxes, while the cloud radiative effect (CRE) characterizes only changes in the downward irradiance.”

As we stated and show now in the definitions section (p.7 l.11), the upward terms cancel for the instantaneous CRF estimate (e.g. Shupe and Intrieri, 2004; Miller et al., 2015) accounting for the reflected residual.

But the reviewer is right, the reflection term needs to be represented, why we changed the formulation (Eq. 3 - 6). Assuming an emissivity of 0.99 (Warren, 1982) the reflected residual is 1 % of the CRE, and thus, will cause a difference in the derived long CRF below 1 Wm^{-2} . (Average values in the Fig. 10, section 4.2 changed slightly)

(7) P5L28: Multiple scattering also depends on the albedo of the sky. How do you account for this?

The albedo of the sky (scattering processes of the atmosphere) is implemented by the radiative transfer simulation of the local atmospheric profile. We continuously update/run the simulation along the flight track using the closest thermodynamic profile and the local estimated areal averaged albedo.

For the smoothing kernel of the areal average albedo estimated by the idealized 3D radiative transfer study we had to fix the atmosphere (represented by the subarctic summer standard profile), which will influence only the smoothing filter, and thus, will induce only a minor impact on the resulting 1D online simulations using the smoothed albedo.

(8) P6L30: Is 60deg SZA representative of the flight conditions?

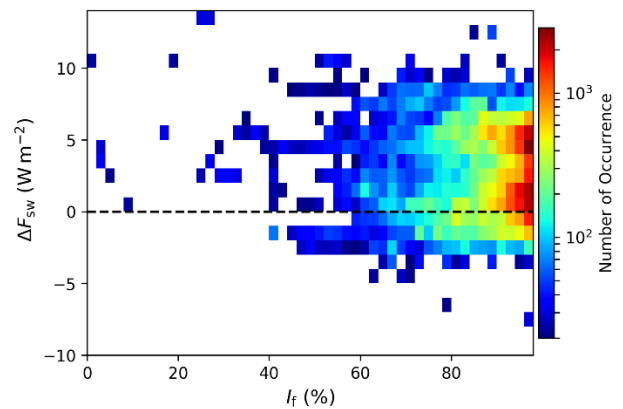
These are rounded values but representative for the conditions over sea ice during that flight. To clarify that we only used this fixed values for this sensitivity study to avoid an impact of changing SZA and surface albedos during the specific profiles and only focus on the thermodynamic impact in this section 3.3 we added (p.9 l.7):

“The surface albedo and SZA is fixed for this sensitivity study to 0.8 and 60 respectively, similar to the observed conditions over sea ice during that flight, in order to avoid any effects induced by changing SZA or surface albedo.”

(9) P9L20: You might also consider that your pyranometer is at best a 2% instrument and thus you might expect uncertainty of around 10 Wm⁻² in the measurement. Thus, Figure 4 looks quite good. I am however curious about the source of the bimodality of the solar CRF in Figure 4. My first thought is that one of these peaks is associated with ice-covered areas and the other with open water, pointing to some residual bias in the method.

To rule that out, we show in Fig. 4 (in this document) the 2D histogram of this shortwave CRF distribution of Fig. 4 (in the manuscript) as a function of sea ice concentration. The occurrence of leads do not induce a bias in the derived downward irradiance as the bimodal distribution can be seen also in the 2D distribution. Only the data of the Polar 5 aircraft produce this bimodality. We found a slight correlation to aircraft heading for this aircraft, what might indicate an issue related to the observations not the radiative transfer simulations. However, we have double checked the processing and could not find any issues regarding the offsets for the correction applied by the approach from Bannehr and Schwiesow (1993) and Boers et al. (1998) as described in Ehrlich et al. 2019b.

In Ehrlich et al. 2019b also a comparison between the two aircraft is shown indicating a good agreement. Unfortunately, we cannot resolve this bimodality during this flight, it could also be related to slightly different local conditions not captured by the in situ profiles or aerosol/haze layers as a huge area was covered. But we should be aware that these differences are well below the measurement uncertainty (<3 %) of these instruments and the albedo smoothing method is not the cause of this deviation.



(10) Section 3.4: It would substantially increase the value of this section if you contextualized your simulated biases with your observations. For example, it would be interesting to see the biases from Figure 3c plotted over Figure 7 in the phase space of the figure panel that is most appropriate.

Figure 4 2D histogram of shortwave CRF derived during the clear-sky flight (as shown in the manuscript Fig. 4) as a function of observed sea ice fraction (I_f).

We do not fully understand the point of the reviewer here. The bias from figure 3c is attributed to the changing downward shortwave irradiance due to multiple scattering, while Figure 7 shows a completely different process and a quantitative estimate of surface albedo-cloud interactions.

In Fig. 10 we show the impact of the surface albedo-cloud interaction (Fig. 7) on the ALOUD observations by comparing the different approaches.

(11) P18L9: You have mentioned SHEBA a couple times, but have not referenced it (Uttal et al., 2002), nor have you defined the acronym.

We give now an appropriate citation and the introduced the acronym.

Reassessment of ~~the common concept to derive the~~ shortwave surface cloud radiative forcing in the Arctic: Consideration of surface albedo – cloud interactions

Johannes Stapf¹, André Ehrlich¹, Evelyn Jäkel¹, Christof Lüpkes², and Manfred Wendisch¹

¹Leipzig Institute for Meteorology (LIM), University of Leipzig, Germany

²Alfred Wegener Institute for Polar and Marine Research, Bremerhaven, Germany

Correspondence: Johannes Stapf (johannes.stapf@uni-leipzig.de)

Abstract. The concept of cloud radiative forcing (CRF) is commonly ~~used~~ applied to quantify the ~~warming or cooling effect due to impact of~~ clouds on the surface radiative energy budget (REB). In the Arctic, radiative interactions between ~~micro-~~ microphysical and macrophysical properties of clouds and the surface ~~influence the CRF and complicate its estimate~~ modify the warming or cooling effect of clouds, complicating the estimate of CRF obtained from observations or models. ~~In this study~~ the individual components and processes related to the surface CRF are analysed separately using simulations and measurement from low-level airborne observations of the REB. ~~Clouds tend to increase the broadband surface albedo over snow surfaces, compared to cloud-free conditions. However, this effect is not adequately represented in the derivation of CRF in the Arctic so far. Therefore, in this study we quantify the effects caused by surface albedo-cloud interactions on the CRF using radiative transfer simulations and below-cloud airborne observations~~ in the heterogeneous springtime marginal sea ice zone (MIZ) ~~–The measurements were obtained~~ during the Arctic CLOUD Observations Using airborne measurements during polar Day (ACLOUD) campaign. The ~~effect of changing surface albedo, due to impact of a modified surface albedo in~~ the presence of clouds, as compared to cloud-free conditions, and its dependence on cloud optical thickness ~~was is~~ found to be relevant for the estimation of the solar shortwave CRF. A method to ~~correct this~~ consider this surface albedo effect by continuously retrieving the cloud-free surface albedo from observations under cloudy conditions is proposed. ~~The application of this new concept to~~ ACLOUD data shows, using an available snow and ice albedo parameterization. Applying ACLOUD data it is shown that the estimated average solar shortwave cooling effect by clouds almost doubles over snow and ice covered surfaces (~~-63-62~~ $W m^{-2}$ instead of ~~-33-32~~ $W m^{-2}$), if surface albedo-cloud interactions are considered. Concerning the seasonal cycle of the surface albedo ~~, this effect would potentially enhance solar~~ it is demonstrated that this effect enhances shortwave cooling in periods where ~~cold snow and ice dominate the surface and weaken~~ snow dominates the surface, and potentially weakens the cooling by optical thin clouds ~~and surface albedos commonly found~~ during the summertime ~~Arctic~~ melting season. These findings suggest ~~that the surface albedo-cloud interaction~~ needs to be represented should be considered in global climate models and in long-term ~~observations~~ studies to obtain a realistic estimate of the ~~solar CRF and a reasonable representation of cloud radiative feedback mechanisms in the Arctic and~~ shortwave CRF in order to quantify the role of clouds in Arctic amplification.

1 Introduction

Interdisciplinary research conducted within the last decades has led to a broader, but not yet complete understanding of the rapid and, compared to mid-latitudes, enhanced warming in the Arctic (so-called Arctic amplification) ~~which is triggered by global warming~~ (Gillett et al., 2008; Overland et al., 2011; Serreze and Barry, 2011; Stroeve et al., 2012; Jeffries et al., 2013; Cohen et al., 2014; Wendisch et al., 2017). Since the ~~interrelationships~~ numerous interactions of physical processes, responsible for ~~the Arctic amplification are complex~~ Arctic amplification, are intertwined and difficult to observe, climate models are needed to quantify the individual ~~contribution of potential~~ contributions of feedback processes to Arctic climate change (Screens and Simmonds, 2010; Pithan and Mauritsen, 2014). However, the model results show a large spread in representing the feedback mechanisms. One prominent example is the cloud radiative feedback, which includes the effects of an increasing cloud amount in the Arctic. ~~While the cooling cloud radiative effect (reflection of solar radiation back to space causing a near-surface cooling of the Arctic surface) dominates in summer, a warming cloud radiative effect enhances the near-surface air temperature in winter, when the emitted terrestrial radiation determines the surface energy budget. In order to enable reliable model,~~ balancing between the potential increase of both longwave downward radiation (positive) and cloud top reflectivity (negative). To enable reliable projections of future climate changes in the Arctic, the understanding of the individual physical processes and feedback mechanisms ~~of causing~~ Arctic amplification is required (Pithan and Mauritsen, 2014; Goosse et al., 2018), as well as observations of how clouds influence the Arctic surface radiative energy budget (REB).

To quantify the ~~instantaneous~~ radiative effect of clouds on the ~~surface radiative energy budget (REB), the~~ REB, the concept of cloud radiative forcing (CRF, expressed as ΔF) is defined as the difference between the net radiative energy flux densities,

$$F_{\text{net}} = F^{\downarrow} - F^{\uparrow}, \quad (1)$$

also called irradiances, in ~~cloudy (all-sky)~~ ($F_{\text{net,cld}}$ conditions ($F_{\text{net,all}}$) and cloud-free ($F_{\text{net,cf}}$) conditions (Ramanathan et al., 1989),

$$\Delta F = F_{\text{net,cld}} - F_{\text{net,cf}}. \quad (2)$$

A warming effect ~~of clouds~~ at the surface will be ~~induced~~ caused by clouds if the net radiative flux densities in a cloudy atmosphere are larger than in corresponding cloud-free conditions. ~~To derive the CRF from observations, simultaneous measurements of net irradiances in cloudy and cloud-free situations would be needed, which is impossible from a practical point of view. Therefore, the net irradiances of the cloud-free state are commonly obtained from radiative transfer simulations based on measurements of the observed surface conditions. The downward terrestrial irradiance in cloud-free atmospheric conditions ($F_{t,cf}^{\downarrow}$) depends on the profiles of atmospheric temperature, absorber gas and aerosol particle concentrations~~ Long-term ground-based observations of CRF in the Arctic (Walsh and Chapman, 1998; Shupe and Intrieri, 2004; Dong et al., 2010; Miller et al., 2015) show that in the longwave wavelength range clouds tend to warm the surface. The magnitude of the warming is influenced by macrophysical and microphysical cloud properties (e.g., Shupe and Intrieri, 2004) and by regional characteristics (Miller et al., 2015) and climate change (Cox et al., 2015). In the solar wavelength range, $F_{s,cf}^{\downarrow}$ is influenced by spectral range, clouds rather cool, whereby the strength and timing over the year is determined, besides cloud microphysical properties, by the solar zenith angle

(SZA) , atmospheric profiles of gases and aerosol particle properties, as well as the surface albedo. To estimate the and the seasonal cycle of surface albedo (e.g., Intrieri et al., 2002; Dong et al., 2010; Miller et al., 2015). However, the required cloud-free atmospheric state, the input of the radiative transfer simulations is based on observations of the atmosphere and surface conditions reference ($F_{\text{net,cf}}$) poses a serious problem to all observations in the cloudy state. However, e.g., the surface albedo in cloudy conditions is not necessarily identical to the one in Arctic (Shupe et al., 2011), as the unknown thermodynamic and surface albedo conditions in cloud-free environments is modified by the presence of clouds itself.

Low-level clouds in the Arctic boundary layer cause elevated temperature inversions, modified thermodynamic profiles, and changed turbulent energy and momentum fluxes, as compared to a cloud-free atmosphere. In the Arctic, the surface albedo, determining the reflected solar radiation at the surface , depends on the snow and sea ice properties, such as specific surface area (SSA, equivalent to the snow grain size), surface roughness, snow height and density, the SZA, but also on the cloud optical thickness (Warren, 1982; Gardner and Sharp, 2010), which alters the spectral shape of the surface albedo and addition, the clouds modify the surface energy budget by the two competing effects of longwave warming and shortwave cooling, with consequences for the surface temperature and turbulent fluxes. This results in two typical states of thermodynamic profiles (Tjernström and Graverson, 2009) and longwave radiative irradiances (Stramler et al., 2011; Wendisch et al., 2019) observed in the Arctic winter. As demonstrated by Walsh and Chapman (1998), the angular distribution of the reflection surface temperature change accompanied by the transitions from cloudy to clear skies is not an instantaneous effect; it rather occurs in the range of hours to days and potentially only advanced boundary layer models might be able to predict the transition between the two states after a given time.

In particular the spectral distribution of the incoming irradiance is shifted to shorter wavelengths in overcast conditions due to absorption within the clouds. In combination with the spectral shape of the snow albedo characterized by higher values for short wavelengths, this effect tends to increase the broadband albedo in cloudy conditions (Grenfell and Perovich, 2008). Furthermore, clouds induce a more isotropic illumination of the surface compared to cloud-free conditions where the direct solar radiation dominates the radiation field. In general, the snow albedo decreases with decreasing SZA (Warren, 1982). In the Arctic with prevailing high SZAs, clouds decrease the effective SZA to approximately 50° . Besides temperature and humidity changes, clouds modify the illumination and reflection of the surface. For highly reflecting snow surfaces, radiative transfer simulations show that two processes are crucial: (i) A cloud-induced weighting of the transmitted downward irradiance to smaller wavelengths, causing an increase of shortwave surface albedo, and (ii) a shift from mainly direct to rather diffuse irradiance in cloudy conditions, which decreases the shortwave albedo (Warren, 1982). Observations have shown that, in general, there is a tendency that the surface albedo is larger in cloudy, compared to cloud-free situation (Warren, 1982), and thus, have a diminishing effect on the surface albedo conditions (e.g., Grenfell and Perovich, 2008), and was demonstrated for a seasonal cycle by Walsh and Chapman (1998) for highly reflecting surface types. Radiative transfer simulations open up the possibility to tackle the processes involved in the cloud-related surface albedo changes. Both processes (i and ii), have been parameterized for snow and ice, for example by Gardner and Sharp (2010) based on simulations, however, . However, their impact on estimates of the CRF in the Arctic have not yet been evaluated.

In this study, the components of CRF, obtained by For this purpose we deploy combined snow surface albedo model and

atmospheric radiative transfer simulations and illustrative low-level (below cloud) airborne observations of the REB in the marginal sea ice zone (MIZ) during the Arctic Cloud Observations Using airborne measurements during polar Day (ACLOUD) campaign (Wendisch et al., 2019). After an introduction of the airborne observations, the instrumentation and the radiative transfer simulations ~~are investigated to improve the estimate of the total (solar plus terrestrial) CRF from observations and~~
5 ~~modelling in the Arctic environment. A method is described~~ (section 2), available approaches to derive the CRF are reviewed in section 3.1. Furthermore, in this section the interaction between spectral surface albedo and cloud optical thickness and its importance for the estimate of shortwave CRF is analyzed and quantified. In section 4 a method is introduced to retrieve the ~~surface broadband albedo in a~~ shortwave surface albedo in the hypothetical cloud-free atmosphere from measurements under cloudy conditions, ~~and to account for the surface albedo heterogeneity, which induces uncertainties in the assumed cloud-free~~
10 ~~downward solar irradiance~~ by using an available snow and ice albedo parameterization from Gardner and Sharp (2010) and a shortwave transmissivity-based retrieval of cloud liquid water path (Appendix A). An application of ~~the approach to airborne low-level (below cloud) observations of REB in the marginal sea ice zone (MIZ) close to Svalbard during the Arctic Cloud Observations Using airborne measurements during polar Day (ACLOUD) campaign (Wendisch et al., 2019) is shown. This dataset extends~~ this approach to ACLOUD airborne observations is presented, extending available REB and CRF ~~datasets/~~observations
15 in the Arctic including horizontal variability in the heterogeneous MIZ.

2 Observation and modelling

2.1 Airborne measurements ~~during ACLOUD~~

The cloudy atmospheric boundary layer (~~ABL~~) in the MIZ north west of Svalbard was studied ~~with two aircraft using the~~ ~~research aircraft Polar 5 and Polar 6 from the Alfred-Wegener Institute (AWI)~~ during the ACLOUD campaign performed
20 in spring between 23 May and 26 June 2017 (Wendisch et al., 2019). Part of the flights ~~with the research aircraft Polar 5 and Polar 6 from the Alfred-Wegener Institute (AWI)~~ were dedicated to characterize the near-surface radiative energy budget below ABL clouds. From all flights, 16 hours of data measured below an altitude of 250 m (average 80 m) covering a distance of 3700 km ~~were~~ ~~are~~ investigated in this paper. The sea ice concentration observed along the low-level ~~flight tracks~~ ~~flights~~ by instruments mounted ~~at on~~ the aircraft is displayed in Fig. 1, together with a ~~(Moderate Resolution Imaging Spectroradiometer)~~
25 ~~MODIS satellite image illustrating a~~ (MODIS) satellite image showing the sea ice distribution ~~being typical for end of May and June 2017. The red (80 %) and light-blue (15 %) contour lines indicate the average sea ice concentration during the ACLOUD campaign~~ calculated from daily sea ice data (Sprenn et al., 2008). ~~During ACLOUD~~ ~~representative for the~~ ~~campaign. During the ACLOUD period, the~~ location of the ~~sea ice edge~~ MIZ, indicated by the contour lines of average sea ice fraction (I_f), was almost stationary (Knudsen et al., 2018). ~~In general, the~~ ~~The~~ sea ice was more compact (higher concentration) north of 81° N
30 ~~geographic latitude~~, and rather heterogeneous towards the west and ~~closer to~~ the open ocean. The ~~low-level flights of Polar 5 and 6 are almost equally distributed over these different sea ice conditions. The~~ majority of flights (66 %) were over sea ice ($I_f > 80\%$), leaving about 17 % over the MIZ as well as 17 % over open ocean ($I_f < 15\%$). As the dataset is merged from different flights covering about six weeks of measurements, it comprises various sea ice characteristics and synoptic situations

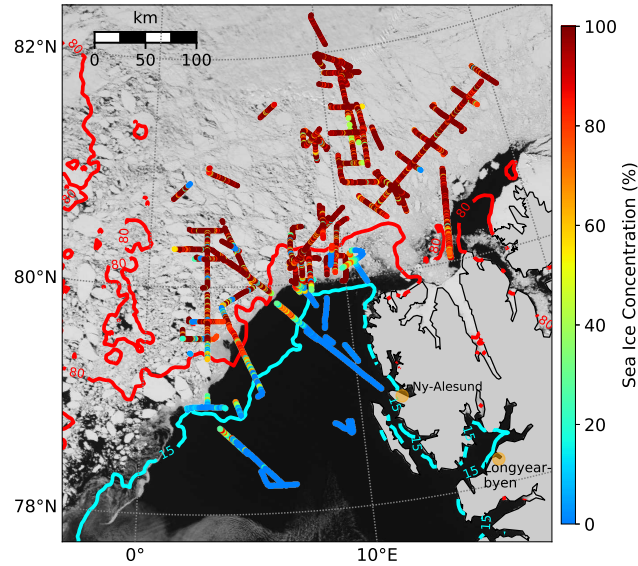


Figure 1. MODIS satellite image on 1 June 2017, representing the typical sea ice distribution during the ACLOUD campaign. All low-level flight sections during the ACLOUD campaign are indicated with the sea ice ~~concentration fraction~~ derived from airborne observations. Red (80 %) and light-blue (15 %) contours indicate the campaign average sea ice ~~concentration fraction~~ from daily sea ice data (Spren et al., 2008).

(Knudsen et al., 2018). However, the data set is still limited and should be considered as a snapshot of the late spring conditions in this region.

2.2 ~~Instrumentation~~Instrumental payload

The comprehensive instrumentation of Polar 5 and Polar 6 during the ACLOUD campaign is described by Wendisch et al. (2019) ~~as well as and~~ by Ehrlich et al. (2019b). ~~The necessary~~ In this paper, shortwave and longwave, upward and downward broadband irradiance have been analyzed from measurements with a frequency of 20 Hz obtained from two sets of Pyranometer (0.2-3.6 μm) and Pyrgeometer (4.5-42 μm). From these irradiance data the net irradiance and surface albedo have been derived. The processing of the Pyranometer and Pyrgeometer data (Stapf et al., 2019), which were used to derive the REB from ACLOUD observations, is ~~described detailed~~ in Ehrlich et al. (2019b). Surface brightness temperature ~~information have been~~ was obtain by a Kelvin Infrared Radiation Thermometer (KT-19) (Stapf et al., 2019). The ~~sea-ice fraction (ice fraction I_f)~~ along the flight track ~~is was~~ estimated from measurements of a digital camera equipped with a hemispheric lens. The geometrically calibrated images ~~are were~~ obtained with a sampling frequency of 6 ~~s from which the cosine-weighted~~; from the images the cosine-weighted sea ice concentration was calculated (Jäkel et al., 2019). The local atmospheric thermodynamic state, including air temperature and relative humidity ~~was measured~~, was determined by dropsondes (Ehrlich et al., 2019a) and

aircraft in situ observations (Hartmann et al., 2019) ~~in vicinity to~~ during ascents and descents in the vicinity of the low-level flight sections.

2.3 Radiative ~~Transfer Simulation~~ transfer simulations

The radiative transfer simulations for the cloud-free conditions ~~are~~ were performed with the libRadtran package (Emde et al., 2016) using the one-dimensional, plane-parallel discrete ordinate radiative transfer solver DISORT (Stamnes et al., 1988) and the molecular absorption parameterization from Kato et al. (1999) for the ~~solar spectral range~~ shortwave spectral range (0.28–4 μm), and from Gasteiger et al. (2014) for the ~~terrestrial wavelengths range~~. ~~Daily ozone concentrations in the flight region of ACLOUD are considered and obtained from~~. ~~The aerosol longwave wavelengths range (4–100 μm)~~. ~~The aerosol particle~~ optical thickness was neglected ~~justified by the fact that in the simulations, because the~~ full column aerosol information ~~are~~ were not available for low-level flights in cloudy conditions. Therefore, the estimated CRF needs to be considered as direct aerosol plus cloud radiative forcing.

The atmospheric state, ~~used in~~ required as input for the radiative transfer simulations to derive the CRF, ~~is~~ was based on radiosoundings performed in Ny-Ålesund (Svalbard) (Maturilli, 2017a, b) and onboard Polarstern (Schmithüsen, 2017), which were partly spatially and temporally separated from the airborne observations by several hundred kilometres and up to three 15 hours. Hence, profiles from in situ measurements of temperature and relative humidity on board of both aircraft and, if available, dropsonde measurements from the Polar 5 aircraft were used to ~~complete the local atmospheric profile data~~ replace the radiosounding layers by the local atmospheric profiles. The atmospheric levels below flight altitude were ~~adjusted linearly interpolated~~ to the surface temperature ~~measured~~ observed by the KT-19 ~~assuming an emissivity of unity~~. ~~The assumption of the black-body emissivity is justified by the high spectral emissivity for nadir observations in this wavelength range~~ (Hori et al., 2006). ~~The sub-Arctic summer profile (Anderson et al., 1986) was used to complete the profiles including gas concentrations up to 120 km altitude. Daily ozone concentrations in the flight region of ACLOUD were considered and obtained from~~ http://exp-studies.tor.ec.gc.ca/cgi-bin/selectMap. ~~The high vertical resolution of the in situ observations was reduced for the radiative transfer simulations to 30 m below 1000 m and stepwise increases to 5 km at 120 km altitude. The surface albedo was obtained from upward and downward looking pyranometers and a method described in section 4.~~

25 Spectral surface albedo values ~~have been~~ for the sensitivity study in section 3.5 were simulated using the spectral Two-stream Radiative TransfEr in Snow model (TARTES) (Libois et al., 2013), ~~which is applied in a sensitivity study in section 3.5~~. 3D radiative transfer simulations ~~are~~ for the albedo smoothing kernels applied in section 3.4 and the appendix A were performed with the open-source Monte Carlo Atmospheric Radiative Transfer Simulator (MCARaTS) (Iwabuchi, 2006; Iwabuchi and Kobayashi, 2008).

3 Components Estimate of the surface cloud radiative forcing

3.1 Definitions

3.1 Common approaches

To derive the CRF from ground-based observations, simultaneous measurements of net irradiances in cloudy and cloud-free conditions would be needed. From a practical point of view it is impossible to simultaneously measure in cloudy and in cloud-free conditions at the same location. Therefore, the common approach is to measure net irradiances in cloudy conditions, and estimate the respective net irradiances in the hypothetical cloud-free atmosphere. For ground-based observations, two general approaches have been realised to estimate the $F_{\text{net,cf}}$.

Firstly, a radiative transfer based approach, which aims to estimate the instantaneous CRF by simply removing in the simulations the cloud from the observed atmosphere, neglecting changes of the thermodynamic state over time or differences of the cloudy and cloud-free surface albedo (Intrieri et al., 2002; Shupe and Intrieri, 2004; Sedlar et al., 2011; Cox et al., 2015; Wang et al., 2018) and partly Miller et al. (2015) (using cloud-free albedo observations). A second, more climatological approach (Walsh and Chapman, 1998; Dong et al., 2010) uses observations in cloud-free conditions to extrapolate the cloud-free state during cloudy periods. In this technique, fitting algorithms from Long and Ackerman (2000) and Long and Turner (2008) are applied, or observed cloud-free/cloudy irradiances are averaged to represent monthly values (Walsh and Chapman, 1998) and partly Dong et al. (2010) (averaging upward longwave irradiance). The cloud-free, shortwave upward irradiance can be obtained from methods described in Long (2005).

In all these methods the physical processes involved in the estimate of $F_{\text{net,cf}}$ are represented differently, resulting in systematic differences in the derived CRF of the individual approaches. From autumn to spring, the longwave CRF derived from the radiative transfer based approach should tend to produce a more positive (warming) CRF compared to the climatological approach. This is due to the in general colder cloud-free surface temperatures, the presence of surface-based and dissipation of elevated temperature inversions in cloud-free conditions. In spring and summer, the surface temperature difference between cloud-free and cloudy state is smaller (Walsh and Chapman, 1998). Therefore, the difference in the CRF estimate between the climatological and radiative transfer based approach will depend on the prevailing conditions controlled by a neutral or potentially even cooling CRF.

The shortwave CRF is strongly affected by the assumed surface albedo. The typically lower values of surface albedo in the cloud-free state (Walsh and Chapman, 1998) should result in more positive shortwave $F_{\text{net,cf}}$, and thus, an increase of the cooling effect of clouds retrieved from the climatological approach relative to the instantaneous radiative transfer based CRF, where a percent deviation of albedo can be related to the deviation of shortwave $F_{\text{net,cf}}$. For the instantaneous CRF, changes in surface albedo between cloudy and cloud-free state have been neglected so far by the use of the observed albedo in the radiative transfer simulations (Intrieri et al., 2002; Shupe and Intrieri, 2004; Sedlar et al., 2011; Wang et al., 2018). Miller et al. (2015) used cloud-free observations of surface albedo fitted linearly as a function of SZA to obtain cloud-free albedo values during cloudy periods. This approach neglects the non-linear dependence of the albedo with SZA (Gardner and Sharp, 2010), the impact of snow grain size and potential seasonal changes of cloud-free surface albedo indicated by the observed albedo shown in

Miller et al. (2018), and thus, induces large uncertainties in the estimate of cloud-free shortwave net irradiance and may even distort the obtained seasonal cycle of CRF. The climatological approach from Long (2005) tries to estimate the cloud-free surface albedo during cloudy periods based on cloud-free observations, taking the prevailing SZA into account. However, it should be noted that for longer cloudy periods the cloudy-sky (observed) albedo is used in combination with downward cloud-free irradiance to represent the upward shortwave irradiance, because an extrapolation in changing albedo conditions caused by precipitation and melting events (changes in snow microphysical properties) is not possible. An application of the climatological approach is primarily limited by the high cloud fraction commonly observed in the Arctic (Shupe et al., 2011). It causes large uncertainties in the estimated cloud-free irradiance, as reported by Intrieri et al. (2002), preventing an application to long-term observations with reported high cloud fractions (e.g., Sedlar et al., 2011). Although the climatological approach will produce a more realistic estimate of CRF (especially longwave) with reduced uncertainties and representation of humidity changes (Dong et al., 2006), it remains unclear how representative a monthly average of cloud-free irradiance with a monthly averaged cloud fractions often well above 90 % can be.

By comparing the available studies, using different approaches to estimate the CRF, it becomes evident that the variety of strategies and the handling of physical processes involved in the CRF in the Arctic limits the comparability of the individual studies and our understanding of CRF in the Arctic.

3.2 Definitions

In this study, we aim to derive the radiative transfer based instantaneous CRF. However, we provide reasons and a solution for the derivation of shortwave CRF using a continuous estimate of the cloud-free surface albedo of snow and ice obtained from observations in cloudy conditions.

To assign processes related to single components of the surface CRF, Eq. 2 is separated in ~~terrestrial and solar~~ longwave and shortwave terms. The ~~terrestrial~~ longwave term reads:

$$\Delta F_{\text{tlw}} = \left(F_{\text{t,cldlw,all}}^{\downarrow} - F_{\text{t,cldlw,all}}^{\uparrow} \right) - \left(F_{\text{t,cflw,cf}}^{\downarrow} - F_{\text{t,cflw,cf}}^{\uparrow} \right). \quad (3)$$

~~It can be assumed to be independent of the upward irradiance ($F_{\text{t,cld}}^{\uparrow} = F_{\text{t,cf}}^{\uparrow}$) as a high surface emissivity enables to neglect a reflection term and for the instantaneous CRF the surface temperature is assumed to be identical for the cloudy and clear sky. As was stated by Cox et al. (2015) the CRF definition refers to net irradiances, while the cloud radiative effect (CRE) characterizes only changes in the downward irradiance. By splitting the upward terms in a component emitted by the surface with a temperature T_s and broadband surface emissivity ϵ_s of 0.99 (Warren, 1982) as well as a reflected residual of $F_{\text{t}}^{\downarrow}$, the upward term:~~

$$-F_{\text{lw,all}}^{\uparrow} + F_{\text{lw,cf}}^{\uparrow} = -\epsilon_s \cdot \sigma \cdot T_s^4 - (1 - \epsilon_s) \cdot F_{\text{lw,all}}^{\downarrow} + \epsilon_s \cdot \sigma \cdot T_s^4 + (1 - \epsilon_s) \cdot F_{\text{lw,cf}}^{\downarrow}, \quad (4)$$

reduces to:

$$-F_{\text{lw,all}}^{\uparrow} + F_{\text{lw,cf}}^{\uparrow} = (1 - \epsilon_s) \cdot (F_{\text{lw,cf}}^{\downarrow} - F_{\text{lw,all}}^{\downarrow}). \quad (5)$$

This approach assumes a constant surface temperature in cloudy and cloud-free ~~case. Hence, the state, and thus, represents the~~ commonly defined instantaneous longwave CRF similar to Shupe and Intrieri (2004); Sedlar et al. (2011); Miller et al. (2015) and should be considered in the interpretation of the CRF values as discussed in the previous section. The essential input for radiative transfer ~~are is~~ the atmospheric temperature, the absorber gas profile and aerosol. ~~Thus the terrestrial CRF. Hence, the~~

5 ~~longwave instantaneous CRF is independent on the upward irradiance and~~ reduces to:

$$\Delta F_{\underline{t}lw} = F_{\underline{t},cldlw,all}^{\downarrow} - F_{\underline{t},cflw,cf}^{\downarrow} + \left(1 - \epsilon_s\right) \cdot \left(F_{lw,cf}^{\downarrow} - F_{lw,all}^{\downarrow}\right). \quad (6)$$

The ~~solar shortwave~~ component of the CRF is given by:

$$\Delta F_{\underline{s}sw} = \left(F_{s,cldsw,all}^{\downarrow} - F_{s,cldsw,all}^{\uparrow}\right) - \left(F_{s,cfsw,cf}^{\downarrow} - F_{s,cfsw,cf}^{\uparrow}\right). \quad (7)$$

~~As the observations aim to quantify the local CRF, the local~~ The surface albedo α as a ratio of ~~F_s^{\uparrow} and F_s^{\downarrow}~~ F_{sw}^{\uparrow} and F_{sw}^{\downarrow}

10 measured during low-level flights is introduced into Eq. 7, which leads to \div

$$\Delta F_s = \left(F_{s,cld}^{\downarrow} - \alpha \cdot F_{s,cld}^{\downarrow}\right) - \left(F_{s,cf}^{\downarrow} - \alpha \cdot F_{s,cf}^{\downarrow}\right).$$

~~The three essential components for the radiative transfer, and thus, for the derivation of the solar CRF are the profiles of atmospheric thermodynamic parameters (pressure, temperature, humidity), the downward solar~~ the instantaneous shortwave CRF definition:

$$15 \Delta F_{sw} = \left(F_{sw,all}^{\downarrow} - \alpha \cdot F_{sw,all}^{\downarrow}\right) - \left(F_{sw,cf}^{\downarrow} - \alpha \cdot F_{sw,cf}^{\downarrow}\right). \quad (8)$$

~~The downward shortwave irradiance at the surface in cloud-free conditions ($F_{s,cf}^{\downarrow}$) as well as the surface albedo α in the unobserved cloud-free conditions. The $F_{s,cf}^{\downarrow}$ is modulated by the atmospheric profile parameters~~ modulate the downward radiation, reaching the surface in cloud-free conditions. Additionally, the surface albedo controls the ~~,~~ but also by the surface albedo. For highly reflective surface types like snow the upward irradiance is significantly higher compared to over mostly

20 absorbing surfaces like ocean water. A part of this upward irradiance is scattered back towards the surface (often referred to as multiple scattering), and thus, contributes to the downward irradiance. Consequently the multiple scattering between surface and atmosphere ~~enhancing the downward irradiance reaching the ground over highly reflective surface types such as snow and sea ice as compared to mostly absorbing surface like~~ causes an increase of downward irradiance over snow and ice compared to open ocean. Photons reflected from a bright surfaces like an ice flow might scatter back to the surface

25 increasing the downward radiation over dark areas like surrounding ocean water. ~~The MIZ is~~ For airborne observations in the MIZ, characterized by strong variability in surface albedo due to the variable sea ice cover. ~~For airborne observations close to the MIZ,~~ as well as ground based measurements in heterogeneous terrain, ~~this, often referred to as,~~ horizontal photon transport due to multiple scattering from the surrounding area to the actual point of observation is not negligible for the estimate of F_s^{\downarrow}

~~(Ricchiuzzi and Gautier, 1998; Kreuter et al., 2014). F_{sw}^{\downarrow} (Ricchiuzzi and Gautier, 1998; Kreuter et al., 2014).~~

30 To address this problem, the downward irradiance for the cloud-free conditions ~~and in regions with~~ heterogeneous surface

albedo fields needs to be simulated with an areal averaged albedo α_{ar} , also called effective albedo (Weihs et al., 2001; Wendisch et al., 2004). For example, a local surface albedo over a small lead embedded in homogeneous sea ice is not representative for the areal average surface albedo, determining the scattering processes in cloud-free conditions. To illustrate this approach, we modify Eq. 8 to:

$$5 \quad \Delta F_{\underline{s}sw} = \left(F_{\underline{s},\underline{c}ldsw,\underline{a}ll}^{\downarrow} - \alpha \cdot F_{\underline{s},\underline{c}ldsw,\underline{a}ll}^{\downarrow} \right) - \left(F_{\underline{s},\underline{c}fsw,\underline{c}f}^{\downarrow} \Big|_{\alpha_{ar}} - \alpha \cdot F_{\underline{s},\underline{c}fsw,\underline{c}f}^{\downarrow} \Big|_{\alpha_{ar}} \right), \quad (9)$$

where $F_{\underline{s},\underline{c}f}^{\downarrow} \Big|_{\alpha_{ar}}$ represents the downward solar shortwave irradiance at the surface simulated with the areal average albedo in cloud-free conditions.

Besides affecting the F_s^{\downarrow} , the local F_{sw}^{\downarrow} , the surface albedo α in Eq. 9 changes for different illumination situations-conditions (cloudy, cloud-free) and cloud optical thickness Warren (1982). Thus, to complete the formulation of the solar-CRF shortwave
 10 CRF used in this study, the local surface albedo has to be separated in a cloudy albedo (α_{cld}) and an albedo representing-
which continuously represents the cloud-free state α_{cf} . As a result Eq. 9 reads:

$$\Delta F_{\underline{s}sw} = \left(F_{\underline{s},\underline{c}ldsw,\underline{a}ll}^{\downarrow} - \alpha_{\underline{c}ld} \cdot F_{\underline{s},\underline{c}ldsw,\underline{a}ll}^{\downarrow} \right) - \left(F_{\underline{s},\underline{c}fsw,\underline{c}f}^{\downarrow} \Big|_{\alpha_{ar}} - \alpha_{\underline{c}f} \cdot F_{\underline{s},\underline{c}fsw,\underline{c}f}^{\downarrow} \Big|_{\alpha_{ar}} \right). \quad (10)$$

In the following sections, these three-two key components (thermodynamic state (section 3.3), $F_{\underline{s},\underline{c}f}^{\downarrow} \Big|_{\alpha_{ar}}$ (section the impact of
horizontal photon transport $F_{sw,\underline{c}f}^{\downarrow} \Big|_{\alpha_{ar}}$ (section 3.4) and the impact of clouds on α_{cf} of the CRF estimate (section 3.5)) of the
 15 CRF estimate are analysed using synthetic radiative transfer simulations and illustrative ALOUD observations, in order to quantify their separate impact on the CRF in the Arctic.

3.3 Impact of local thermodynamic atmospheric state

In the MIZ, the thermodynamic state of the atmosphere changes within short distances due to the influence of the surface on the air mass (warm air moving north over cold sea ice, cold air moving south over warm open ocean) (Lampert et al., 2012). In
 20 this case, differences in the collocation of airborne in-situ measurements of atmospheric profiles and low-level flights might be significant and effect the radiative transfer simulations, and thus, the local-CRF estimate. Exemplarily (e.g., Lampert et al., 2012).
As was shown by Tjernström et al. (2015, 2019) such events might significantly impact the local energy budget along the trajectory. As an example of temperature profiles being influence by large scale processes, the spatial variability of air temperature profiles measured on 2 June 2017 by the aircraft instruments (Polar 6) and dropsondes is illustrated in Fig. 2a. The
 25 synoptical situation during this flight (west of Svalbard) was characterized by warm air advection with optically thick clouds moving from the open ocean over the MIZ. The consecutive in situ profiles illustrate the changes in inversion height along the flight leg, which changed from roughly 800 m over the ocean to 250 m over the sea ice within 50 to 100 km. The relative humidity (not shown here) changed accordingly.

For all the shown profiles, radiative transfer simulations have been run to calculate $F_{\underline{s},\underline{c}f}^{\downarrow}$ and $F_{\underline{t},\underline{c}f}^{\downarrow}$ are performed to calculate
 30 $F_{\underline{s}w,\underline{c}f}^{\downarrow}$ and $F_{\underline{i}w,\underline{c}f}^{\downarrow}$ for the cloud-free reference case. The surface albedo and SZA were fixed-is fixed for this sensitivity study

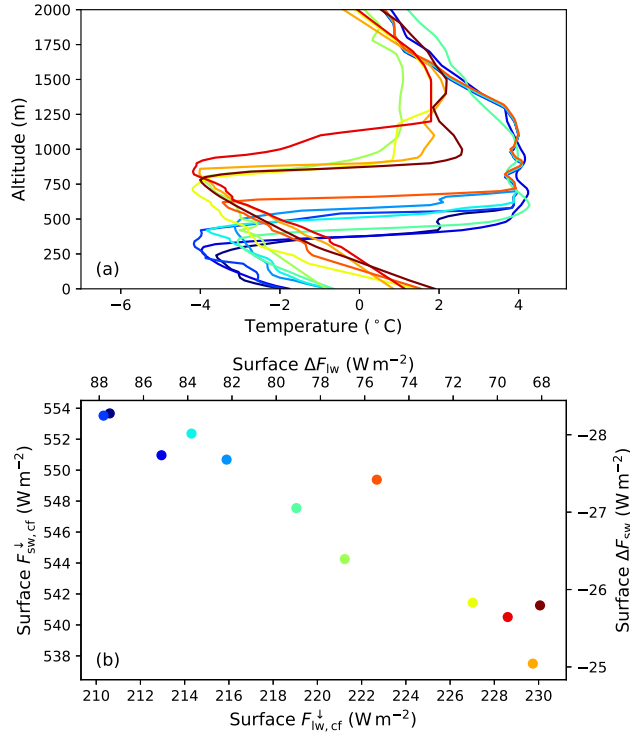


Figure 2. (a) Temperature profiles observed during the warm air intrusion on 2 June 2017. The profiles are obtained from dropsonde and in situ measurements (merged with radiosoundings) and are color-coded by the air temperature in the lowest 200 m. (b) Correlation between simulated cloud-free $F_s^{\downarrow}-F_{sw}^{\downarrow}$ and $F_t^{\downarrow}-F_{lw}^{\downarrow}$ assuming the observed atmospheric profiles from (a) (same color code). The second x and y axis estimates shows the expected terrestrial longwave/solar shortwave CRF at the surface by assuming a constant $F_{s,cld}^{\downarrow}-F_{sw,all}^{\downarrow}$ (412 W m⁻²) and $F_{t,cld}^{\downarrow}-F_{lw,all}^{\downarrow}$ (298 W m⁻²) based on observations. For a better comparability, the simulations the surface albedo and the SZA was fixed in the simulations to 0.8 and the SZA to 60°, respectively.

to 0.8 and 60° ,respectively respectively, similar to the observed conditions over sea ice during that flight, in order to avoid any effects induced by changing SZA or surface albedo. Fig. 2b shows the simulated downward irradiance and corresponding values of the solar and terrestrial shortwave and longwave CRF. While terrestrial longwave irradiance increases with increasing humidity and temperature (enhanced emission), the solar shortwave irradiance decreases (enhanced scattering and absorption).

- 5 The CRF for each case is estimated using the average observed $F_{s,cld}^{\downarrow}$ and $F_{t,cld}^{\downarrow}$ $F_{sw,all}^{\downarrow}$ and $F_{lw,all}^{\downarrow}$ during the low-level section on 2 June 2017. The results show a strong variability in ΔF induced by changes in the thermodynamic structure. The relative deviations range up to 29 % for the terrestrial longwave and 11 % for the solar shortwave CRF, which highlights that neglecting changes of the atmospheric thermodynamic state within a few kilometers can cause significant errors in the retrieved CRF. Especially for air mass transformation like warm air intrusions and cold air outbreaks in the Arctic (Pithan et al., 2018), this is
- 10 a relevant issue, and requires a precise representation of air mass transformations by models or local in situ observations along

the trajectory.

Time series (covered distance) of measured broadband surface albedo (black) (a) and simulated $F_{s,cf}^{\downarrow}$ (b) along the low-level flight track during the 23 May 2017. The red line in (a) shows the areal averaged albedo using the kernel embedded in (b). (b) The gray area shows the potential variability of $F_{s,cf}^{\downarrow}$ due to surface albedo changes. The black and red scatter shows the $F_{s,cf}^{\downarrow}|_{\alpha}$ and $F_{s,cf}^{\downarrow}|_{\alpha_{ar}}$ respectively. (c) Difference in solar CRF estimate between $\Delta F_s(\alpha_{ar})$ and $\Delta F_s(\alpha)$. Another aspect regarding the thermodynamic state of the atmosphere is the impact of the average aircraft flight altitude (here 80 m) on the estimate of CRF. The $F_{t,cf}^{\downarrow}$ $F_{lw,cf}^{\downarrow}$ is simulated for local flight altitude and not exactly for the surface. Due to the fact that the vertical gradient dF_t^{\downarrow}/dz dF_{lw}^{\downarrow}/dz and dF_{lw}^{\uparrow}/dz below clouds remains almost the same in the cloudy and cloud-free state with or without a cloud in the radiative transfer simulations (for atmospheric profiles as observed during ALOUD), the observed CRF in flight altitude can be safely related to surface CRF values causing uncertainties below $\pm 5 \text{ W m}^{-2}$. For an interpretation of single terrestrial irradiance directions (longwave irradiance directions and a comparison to surface observations (both not shown in this study) and a comparison to surface observations, changes due to prevailing near-surface temperature profile have to be expected.

3.4 Impact of areal versus local surface albedo

In Fig. 1 the variability of the observed sea ice fraction I_f can directly be related to the heterogeneous variability in the surface albedo distributions in the MIZ and will influence the observed field of downward shortwave irradiance. For the observations carried out on 23 May 2017, the measured broadband surface albedo along the flight track is shown in Fig. 3a. The low-level section started in the MIZ over large ice floes and small leads and ended over the open ocean in vicinity of the ice edge with occasionally scattered sea ice floe fields. Leads with the size of a few tens of meters up to a few kilometers caused a highly variable local surface albedo.

In Fig. 3b the simulated $F_{s,cf}^{\downarrow}$ $F_{sw,cf}^{\downarrow}$ using the observed 20 Hz surface albedo illustrates the problem of albedo heterogeneity. Without an appropriate smoothing the simulated $F_{s,cf}^{\downarrow}$ would change problems related with strong albedo fluctuations. The simulated $F_{sw,cf}^{\downarrow}$ changes on small horizontal scale scales by up to 35 W m^{-2} (SZA average: 59.2°) within the range of $F_{s,cf}^{\downarrow}$ influenced by multiple scattering. However, due to horizontal photon transport from surrounding ice fields, in reality the changes in $F_{sw,cf}^{\downarrow}$ are less pronounced. The quantitative impact of multiple scattering on $F_{sw,cf}^{\downarrow}$ is indicated by the gray shaded area in Fig. 3b with a maximum contribution of almost 40 W m^{-2} (relative to open ocean). Therefore, the downward irradiance for the cloud-free conditions, required for Eq. 10, needs to be simulated with an appropriate areal averaged albedo representing the multiple scattering contribution from the surrounding albedo fields.

For the low-level flights during ALOUD a moving average filter using a kernel with the shape similar to a Laplace distribution was applied to estimate the areal averaged surface albedo. The filter shape and width was estimated by To estimate a required filter shape and width to obtain an areal averaged albedo, 3D radiative transfer simulations of a typical scenario are performed (not shown here), where leads of different sizes are embedded in homogeneous sea ice (not shown here) similar to the study from Podgorny et al. (2018). The simulated irradiance of the 3D model output over the heterogeneous surface albedo field was in the vicinity of the leads is reproduced by 1D simulations by applying the filter embedded in Fig. 3b to the albedo field

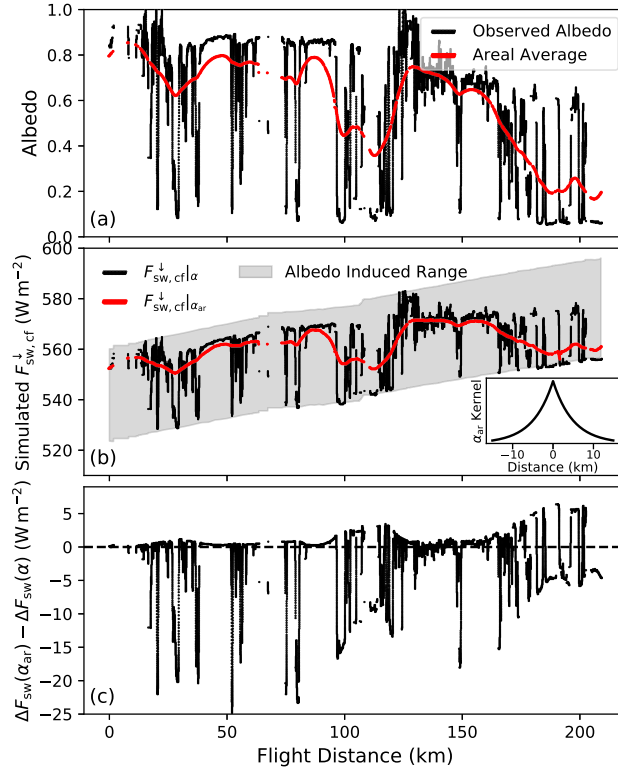


Figure 3. Time series (covered distance) of measured broadband surface albedo (black) (a) and simulated $F_{sw,cf}^{\downarrow}$ (b) along the low-level flight track during the 23 May 2017. The red line in (a) shows the areal averaged albedo using the kernel embedded in (b). (b) The gray area shows the potential variability of $F_{sw,cf}^{\downarrow}$ due to surface albedo changes. The black and red scatter shows the $F_{sw,cf}^{\downarrow}|_{\alpha}$ and $F_{sw,cf}^{\downarrow}|_{\alpha_{ar}}$ respectively. (c) Difference in shortwave CRF estimate between $\Delta F_{sw}(\alpha_{ar})$ and $\Delta F_{sw}(\alpha)$.

and theoretically observed albedo and by using the obtained effective areal averaged albedo for the 1D model simulations to continuously estimate the $F_{sw,cf}^{\downarrow}$. The appropriate weighting of near-field and far-field albedo is applied by kernel k defined by a Laplace-distribution:

$$k(x, \mu, \gamma) = \frac{1}{2\gamma} \left(-\frac{|x - \mu|}{\gamma} \right), \quad (11)$$

- 5 with γ of 5 km, the median μ and a scale x of 30 km. This rather large filter width indicates that small leads of up to below 1 km embedded in homogeneous sea ice show a minor impact. Applying the moving average kernel to the observed local albedo results in the on F_{sw}^{\downarrow} in cloud-free conditions.

The resulting areal averaged albedo is shown in Fig. 3a and the simulated $\Delta F_s(\alpha_{ar})$, together with the simulated $F_{sw,cf}^{\downarrow}|_{\alpha_{ar}}$ (Fig. 3b), which follows the large scale trends of surface albedo but mitigates small scale fluctuations. Neglecting these effects would result in uncertainties of the local solar shortwave CRF estimate, as shown in Fig. 3c. On average, the effect for flight

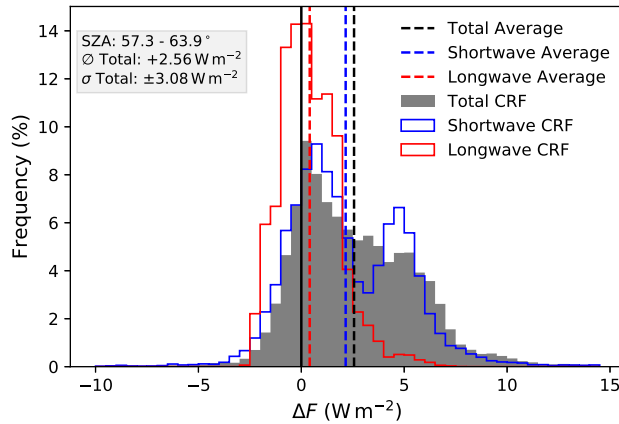


Figure 4. Histogram of solar shortwave, terrestrial longwave and total ΔF derived during the cloud-free ACLOUD flight on 25 June 2017. Statistics are given in the gray box (mean \emptyset , standard deviation σ).

section in Fig. 3 is of minor importance (average $-2.1.9 \text{ W m}^{-2}$), because under- and overestimation of solar shortwave CRF cancel in this specific example, similar to results from Benner et al. (2001). Nevertheless, on a local scale the difference between the two approaches it should be highlighted that due to horizontal photon transport the $F_{sw,ef}^{\downarrow}|_{\alpha_{ar}}$ is up to 28 W m^{-2} larger above leads compared to the $F_{sw,ef}^{\downarrow}|_{\alpha}$. The difference in the derived CRF reaches values between -22.25 W m^{-2} over open water in the vicinity of ice floes embedded in homogeneous sea ice, where the $F_{s,cf}^{\downarrow}$ would be $F_{sw,cf}^{\downarrow}$ is underestimated by applying the local albedo, and $+6 \text{ W m}^{-2}$ in above scattered ice floe fields in the ocean with an overestimation of $F_{s,cf}^{\downarrow} F_{sw,ef}^{\downarrow}$. Hence, the uncertainties and potential noise is limited, which artificial fluctuations in CRF are limited by applying the smoothed albedo in the $F_{sw,cf}^{\downarrow}$ simulations. This enables a more reliable estimate of the CRF in the MIZ heterogeneous MIZ and over the specific surface types, taking into account that the complexity of surface albedo fields in the MIZ can only be insufficiently represented by this simplified approach to estimate the areal averaged albedo.

3.4.1 Uncertainty estimate in cloud-free conditions

During ACLOUD a flight in cloud-free conditions on 25 June 2017 was can be used for a comparison between measured and simulated irradiances to estimate the accuracy of this dataset. The difference between observed and simulated F_{cf}^{\downarrow} for the low level flights of both aircraft (2.1 hours of data) was -6.5 is 5.7 ± 7.3 7.1 W m^{-2} (-21.1%) in the solar shortwave and $0.41 \pm 1.45 \text{ W m}^{-2}$ (0.2%) in the terrestrial longwave irradiance. The histograms of the CRF for that day are shown in Fig. 4. The mean values of the entire flight section was -2.45 is 2.15 W m^{-2} in the solar shortwave and 0.41 W m^{-2} in the terrestrial longwave. The slightly positive CRF might be caused by the upper air sounding approximately 300 km in the south of the flight track or the aerosol conditions (aerosol optical thickness was set to zero in the simulation). Additionally to measurement uncertainties, In addition to the measurement uncertainties of the used broadband radiometer ($<3\%$, (Ehrlich et al., 2019b)),

the radiative transfer modelling can induce a bias ~~in the solar (<2%) in the shortwave~~ wavelength ranges (Randles et al., 2013). Due to the absence of cloud-free conditions during other low-level flights of the ACLOUD campaign this comparison can be considered as a rough estimate of potential uncertainties during the whole ACLOUD campaign.

3.5 Impact of clouds on the surface albedo

5 The effect of clouds on the broadband surface albedo, implemented in Eq. 10, is analysed by a set of spectral albedos of three sea ice types common in the Arctic for different seasons. Different snow packs with a density of 300 kg m^{-2} are specified with various values of snow geometric thickness and specific surface area (SSA), ~~a measure of snow grain size~~ (Gardner and Sharp, 2010), and located above a layer representing bare sea ice with a wavelength constant broadband albedo of 0.5. Fresh cold and dry snow (SSA = $80 \text{ m}^2 \text{ kg}^{-1}$, 20 cm thick) represents early to late spring conditions, melting snow
10 (SSA = $5 \text{ m}^2 \text{ kg}^{-1}$, 20 cm thick) the melting season in late spring early summer, and thin melting snow/white ice (SSA = $5 \text{ m}^2 \text{ kg}^{-1}$, 1 cm thick) summer conditions, before the melt pond formation. The spectral albedo for each type ~~was is~~ simulated with the TARTES model for 65° SZA; the respective results are shown in Fig. 5 (solid lines) together with simulated downward irradiances from the atmospheric radiative transfer simulations using libRadtran (shaded spectra).

The general impact of snow properties on the spectral albedo is characterized by stronger absorption at longer wavelengths with
15 decreasing SSA (increasing effective grain size) and can be seen by comparing the albedo of fresh and melting snow in Fig. 5. A decreasing SSA amplifies the contrast between shorter and longer wavelength. A thinning of the snow layer or impurities in snow enhance the absorption mainly in the shorter visible wavelength range, as illustrated by the albedo of melting snow in comparison to that of white ice.

~~Broadband albedo integrated from simulated up- and downward spectral irradiance as a function of cloud LWP using the color-related spectral albedos of Fig 5. The approximate area of direct dominated/ cloud free radiation is indicated by the gray shading (SZA of 65°). The horizontal line indicates the cloud free albedo as a reference.~~ Two processes influencing the broadband snow albedo are related to the transition from cloud-free to cloudy atmospheric conditions. In an overcast atmosphere with clouds of sufficient optical thickness, mainly diffuse radiation illuminates the surface as compared to cloud-free conditions, when the direct ~~solar shortwave~~ radiation dominates. In the Arctic, large values of SZA ($> 50^\circ$) are common.
25 In overcast conditions, scattering processes in clouds decrease the averaged incoming (effective) angle of the mainly diffuse irradiance to approximately 50° above snow (Warren, 1982). With decreasing effective SZA, the penetration depths of photons into the snow and ice surface increases, enhancing the probability of absorption, and thus decrease the overall broadband surface albedo (Warren, 1982). In Fig. 5 this effect is illustrated by the attenuated lines representing the respective diffuse albedo values. Compared to the surface albedo ~~of fresh snow~~ in cloud-free atmospheric conditions ~~of fresh snow (black line)~~
30 the change of effective SZA (in this example from 65° to approximately 50° SZA) causes a lower spectral surface albedo ; ~~especially (attenuated black line)~~ in the non-visible wavelength range, while the highly reflective visible wavelengths are not affected. ~~The downward solar irradiance spectra, exemplarily shown for cloudy conditions with LWP of 80 (gray). Thus, for this surface type only a small impact on the actual broadband albedo can be expected, because for the majority of the related downward shortwave irradiance (e.g. grey shaded area in Fig. 5) ; indicate that the main part of F_s^\downarrow (shorter wavelengths) is not~~

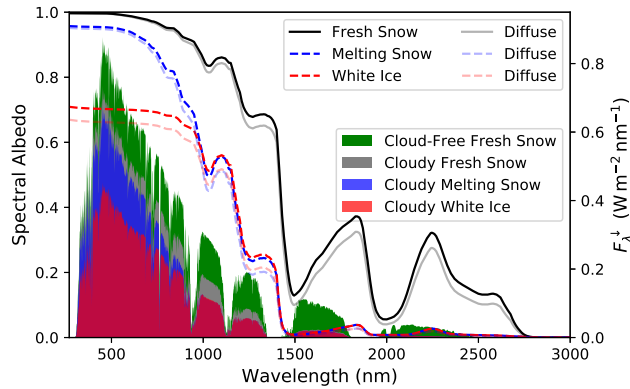


Figure 5. Spectral Simulated spectral snow albedo of three seasonal sea ice types for different SSA and snow thickness above sea ice with spectrally neutral albedo of 0.5. Non-attenuated Non-attenuated lines show the albedo of the cloud-free situations (SZA of 65°), attenuated lines the albedo for overcast conditions. The downward irradiance (right y-axis) simulated for these cases are exemplary shown by the shaded areas. Green shows the cloud-free spectra over fresh snow, gray, blue and red under cloudy conditions (LWP of 80 g m^{-2}) for the surface albedo related by the colors.

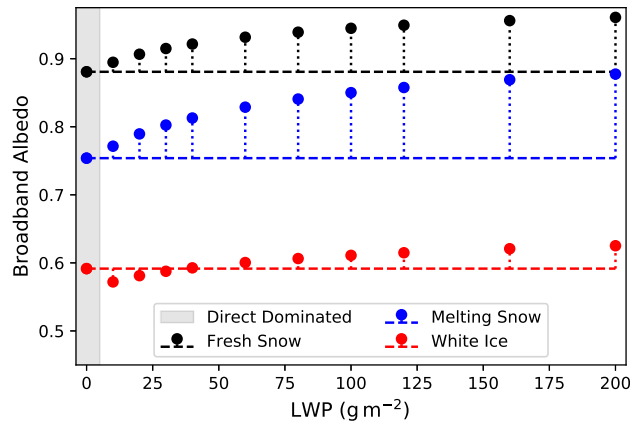


Figure 6. Broadband albedo integrated from simulated up- and downward spectral irradiance as a function of cloud LWP using the color-related spectral albedos of Fig 5. The approximate area of direct dominated/ cloud free radiation is indicated by the gray shading (SZA of 65°). The horizontal line indicates the cloud-free albedo as a reference.

affected by this change and a weak impact on the broadband albedo is expected for fresh snow. For albedo values the albedo remains high. However, for surface types with a spectral albedo characterized by stronger absorption in the visible wavelength range (albedo of white ice, red line in Fig. 5), a stronger change also stronger changes between direct-dominated and diffuse broadband albedo is expected are expected (attenuated red line).

- Besides the changing effective SZA, clouds reduce the incident irradiance by attenuating especially in the near-infrared wave-

length range (Grenfell and Perovich, 2008), which can be seen in Fig. 5 by comparing the green and gray shaded spectrum representing cloud-free, cloudy conditions with a liquid water path (LWP) of 80 g m^{-2} , respectively. With increasing cloud optical thickness the spectral slope of downward irradiance is imprinted in the surface spectra, which can be seen in Fig. 5 by comparing the green shaded (cloud-free) and the gray shaded (cloudy) spectrum. The As the spectral albedo of ice and snow is higher for short wavelengths resulting in a increasing wavelength-integrated shorter wavelengths (e.g. black line in Fig. 5) and the downward irradiance spectra is shifted to shorter wavelength, the wavelength integrated (broadband) surface albedo with increasing cloud optical thickness albedo will increase. This effect becomes the stronger the more pronounced the slope between visible and near-infrared wavelength becomes, which can be induced by two processes: either stronger absorption by clouds due to a higher LWP, or by spectral changes in the albedo. With decreasing SSA, the underlying surface albedo with decreasing near-infrared albedo. The latter is controlled by decreasing SSA (transition from fresh to melting snow, more radiation is absorbed in the), resulting reduced near-infrared reflection of the surface (compare black and blue lines in Fig. 5), which affects F_s^\downarrow (indirectly affects F_{sw}^\downarrow by reduced multiple scattering between surface and clouds in this wavelength range (compare grey and blue shaded spectra). For However, for the spectral albedo of white ice (red shaded area line) the slope in the spectra F_{sw}^\downarrow spectra (red shaded) is less pronounced, and a weaker increase of broadband albedo is expected for increasing LWP.

For all three surface albedo types shown in Fig. 5, the effect of clouds on the broadband surface albedo (as a function of LWP) on the broadband surface albedo, is presented in Fig. 6 for a SZA of 65° . An effective cloud droplet radius (r_{eff}) of $8 \mu\text{m}$ is used. The gray area indicates the direct-dominated radiation in cloud-free conditions; dashed lines represent the cloud-free albedo value as a reference.

For the different surface types a significant change of up to 12% relative to the individual cloud-free values of albedo can be found with increasing cloud optical thickness, which is modulated by the interaction of surface and cloud radiative properties. In general, the lower the ratio of spectral albedo between shorter and longer wavelengths, the stronger is the increase of broadband albedo with increasing LWP, exemplary as shown for the black and blue scatter in Fig. 6 representing fresh and melting snow, respectively. Spectral absorption of the surface in shorter wavelengths strongly decreases the broadband albedo, but it will also alter the behaviour with increasing LWP (Fig. 6, red). For low LWP values, the broadband albedo is lower compared to cloud-free conditions due to a significant lower spectral diffuse albedo (dashed and attenuated dashed red in Fig. 5) at shorter wavelengths. However, with increasing LWP the weighting effect in transmitted F_s^\downarrow F_{sw}^\downarrow to shorter wavelength compensates/dominates and, as a consequence, it increases the broadband surface albedo compared to cloud-free conditions.

3.5.1 Albedo-cloud Surface albedo-cloud interaction and CRF

In calculations of the instantaneous CRF based on measurements radiative transfer, the observed surface albedo below clouds commonly serves as a reference for the simulations of $F_{s,cf}^\downarrow - F_{\text{net},cf}$ and calculation of $\Delta F_s \Delta F_{sw}$. Also weather and climate models, where the change of the broadband albedo with increasing LWP are notis not, or only poorly, parameterized, may have a bias in the estimated CRF as well as in the $F_{\text{net},cf}$ in cloudy conditions. To estimate the significance of this effect the surface albedo-cloud interaction, radiative transfer simulations have been are used to calculate the solar shortwave CRF, ei-

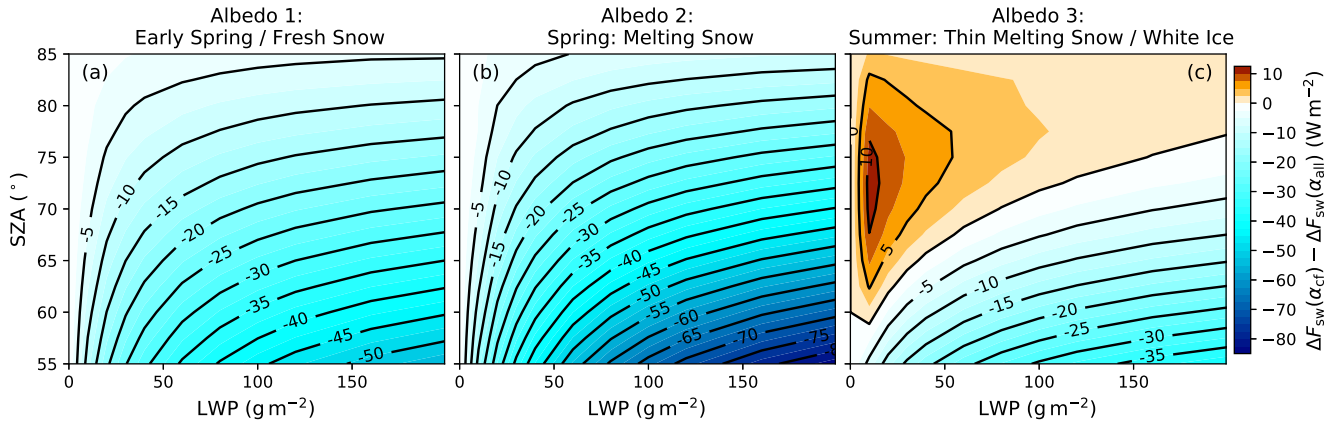


Figure 7. Bias of the solar-shortwave CRF ($\Delta F_s(\alpha_{cf}) - \Delta F_s(\alpha_{cid})$, $\Delta F_{sw}(\alpha_{cf}) - \Delta F_{sw}(\alpha_{all})$) caused by neglecting the change between observed cloudy and cloud-free surface albedo as a function of cloud LWP and SZA. The three albedo types from Fig. 5 have been assumed, (a) fresh snow representative for early spring, (b) melting snow during late spring, and (c) thin melting snow/white ice found in early summer.

ther assuming the correct cloud-free albedo or the wrong cloudy albedo as a reference, or the prevailing cloudy albedo, as shown in Fig 6. The difference $\Delta F_s(\alpha_{cf}) - \Delta F_s(\alpha_{cid})$ between both runs in CRF $\Delta F_{sw}(\alpha_{cf}) - \Delta F_{sw}(\alpha_{all})$ between both approaches, and thus, an underestimate of the solar-shortwave cooling effect if the cloudy albedo is used, are is shown in Fig. 7 as a function of SZA and LWP ($r_{eff} = 8 \mu m$). Negative (bluish) values indicate a stronger solar-shortwave cooling effect for $\Delta F_s(\alpha_{cf})$ $\Delta F_{sw}(\alpha_{cf})$. The simulations have been are performed for all three sea ice types in Fig. 5 and changes in direct/diffuse radiation due to SZA have been are taken into account.

In case of snow surfaces, influenced by the SSA (Fig. 7a and b), the cooling effect of clouds on the surface is underestimated (blue colors), if the cloudy albedo is used to derive the solar-shortwave CRF. In general, the lower the SZA and the higher the LWP, the stronger the underestimation of the cooling effect becomes. Additionally Furthermore, the coarser the snow grains (melting snow) the stronger the underestimation. In contrast, during summer and for thin melting snow or white ice (Fig. 7c), the cooling effect is overestimated for low sun and optically thin clouds, if the apparent cloudy albedo is used for ΔF_s ΔF_{sw} , and shifts towards the underestimation for optically thick clouds and/or lower SZA.

The values of under-underestimation/overestimation indicate that the surface albedo-cloud interaction might significantly impact the estimate of solar-CRF-shortwave CRF and the obtained values from the different approaches in the available CRF studies in the Arctic. Especially for clouds over snow, the cooling effect of clouds is considerably larger. Due to the dependence of on specific spectral surface albedo shape types, a seasonal dependence of this surface albedo-cloud interaction, and thus, the solar-shortwave CRF, is indicated.

In Fig. 8 a hypothetical scheme of the modified seasonal cycle of CRF due to the surface albedo-cloud interaction, is proposed. The time series of surface albedo as observed during the SHEBA-campaign is shown Surface Heat Budget of the Arctic Ocean (SHEBA) campaign (Uttal et al., 2002) is shown, to illustrate the seasonal transition as reported by Perovich et al. (2002),

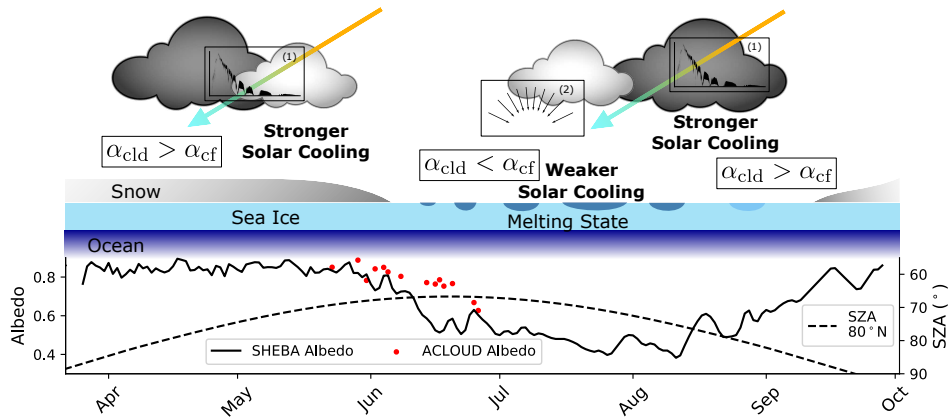


Figure 8. Hypothetical scheme of the seasonal cycle of surface albedo-cloud interaction related modification of solar shortwave CRF. Dominant processes influencing the transition from cloudy (cld) to cloud-free surface albedo in the specific season are represented by the icons (1-) (weighting of downward irradiance to shorter wavelength with increasing LWP) and (2-) (transition from direct to diffuse radiative transfer). The seasonal cycle of surface broadband albedo is shown by SHEBA observations (200 m albedo line). Averaged ACLLOUD observations for homogeneous sea ice ($I_f > 95\%$) are shown in red scatter points. Computed daily averaged SZA for 80° N in dashed black.

together with a daily averaged SZA for 80° N. During spring, early summer and autumn surface albedo values related to snow on sea ice are found. The results from Fig. 7 indicate that the shift of transmitted irradiance towards shorter wavelength (process 1 in Fig. 8) is dominant in these situations and clouds induce a stronger cooling effect on the surface. With the beginning of the melting season, the change between diffuse and direct albedo will dominate (process 2) for optical thin clouds and high SZA, potentially reducing the cooling effect on the surface in dependence of the conditions. In this period the onset of melting (rapidly decreasing albedo), the melt pond fraction, and the SZA (dashed black line in Fig. 8) together with the cloud optical thickness would critically influences the sign of this modification. However, as was reported by Walsh and Chapman (1998), for regions where even in summer snow or bare sea ice is found, all year long a lower albedo in cloud-free conditions, and thus, a stronger cooling effects of clouds can be expected. Though, conclusions about the annual averaged shortwave CRF influence by surface albedo-cloud interactions are not yet possible, as coupled surface-atmosphere radiative transfer models capable of representing surface types like melt ponds are required to study the full seasonal cycle. Also for climate models with simple albedo parameterizations, the results from Fig. 7 can be interpreted as a potential bias in the shortwave F_{net} and CRF depending on the cloud optical thickness.

For the ACLLOUD campaign, snow on ice was the dominant surface type (Jäkel et al., 2019), which explains the slightly later decrease in surface albedo (Fig. 8, red lines scatter points) compared to SHEBA data (black) and represents the transition from cold and fresh snow to melting snow. Transferred to the results from Fig. 7 a stronger cooling effect of the clouds should be expected during ACLLOUD. Though, conclusions about the yearly impact on the estimate of solar forcing are not yet possible, as coupled surface-atmosphere radiative transfer models capable of representing surface types like melt ponds are required to study the full seasonal cycle of solar CRF influence by surface albedo-cloud interactions.

4 Cloud radiative forcing during ACLOUD

The problems of calculating the CRF, as discussed in sections 3.3, 3.4 and 3.5 are considered in the data processing of the ACLOUD measurements. Therefore, the closest available atmospheric profile ~~was~~ is applied in the radiative transfer simulations as well as the areal averaged surface albedo, required for the simulations of ~~$F_{s,cf}^{\downarrow}$~~ , ~~has been~~ ~~$F_{sw,cf}^{\downarrow}$~~ are calculated for the
5 low-level flights. The final step is to continuously retrieve the local surface albedo under cloud-free atmospheric conditions from the observed cloudy-sky albedo, in order to obtain a more realistic estimate of the CRF.

4.1 Retrieving the cloud-free albedo from cloudy-sky observations

To obtain an estimate of the cloud-free albedo, the broadband albedo parameterization developed by Gardner and Sharp (2010) for snow and ice surfaces ~~was~~ is applied. Gardner and Sharp (2010) considered the dependence of broadband albedo with
10 respect to SZA, SSA, concentration of absorbing carbon, as well as the cloud optical thickness. The parameterization is valid for homogeneous snow and ice including a cloud optical thickness below 30 (LWP of 133 g m^{-2} ~~for an effective cloud droplet radius~~ with $r_{\text{eff}} = 8 \mu\text{m}$). During ACLOUD, the observed albedo ranged between 0.9 for homogeneous sea ice covered with cold snow and values below 0.6 during the ~~melting season~~ later stage of the campaign with the onset of melting (Wendisch et al., 2019; Jäkel et al., 2019). To include these data in the analysis and cover this albedo range only as a function of grain
15 size (SSA), an impurity load of absorbing carbon of 0.1 ppmw ~~was~~ is chosen, which causes a similar spectral behaviour of the albedo as changes in snow thickness. As shown by Jäkel et al. (2019), snow overlaying sea ice was the predominant surface type over closed sea ice during ACLOUD. Nevertheless, the potential variability in the spectral surface albedo with respect to absorption in the short wavelength ranges during the campaign is only roughly covered by this approach and needs to be considered in the interpretation of the obtained cloud-free albedo values.

20 The parameterization is used to generate lookup tables ~~as~~ as a function of observed variables of cloudy-sky albedo, LWP and local SZA. Isolines of SSA are used to extrapolate the cloud-free albedo ($\text{LWP} = 0 \text{ g m}^{-2}$). To apply the albedo parameterization by Gardner and Sharp (2010) the cloud optical thickness or LWP is required. As the cloud properties change on small horizontal scales, a retrieval of LWP based on the airborne measurements of cloud transmissivity was used, which is described in the appendix A.

25 4.1.1 Application to the observations

The dependence of the surface albedo on the cloud LWP is shown in Fig. 9 as measured over homogeneous sea ice (selected $I_f > 98\%$) on 14 June 2017. ~~Additionally~~ In addition, the albedo parameterization by Gardner and Sharp (2010) for the averaged SZA (63.7°) and different values of SSA is shown. During 1.7 hours of low-level flights below clouds, a large area was mapped ($80.7\text{-}81.8^\circ \text{ N}, 9.8\text{-}12.7^\circ \text{ E}$) and a strong variability in optical thickness including occasional openings with direct illumination
30 of the surface and optical thick multilayer clouds was covered. The surface temperatures were close to zero, indicating the beginning melting season (Jäkel et al., 2019). The observed albedo values averaged for 6 g m^{-2} bins (dashed red in Fig. 9) change from 0.7 for low values of LWP to ~~0.83~~ albedo values above 0.8 for a LWP larger than 100 g m^{-2} . While the overall

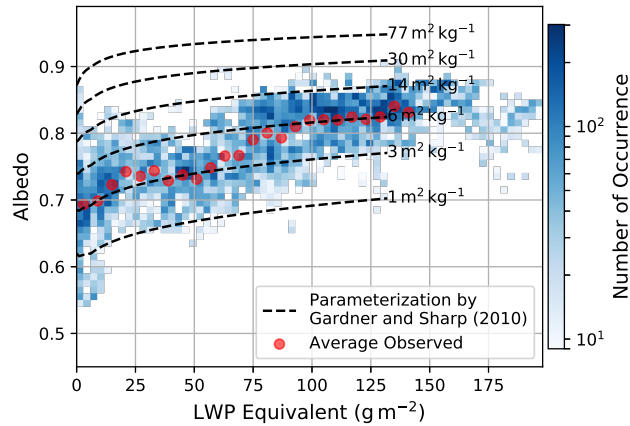


Figure 9. Relation between broadband albedo and retrieved LWP equivalent observed on 14 June 2017 ACLOUD [flight](#) over homogeneous sea ice ($I_f > 98\%$). The broadband albedo parameterization by Gardner and Sharp (2010) is shown for different SSA and the average SZA by [the](#) dashed lines (impurity load of 0.1 ppmw). Averaged observations (6 g m^{-2} bins) are shown in red scatter.

trend of increasing albedo with increasing LWP is represented, the slope follows the parameterization for a SSA between $3 \text{ m}^2 \text{ kg}^{-1}$ ([+](#)) for lower LWP values and $6 \text{ m}^2 \text{ kg}^{-1}$ ([0.5](#)) for higher LWP. This [effect](#) might be related to different observed cloud and surface areas as the distribution includes data from both aircraft.

Extrapolating the observations (pair of variates) of LWP equivalent and surface albedo along isolines of SSA to a LWP of zero gives an estimate of the cloud-free surface albedo. For the example given here, for [an](#) α_{cloud} [a](#) α_{all} of 0.82 and LWP of 100 g m^{-2} a cloud-free albedo of 0.74 would be estimated, and thus, 0.06 lower than the observed one in overcast conditions. [Due to the non-linear increase of \$\alpha_{\text{cloud}}\$ with LWP the potential error induced by uncertainties in the retrieved LWP is larger for lower LWP and additionally depends on the prevailing surface types.](#) For LWP values exceeding the limitation of the parameterization the maximum valid LWP was applied. [Rarely occurring surface albedo values above/below the range of the parameterization from Gardner and Sharp \(2010\) have been filtered out.](#)

A comparison of measured ([overcast](#)) α_{cloud} [all-sky](#) α_{all} and extrapolated cloud-free albedo α_{cf} is shown in Fig. 10a. The frequency distributions are calculated for all low-level flights during ACLOUD over homogeneous sea ice ($I_f > 98\%$). The broad distribution of observed albedo illustrates the seasonal transition of sea ice properties from a cold period end of May 2017 into the melting season in June 2017 (Wendisch et al., 2019; Jäkel et al., 2019). On average, the [overcast albedo](#) [cloudy albedo](#) ($\text{LWP} > 1 \text{ g m}^{-2}$) was about 0.8. The estimated cloud-free albedo gives an average value of 0.74, which is approximately 6% lower than α_{cloud} α_{all} . The distribution of α_{cf} is slightly narrower than [measured the measured one](#) in cloudy conditions, because the majority of cloud-free flight sections [takes took](#) place close to the end of the campaign with low values of surface albedo, and thus, [give gives](#) a lower bound to the distribution.

[The uncertainties in the estimate \$\alpha_{\text{cf}}\$ and the shortwave \$F_{\text{net,cf}}\$ depend mainly on the observed \$\alpha_{\text{all}}\$, as was investigated by applying synthetic albedo and LWP distributions to the lookup tables. Due to the non-linear increase of \$\alpha_{\text{all}}\$ with LWP, the](#)

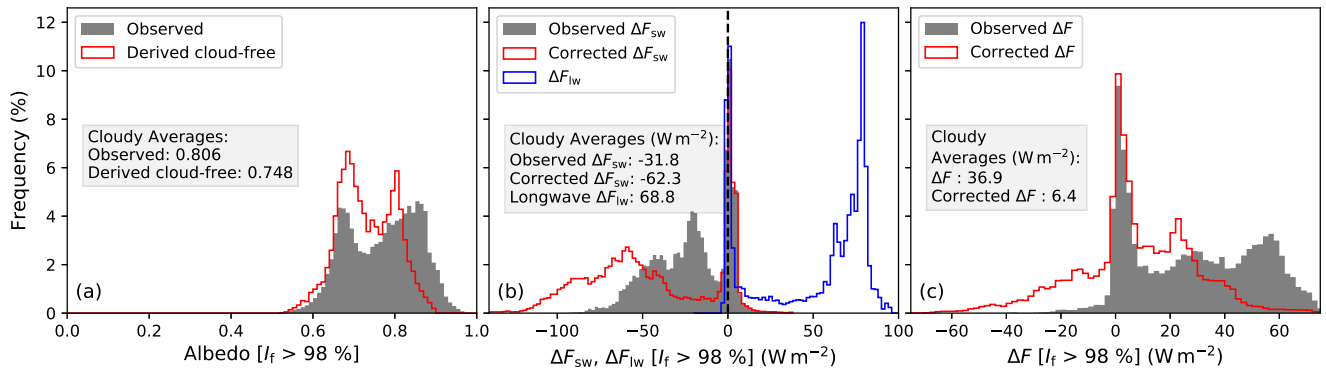


Figure 10. (a) Frequency distribution of the observed (gray) and cloud-free estimated (red) surface albedo for all ACLOUD measurements obtained over homogeneous sea ice ($I_f > 98\%$). (b) Terrestrial (blue) and shortwave CRF using the observed albedo (gray) and the shortwave CRF applying the estimated cloud-free albedo (red). (c) The total (shortwave + longwave) CRF calculated with both albedo estimates are shown in panel (c). Average values for cloudy conditions ($LWP > 1 \text{ g m}^{-2}$) are given in the embedded text boxes of each panel.

potential error induced by uncertainties in the retrieved LWP is larger for lower LWP. Additionally, the effect depends on the prevailing surface types. The overall uncertainty in the cloud-free shortwave net irradiances using the retrieved α_{cf} can be expected to range below 20% above homogeneous high surface albedos, decreasing with decreasing surface albedo.

Fig. 10a shows only measurements conducted over homogeneous sea ice, which was frequently observed during ACLOUD.

- 5 In the MIZ, though, the heterogeneous sea ice and the corresponding reduced surface albedo prevents an application of the original parametrization by Gardner and Sharp (2010). However, making use of the cosine weighted sea ice fraction I_f and its linear relation to the albedo, changes due to the surface albedo-cloud interaction can be scaled to the prevailing I_f by assuming diffuse radiative transfer (Lambertian albedo) ;

$$\alpha(I_f) = (\alpha - \alpha_w) \cdot I_f + \alpha_w,$$

- 10 with $\alpha_w = 0.07$ (average open ocean albedo during ACLOUD). Below an I_f of 10% no correction have been applied because the cloud effect on the surface albedo can be neglected. (not shown in this study).

4.2 Correction of CRF

To illustrate the effect of surface albedo-cloud interactions on the calculation of the CRF during the ACLOUD campaign, the CRF was is computed using both measured cloudy albedo (α_{all}) and the estimated cloud-free albedo (α_{cf}). Fig. 10b shows the frequency distribution of the solar-shortwave CRF for both solutions, observed over homogeneous sea ice ($I_f > 98\%$). The CRF based on the observed albedo (gray bars) shows a bimodal distribution. The mode around 0 W m^{-2} represents cloud-free situations and heterogeneous optically thin clouds, where 3D effects induced occasionally positive solar-shortwave CRF values as reported in Wendisch et al. (2019). The broader mode between -60 W m^{-2} and -20 W m^{-2} characterizes the cloudy mode as a function of the prevailing surface albedo and LWP. Applying the estimated cloud-free albedo (red histogram in Fig. 10a),

shifts the solar shortwave CRF in Fig. 10b of the cloudy mode to more negative values, indicating a stronger cooling effect. The non-linearity in the functional dependence of ~~the solar CRF and surface albedo~~ surface albedo and LWP spreads the frequency distribution of corrected CRF, while the mode for cloud-free conditions is not affected.

In total the ~~solar CRF showed~~ shortwave CRF shows on average a weak cooling effect of ~~-33-32~~ W m^{-2} using the observed albedo values under cloudy conditions ($\text{LWP} > 1 \text{ g m}^{-2}$). Applying the ~~correct~~ surface albedo for cloud-free conditions almost doubles the solar shortwave cooling effect to ~~-63-62~~ W m^{-2} . These values hold for the ACLOUD observations with an average LWP during cloudy conditions over sea ice of 58 g m^{-2} and a SZA of 59.61° . In combination with the distribution of the terrestrial longwave CRF (blue histogram in Fig. 10b), which averages to 69 W m^{-2} in cloudy conditions, the total (solar plus terrestrial shortwave plus longwave) CRF estimate (Fig. 10c) shifts from a significant warming effect of 37 W m^{-2} over sea ice to an in average almost neutral effect (6 W m^{-2}). Also the distribution of the corrected CRF indicates that during the end of the campaign already the cooling effect was dominant (uncorrected mainly positive). Considering that the predominant surface type of the campaign was still sea ice covered by snow, the transition from warming to cooling effect of clouds could already start early in the season, before the formation of melt ponds and the rapid drop in surface albedo, which underlines the potential impact of surface albedo-cloud interactions. ~~(a) Frequency distribution of the observed (gray) and cloud-free estimated (red) surface albedo for all ACLOUD measurements obtained over homogeneous sea ice ($I_t > 98\%$). (b) Terrestrial (blue) and solar CRF using the observed albedo (gray) and the solar CRF applying the estimated cloud-free albedo (red). (c) The total (solar + terrestrial) CRF calculated with both albedo estimates are shown in panel (c). Average values for cloudy conditions ($\text{LWP} > 1$) are given in the embedded text boxes of each panel.~~

5 Conclusions

To estimate the ~~instantaneous~~ warming or cooling effect of clouds on the surface REB in the Arctic from observations or models, a precise knowledge characterization of the cloud-free state is ~~indispensable~~ required. Especially in the transition region between open ocean and closed sea ice (the MIZ), the thermodynamic state of the atmosphere changes on horizontal scales of a few kilometers, which ~~significantly~~ influences the simulated cloud-free radiative field. ~~To obtain reliable information of CRF related to air mass transformations like~~ Also, to obtain reliable estimates of CRF along meridional air mass transports into and out of the Arctic, such as warm air intrusions or cold air outbreaks ~~in the Arctic (Tjernström et al., 2015; Pithan et al., 2018); (Tjernström et al., 2015; Pithan et al., 2018; Tjernström et al., 2019), a high temporal and spatial resolution is required to obtain reliable values of local CRF induced by these large scale processes of thermodynamic profile measurements along the trajectory are required.~~

Variability in sea ice concentration is closely linked with fluctuations in ~~the local~~ surface albedo. The derivation of ~~cloud-free downward irradiance in these condition~~ downward irradiances under cloud-free conditions requires an estimate of the effective areal average surface albedo, determining the multiple scattering on large ~~scales~~ Moving spatial scales. For airborne observations, moving average filters with shapes appropriate of reproducing 3D radiative transfer need to be applied to obtain ~~a reliable local solar CRF~~ values of shortwave CRF adapted to the environment.

The transition between cloudy and ~~cloudy-free~~ cloud-free atmospheric states is accompanied by changes in the radiative transfer, affecting the surface albedo, and ~~thus,~~ the CRF. In the available CRF studies in the Arctic, either observations during cloud-free periods have been used to extrapolate the expected cloud-free surface albedo during cloudy periods, or simply the surface albedo observed in cloudy conditions have been used. As the snow and ice albedo depends on parameters like snow
5 grain size, prevailing SZA, and cloud optical thickness, the available approaches only insufficiently represent the cloud-free albedo in the cloudy Arctic.

Combining spectral snow surface albedo models with atmospheric radiative transfer ~~models~~ simulations enables to quantify the impact of two processes related to spectral surface albedo-cloud interactions. The spectral weighting effect of downward irradiance appears to be dominant for snow surfaces and enhances the cooling effect of clouds ~~on~~ at the surface. For the second
10 process, a change ~~between direct dominated from mainly direct~~ radiation in the cloud-free state ~~and to rather~~ diffuse radiation in the cloudy state, the sign of the modification depends on SZA, cloud optical thickness, and the melting state of sea ice. The changes in shortwave surface albedo with increasing cloud optical thickness are significant and directly impact the shortwave net irradiances, and thus, the estimate of shortwave CRF.

For the ACLOUD campaign, characterized by snow on sea ice in the beginning melting season, the averaged ~~solar~~ shortwave
15 CRF estimate over homogeneous sea ice of ~~-33~~ -32 W m^{-2} (cooling) almost ~~doubled~~ doubles to -62 W m^{-2} , when surface albedo-cloud interactions ~~were~~ are taken into account (~~-63~~). The campaign averaged total CRF ~~was thereby~~ is shifted from a mainly warming effect of clouds over sea ice to an ~~on average~~ almost neutral effect, for the ACLOUD observations with ~~low~~ relatively small SZA. Hence, the observed albedo trend during the campaign (Fig. 8) ~~induced~~ induces a transition in CRF from a warming to a cooling already for snow covered surface types, and thus, earlier in the season ~~as reported during~~
20 SHEBA. In addition, the instantaneous longwave CRF approach might additionally induce an overestimate of the warming effect potentially shifting the total CRF further to cooling. This indicates a ~~potential prolongation possible extension~~ of the period in which clouds ~~are expected to have a cooling effect on~~ cool the surface and highlights the impact of surface albedo-cloud interactions and a required reassessment of the CRF in the Arctic.

Long-term measurements, such as those performed during the SHEBA campaign or ~~planned~~ currently within the Multidisciplinary drifting Observatory for the Study of Arctic Climate (MOSAiC) expedition (www.mosaic-expedition.org), with an
25 appropriate instrumentation and radiative transfer modelling will be required to quantify these effects and ~~its~~ their potential seasonal dependence ~~by continuously estimating the cloud-free albedo in cloudy conditions. The proposed method to estimate the surface albedo in cloud-free conditions using the parameterization from Gardner and Sharp (2010) can be easily applied to common Arctic long-term observations above snow and ice surface types, especially if high quality LWP measurements are~~
30 available.

~~Besides observation, also~~ Besides observations, global climate models and their estimate of the cloud radiative feedback are based on the impact of clouds on the surface REB, for which the surface albedo is fundamental. For specific surface types, often fixed values of ~~broadband~~ shortwave surface albedo are assigned and ~~modulated by temperature dependences~~ parameterized using surface temperature. However, these simplified parameterizations are not ~~capable of describing appropriate to accurately~~
35 describe surface albedo-cloud interactions. The use of parameterizations accounting for these effects ~~like the one from Gardner and Sharp (2010)~~

such as that of Gardner and Sharp (2010), are necessary and highlight the need for coupled surface atmosphere models with represented including representative surface microphysical properties. The shortwave net irradiances depend not alone on cloud transmissivity and surface albedo, moreover the interaction between both needs to be represented.

- Further effort in coupled surface atmosphere radiative transfer modelling with a representation of common surface albedos
- 5 albedo types like the ones from melt ponds in the Arctic are required to track the true-seasonal cycle of solar-shortwave CRF. Spectral albedo observations combined with the common broadband ~~devises-would~~ devices will help to account for the spectral features in surface albedo and trace changes in SSA. The proposed approach of reproducing the cloud-free albedo can not adequately reflect the diversity of spectral surface ~~albedos~~ albedo types and issues related to the surface albedo-cloud interaction, especially in summer.
- 10 Considering the surface albedo-cloud interaction in global climate models and upcoming long-term observations such as ~~MOSAIC~~ MOSAIC will further improve our understanding of CRF and cloud radiative feedback in the Arctic environment and its role for Arctic amplification.

Data availability. The pyranometer and pyrgeometer broadband irradiance and KT-19 nadir brightness temperature from AWI aircraft Polar 5&6 during the May to June 2017 ACLOUD campaign are published on the PANGAEA database (Stapf et al., 2019). The retrieved CRF,

15 LWP equivalent and cloud-free albedo are made available on PANGAEA. Air temperature, relative humidity and pressure in situ profiles from both aircraft are used from (Hartmann et al., 2019). Polar 5 Dropsondes: (Ehrlich et al., 2019a). Calibrated fisheye camera images: (Jäkel and Ehrlich, 2019; Jäkel et al., 2019). Radiosoundings from Polarstern (Schmithüsen, 2017) and Ny-Ålesund (Maturilli, 2017a, b).

Appendix A: ~~Transmissivity-based~~ Transmissivity-based retrieval of LWP equivalent

The cloud transmissivity is defined by the ratio of measured $F_{s,cld}^{\downarrow} \sim F_{sw,all}^{\downarrow}$ and the simulated cloud-free $F_{s,cf}^{\downarrow} \sim F_{sw,cf}^{\downarrow}$ downward

20 irradiance:

$$\mathcal{T} = \frac{F_{s,cld}^{\downarrow} F_{sw,all}^{\downarrow}}{F_{s,cf}^{\downarrow} F_{sw,cf}^{\downarrow}}. \quad (A1)$$

\mathcal{T} can be converted into cloud optical thickness or LWP, however, it is important to account for the surface albedo dependences due to multiple scattering. The \mathcal{T} for a cloud with the same microphysical properties over snow and ice is higher compared to over open ocean, where the majority of photons will be absorbed by the surface and are not available for new back-scattering

25 events of the upward irradiance in the cloud towards the surface. Taking this dependence into account, the broadband \mathcal{T} ~~was-is~~ is used to derive the cloud optical thickness similar to the approach by Leontyeva and Stamnes (1993).

Lookup tables of \mathcal{T} for a range of surface albedo between 0 and 1 and LWP between 0 and 320 g m⁻² ~~were-are~~ are simulated for the local solar zenith angle and compared to the values derived from the observations along the flight track. In the simulations, vertically homogeneous pure liquid water clouds are assumed to limit the complexity of the simulations. Therefore, in the

30 following the LWP is referred to an equivalent LWP, because no ice water content ~~was-is~~ is assumed. The cloud ~~was-is~~ is located

between 400 m and 600 m with a fixed r_{eff} of $8 \mu\text{m}$, typical for Arctic clouds in this season and region (Mioche et al., 2017). These rather crude assumptions result in uncertainties of the simulated irradiance, which were quantified by Leontyeva and Stamnes (1993) as a function of surface albedo, SZA, r_{eff} and cloud optical thickness.

Similar to the simulations of $F_{s,\text{cf}}^{\downarrow} - F_{\text{sw},\text{cf}}^{\downarrow}$ for heterogeneous surface albedo fields, an effective albedo, which influences the local scattering processes in cloudy conditions needs to be considered in the retrieval simulations of \mathcal{T} (Pirazzini and Raisanen, 2008).

The diversity of potential 3D effects induced by surface and cloud heterogeneities in the MIZ omit a specific solution for the smoothing problem of the areal averaged effective albedo and can only partially be depicted by radiative transfer modelling. To make the retrieval applicable to ACLLOUD measurements and reduce the uncertainties induced by horizontal photon transport, a commonly observed cloud/surface scene, with a cloud base height of 200 m and leads with different sizes, ~~has been are~~ simulated using 3D radiative transfer (not shown here). The estimated kernel k is based on a Cauchy distribution ~~and has a considerably smaller horizontal extent~~:

$$k(x, \mu, \gamma) = \left(\pi \cdot \gamma \cdot \left[1 + \left(\frac{x - \mu}{\gamma} \right)^2 \right] \right)^{-1}, \quad (\text{A2})$$

with γ of 400 m, the median μ and a scale x of 10 km. The horizontal extent is, as expected, smaller compared to the cloud-free kernel introduced in Fig. 3b, due to the ~~the~~ low cloud base height limiting the free photon path length. Applied to the theoretical observed albedo the simulated 1D irradiance adequately reproduces the results obtained from the 3D output, and thus, reduces for these cloud/surface scenes the uncertainties of the retrieved LWP considerably.

Nevertheless, multiple scattering, changes in cloud base height (Pirazzini and Raisanen, 2008) and 3D radiative effects due to inhomogeneous cloud/surface scenes, might induce large uncertainties in this retrieval. However, the observed I_f statistics indicate ~~;~~ that the majority of ACLLOUD flights were conducted over a rather homogeneous surface, where the discussed issue is minor important. The sensitivity of the retrieval is in general higher over open water compared to over ice, since changes in $F_s^{\downarrow} - F_{\text{sw}}^{\downarrow}$ with increasing LWP are more pronounced. The relative uncertainty range of this retrieval for homogeneous clouds and surface can be expected between 15 % and 35 % over open ocean and sea ice respectively.

The conversion from LWP to optical thickness (τ), as required for the parameterization by Gardner and Sharp (2010), ~~was is~~ applied by,

$$\tau = \frac{9}{5} \cdot \frac{\text{LWP}}{\rho_w \cdot r_{\text{eff}}}, \quad (\text{A3})$$

with the density of liquid water ρ_w and the simulated r_{eff} .

Author contributions. All authors contributed to the editing of the manuscript and to the discussion of the results. JS drafted the manuscript and initialized the study. JS processed the radiation data, merged the data sets and performed the radiative transfer simulations. EJ contributed to the radiative transfer simulations and their interpretation. MW, AE and CL designed the experimental basis of this study.

Competing interests. The authors declare that they have no conflict of interest.

Acknowledgements. We gratefully acknowledge the funding by the Deutsche Forschungsgemeinschaft (DFG, German Research Foundation) – Project Number 268020496 – TRR 172, within the Transregional Collaborative Research Center “Arctic Amplification: Climate Relevant Atmospheric and Surface Processes, and Feedback Mechanisms (AC)³”. The authors are grateful to AWI for providing and operating the two aircraft during the ACLOUD campaign. We thank the crews of Polar 5 and Polar 6, the technicians of the aircraft for excellent technical and logistical support. The generous funding of the flight hours for ACLOUD by AWI is greatly appreciated. Observations in Fig. 8 were made by the SHEBA Atmospheric Surface Flux Group, Ed Andreas, Chris Fairall, Peter Guest, and Ola Persson.

References

- [Anderson, G., Clough, S., Kneizys, F., Chetwynd, J., and Shettle, E.: AFGL Atmospheric Constituent Profiles \(0–120 km\), Tech. Rep. AFGL-TR-86-0110, AFGL \(OPI\), Hanscom AFB, MA 01736, 1986.](#)
- Benner, T. C., Curry, J. A., and Pinto, J. O.: Radiative transfer in the summertime Arctic, *J. Geophys. Res.*, 106, 15.173–15.183, 2001.
- 5 Cohen, J., Screen, J. A., Furtado, J. C., Barlow, M., Whittleston, D., Coumou, D., Francis, J., Dethloff, K., Entekhabi, D., Overland, J., and Jones, J.: Recent Arctic amplification and extreme mid-latitude weather, *Nat. Geosci.*, 7, 627–637, <https://doi.org/10.1038/NGEO2234>, 2014.
- [Cox, C. J., Walden, V. P., Rowe, P. M., and Shupe, M. D.: Humidity trends imply increased sensitivity to clouds in a warming Arctic, *Nat. Commun.*, 6, 10 117, <https://doi.org/10.1038/ncomms10117>, 2015.](#)
- 10 [Cox, C. J., Uttal, T., Long, C. N., Shupe, M. D., Stone, R. S., and Starkweather, S.: The Role of Springtime Arctic Clouds in Determining Autumn Sea Ice Extent, *J. Climate*, 29, 6581–6596, <https://doi.org/10.1175/JCLI-D-16-0136.1>, 2016.](#)
- [Dong, X. Q., Xi, B. K., and Minnis, P.: A climatology of midlatitude continental clouds from the ARM SGP central facility. Part II: Cloud fraction and surface radiative forcing, *J. Climate*, 19, 1765–1783, 2006.](#)
- [Dong, X. Q., Xi, B. K., Crosby, K., Long, C. N., Stone, R. S., and Shupe, M. D.: A 10 year climatology of Arctic cloud fraction and radiative forcing at Barrow, Alaska RID F-8754-2011, *J. Geophys. Res.*, 115, D17 212, <https://doi.org/10.1029/2009JD013489>, 2010.](#)
- 15 Ehrlich, A., Stapf, J., Lüpkes, C., Mech, M., Crewell, S., and Wendisch, M.: Meteorological measurements by dropsondes released from POLAR 5 during ALOUD 2017, PANGAEA, <https://doi.org/10.1594/PANGAEA.900204>, 2019a.
- Ehrlich, A., Wendisch, M., Lüpkes, C., Buschmann, M., Bozem, H., Chechin, D., Clemen, H.-C., Dupuy, R., Eppers, O., Hartmann, J., Herber, A., Jäkel, E., Järvinen, E., Jourdan, O., Kästner, U., Kliesch, L.-L., Köllner, F., Mech, M., Mertes, S., Neuber, R., Ruiz-Donoso,
- 20 E., Schnaiter, M., Schneider, J., Stapf, J., and Zanatta, M.: A comprehensive in situ and remote sensing data set from the Arctic CLOUD Observations Using airborne measurements during polar Day (ALOUD) campaign., *Earth Syst. Sci. Data Discuss.*, <https://doi.org/10.5194/essd-2019-96>, in review, 2019b.
- Emde, C., Buras-Schnell, R., Kylling, A., Mayer, B., Gasteiger, J., Hamann, U., Kylling, J., Richter, B., Pause, C., Dowling, T., and Bugliaro, L.: The libRadtran software package for radiative transfer calculations (version 2.0.1), *Geosci. Model Dev.*, 9, 1647–1672,
- 25 <https://doi.org/10.5194/gmd-9-1647-2016>, 2016.
- Gardner, A. S. and Sharp, M. J.: A review of snow and ice albedo and the development of a new physically based broadband albedo parameterization, *J. Geophys. Res.*, 115, F01 009, <https://doi.org/10.1029/2009JF001444>, 2010.
- Gasteiger, J., Emde, C., Mayer, B., Buras, R., Buehler, S. A., and Lemke, O.: Representative wavelengths absorption parameterization applied to satellite channels and spectral bands, *J. Quant. Spectrosc. Ra.*, 148, 99–115, <https://doi.org/10.1016/j.jqsrt.2014.06.024>, 2014.
- 30 Gillett, N. P., Stone, D. A., Stott, P. A., Nozawa, T., Karpechko, A. Y., Hegerl, G. C., Wehner, M. F., and Jones, P. D.: Attribution of polar warming to human influence, *Nat. Geosci.*, 1, 750–754, <https://doi.org/10.1038/ngeo338>, 2008.
- Goosse, H., Kay, J. E., Armour, K. C., Bodas-Salcedo, A., Chepfer, H., Docquier, D., Jonko, A., Kushner, P. J., Lecomte, O., Massonnet, F., Park, H. S., Pithan, F., Svensson, G., and Vancoppenolle, M.: Quantifying climate feedbacks in polar regions, *Nat. Commun.*, 9, 1919, <https://doi.org/10.1038/s41467-018-04173-0>, 2018.
- 35 Grenfell, T. C. and Perovich, D. K.: Incident spectral irradiance in the Arctic Basin during the summer and fall, *J. Geophys. Res.*, 113, D12 117, <https://doi.org/10.1029/2007JD009418>, 2008.

- Hartmann, J., Lüpkes, C., and Chechin, D.: High resolution aircraft measurements of wind and temperature during the ACLOUD campaign in 2017, PANGAEA, <https://doi.pangaea.de/10.1594/PANGAEA.900880>, 2019.
- Hori, M., Aoki, T., Tanikawa, T., Motoyoshi, H., Hachikubo, A., Sugiura, K., Yasunari, T. J., Eide, H., Stordvold, R., Nakajima, Y., and Takahashi, F.: In-situ measured spectral directional emissivity of snow and ice in the 8-14 μ m atmospheric window, *Remote Sens. Environ.*, **100**, 486–502, <https://doi.org/10.1016/j.rse.2005.11.001>, 2006.
- Intrieri, J. M., Fairall, C. W., Shupe, M. D., Persson, P. O. G., Andreas, E. L., Guest, P. S., and Moritz, R. E.: An annual cycle of Arctic surface cloud forcing at SHEBA, *J. Geophys. Res.*, **107**, 8039, 2002.
- Iwabuchi, H.: Efficient Monte Carlo methods for radiative transfer modeling, *J. Atmos. Sci.*, **63**, 2324–2339, 2006.
- Iwabuchi, H. and Kobayashi, H.: Modeling of radiative transfer in cloudy atmospheres and plant canopies using Monte Carlo methods, *Tech. Rep.*, **8**, 199 pp., 2008.
- Jäkel, E. and Ehrlich, A.: Radiance fields of clouds and the Arctic surface measured by a digital camera during ACLOUD 2017, PANGAEA, <https://doi.pangaea.de/10.1594/PANGAEA.901024>, 2019.
- Jäkel, E., Stapf, J., Wendisch, M., Nicolaus, M., Dorn, W., and Rinke, A.: Validation of the sea ice surface albedo scheme of the regional climate model HIRHAM-NAOSIM using aircraft measurements during the ACLOUD/PASCAL campaigns, *Cryosphere*, **13**, 1695–1708, <https://doi.org/10.5194/tc-13-1695-2019>, 2019.
- Jeffries, M. O., Overland, J. E., and Perovich, D. K.: The Arctic shifts to a new normal, *Phys. Today*, **66**, 35–40, 2013.
- Kato, S., Ackerman, T., Mather, J., and Clothiaux, E.: The k-distribution method and correlated-k approximation for a shortwave radiative transfer model, *J. Quant. Spectrosc. Ra.*, **62**, 109–121, 1999.
- Knudsen, E. M., Heinold, B., Dahlke, S., Bozem, H., Crewell, S., Gorodetskaya, I. V., Heygster, G., Kunkel, D., Maturilli, M., Mech, M., Viceto, C., Rinke, A., Schmithüsen, H., Ehrlich, A., Macke, A., Lüpkes, C., and Wendisch, M.: Synoptic development Meteorological conditions during the ACLOUD/PASCAL field campaign near Svalbard in spring-early summer 2017, *Atmos. Chem. Phys.*, **18**, 17995–18022, <https://doi.org/10.5194/acp-18-17995-2018>, 2018.
- Kreuter, A., Buras, R., Mayer, B., Webb, A., Kift, R., Bais, A., Kouremeti, N., and Blumthaler, M.: Solar irradiance in the heterogeneous albedo environment of the Arctic coast: measurements and a 3-D model study, *Atmos. Chem. Phys.*, **14**, 5989–6002, <https://doi.org/10.5194/acp-14-5989-2014>, 2014.
- Lampert, A., Maturilli, M., Ritter, C., Hoffmann, A., Stock, M., Herber, A., Birnbaum, G., Neuber, R., Dethloff, K., Orgis, T., Stone, R., Brauner, R., Kassbohrer, J., Haas, C., Makshtas, A., Sokolov, V., and Liu, P.: The spring-time boundary layer in the central Arctic observed during PAMARCMiP 2009, *Atmosphere-Basel*, **3**, 320–351, <https://doi.org/10.3390/atmos3030320>, 2012.
- Leontyeva, E. and Stamnes, K.: Estimation of cloud optical thickness from ground-based measurements of incoming solar radiation in the Arctic, *J. Climate*, **7**, 566–578, 1993.
- Libois, Q., Picard, G., France, J. L., Arnaud, L., Dumont, M., Carmagnola, C. M., and King, M. D.: Influence of grain shape on light penetration in snow, *Cryosphere*, **7**, 1803–1818, <https://doi.org/10.5194/tc-7-1803-2013>, 2013.
- Long, C. and Ackerman, T.: Identification of clear skies from broadband pyranometer measurements and calculation of downwelling shortwave cloud effects, *J. Geophys. Res.*, **105**, 15609–15626, 2000.
- Long, C. N.: On the estimation of clear-sky upwelling SW and LW, Fifteenth ARM Science Team Meeting Proceedings, Daytona Beach, Florida, March 14–18, 2005.
- Long, C. N. and Turner, D. D.: A method for continuous estimation of clear-sky downwelling longwave radiative flux developed using ARM surface measurements, *J. Geophys. Res.*, **113**, D18206, <https://doi.org/10.1029/2008JD009936>, 2008.

- Maturilli, M.: High resolution radiosonde measurements from station Ny-Ålesund (2017-05), PANGAEA, <https://doi.org/10.1594/PANGAEA.879820>, 2017a.
- Maturilli, M.: High resolution radiosonde measurements from station Ny-Ålesund (2017-06), PANGAEA, <https://doi.org/10.1594/PANGAEA.879822>, 2017b.
- 5 [Miller, N. B., Shupe, M. D., Cox, C. J., Walden, V. P., Turner, D. D., and Steffen, K.: Cloud Radiative Forcing at Summit, Greenland, *J. Climate*, 28, 6267–6280, <https://doi.org/10.1175/JCLI-D-15-0076.1>, 2015.](#)
- [Miller, N. B., Shupe, M. D., Lenaerts, J. T. M., Kay, J. E., de Boer, G., and Bennartz, R.: Process-Based Model Evaluation Using Surface Energy Budget Observations in Central Greenland, *J. Geophys. Res.*, 123, 4777–4796, <https://doi.org/10.1029/2017JD027377>, 2018.](#)
- Mioche, G., Jourdan, O., Delanoë, J., Gourbeyre, C., Febvre, G., Dupuy, R., Monier, M., Szczap, F., Schwarzenboeck, A., and Gayet, J. F.:
- 10 Vertical distribution of microphysical properties of Arctic springtime low-level mixed-phase clouds over the Greenland and Norwegian seas, *Atmos. Chem. Phys.*, 17, 12 845–12 869, <https://doi.org/10.5194/acp-17-12845-2017>, 2017.
- Overland, J. E., Wood, K. R., and Wang, M.: Warm Arctic–cold continents: Impacts of the newly open Arctic Sea, *Polar Res.*, 30, 15 787, doi:10.3402/polar.v30i0.15 787, 2011.
- Perovich, D. K., Grenfell, T. C., Light, B., and Hobbs, P. V.: Seasonal evolution of the albedo of multiyear Arctic sea ice, *J. Geophys. Res.*,
- 15 107, <https://doi.org/10.1029/2000JC000438>, 8044, 2002.
- Pirazzini, R. and Raisanen, P.: A method to account for surface albedo heterogeneity in single-column radiative transfer calculations under overcast conditions, *J. Geophys. Res.*, 113, <https://doi.org/10.1029/2008JD009815>, 2008.
- Pithan, F. and Mauritsen, T.: Arctic amplification dominated by temperature feedbacks in contemporary climate models, *Nature*, 7, 181–184, <https://doi.org/10.1038/ngeo2071>, 2014.
- 20 Pithan, F., Svensson, G., Caballero, R., Chechin, D., Cronin, T. W., Ekman, A. M. L., Neggers, R., Shupe, M. D., Solomon, A., Tjernstrom, M., and Wendisch, M.: Role of air-mass transformations in exchange between the Arctic and mid-latitudes, *Nat. Geosci.*, 11, 805–812, <https://doi.org/10.1038/s41561-018-0234-1>, 2018.
- [Podgorny, I., Lubin, D., and Perovich, D. K.: Monte Carlo Study of UAV-Measurable Albedo over Arctic Sea Ice, *J. Atmos. Ocean. Tech.*, 35, 57–66, <https://doi.org/10.1175/JTECH-D-17-0066.1>, 2018.](#)
- 25 Ramanathan, V., Cess, R. D., Harrison, E. F., Minnis, P., Barkstrom, B. R., Ahmad, E., and Hartmann, D.: Cloud-radiative forcing and climate: Results from the Earth Radiation Budget Experiment, *Science*, 243, 57–63, 1989.
- Randles, C. A., Kinne, S., Myhre, G., Schulz, M., Stier, P., Fischer, J., Doppler, L., Highwood, E., Ryder, C., Harris, B., Huttunen, J., Ma, Y., Pinker, R. T., Mayer, B., Neubauer, D., Hitzenberger, R., Oreopoulos, L., Lee, D., Pitari, G., Di Genova, G., Quaas, J., Rose, F. G., Kato, S., Rumbold, S. T., Vardavas, I., Hatzianastassiou, N., Matsoukas, C., Yu, H., Zhang, F., Zhang, H., and Lu, P.: Intercomparison
- 30 of shortwave radiative transfer schemes in global aerosol modeling: results from the AeroCom Radiative Transfer Experiment, *Atmos. Chem. Phys.*, 13, 2347–2379, <https://doi.org/10.5194/acp-13-2347-2013>, 2013.
- Ricchiuzzi, P. and Gautier, C.: Investigation of the effect of surface heterogeneity and topography on the radiation environment of Palmer Station, Antarctica, with a hybrid 3-D radiative transfer model, *J. Geophys. Res.*, 103, 6161–6178, 1998.
- Schmithüsen, H.: Upper air soundings during POLARSTERN cruise PS106.1 (ARK-XXXI/1.1), PANGAEA, <https://doi.org/10.1594/PANGAEA.882736>, 2017.
- 35 Screens, J. A. and Simmonds, I.: The central role of diminishing sea ice in recent Arctic temperature amplification, *Nature*, 464, 1334–1337, 2010.

- Sedlar, J., Tjernstrom, M., Mauritsen, T., Shupe, M. D., Brooks, I. M., Persson, P. O. G., Birch, C. E., Leck, C., Sirevaag, A., and Nicolaus, M.: A transitioning Arctic surface energy budget: the impacts of solar zenith angle, surface albedo and cloud radiative forcing *RID F-8754-2011, Climate Dyn.*, **37**, 1643–1660, <https://doi.org/10.1007/s00382-010-0937-5>, 2011.
- Serreze, M. C. and Barry, R. G.: Processes and impacts of Arctic amplification: A research synthesis, *Global Planet. Change*, **77**, 85–96, doi:10.1016/j.gloplacha.2011.03.004, 2011.
- Shupe, M. D. and Intrieri, J. M.: Cloud radiative forcing of the Arctic surface: The influence of cloud properties, surface albedo, and solar zenith angle, *J. Climate*, **17**, 616–628, 2004.
- Shupe, M. D., Walden, V. P., Eloranta, E., Uttal, T., Campbell, J. R., Starkweather, S. M., and Shiobara, M.: Clouds at Arctic Atmospheric Observatories. Part I: Occurrence and Macrophysical Properties, *J. Appl. Meteorol.*, **50**, 626–644, <https://doi.org/10.1175/2010JAMC2467.1>, 2011.
- Spreen, G., Kaleschke, L., and Heygster, G.: Sea ice remote sensing using AMSR-E 89-GHz channels, *J. Geophys. Res.*, **113**, C02S03, <https://doi.org/10.1029/2005JC003384>, 2008.
- Stamnes, K., Tsay, S., Wiscombe, W., and Jayaweera, K.: A numerically stable algorithm for discrete-ordinate-method radiative transfer in multiple scattering and emitting layered media, *Appl. Opt.*, **27**, 2502–2509, 1988.
- Stapf, J., Ehrlich, A., Jäkel, E., and Wendisch, M.: Aircraft measurements of broadband irradiance during the ACLOUD campaign in 2017, *PANGAEA*, <https://doi.org/10.1594/PANGAEA.900442>, 2019.
- Stramler, K., Del Genio, A. D., and Rossow, W. B.: Synoptically Driven Arctic Winter States, *J. Climate*, **24**, 1747–1762, <https://doi.org/10.1175/2010JCLI3817.1>, 2011.
- Stroeve, J. C., Serreze, M. C., Holland, M. M., Kay, J. E., Maslanik, J., and Barrett, A. P.: The Arctic’s rapidly shrinking sea ice cover: A research synthesis, *Climatic Change*, **110**, 1005–1027, doi:10.1007/s10584-011-0101-1, 2012.
- Tjernström, M. and Graversen, R. G.: The vertical structure of the lower Arctic troposphere analysed from observations and the ERA-40 reanalysis, *Quart. J. Roy. Meteor. Soc.*, **135**, 431–443, <https://doi.org/10.1002/qj.380>, 2009.
- Tjernström, M., Shupe, M. D., Brooks, I. M., Persson, P. O. G., Prytherch, J., Salisbury, D. J., Sedlar, J., Achtert, P., Brooks, B. J., Johnston, P. E., Sotiropoulou, G., and Wolfe, D.: Warm-air advection, air mass transformation and fog causes rapid ice melt, *Geophys. Res. Lett.*, **42**, 5594–5602, <https://doi.org/10.1002/2015GL064373>, 2015.
- Tjernström, M., Shupe, M. D., Brooks, I. M., Achtert, P., Prytherch, J., and Sedlar, J.: Arctic Summer Airmass Transformation, Surface Inversions, and the Surface Energy Budget, *J. Climate*, **32**, 769–789, <https://doi.org/10.1175/JCLI-D-18-0216.1>, 2019.
- Uttal, T., Curry, J. A., McPhee, M. G., Perovich, D. K., Moritz, R. E., Maslanik, J. A., Guest, P. S., Stern, H. L., Moore, J. A., Turenne, R., Heiberg, A., Serreze, M. C., Wylie, D. P., Persson, O. G., Paulson, C. A., Halle, C., Morison, J. H., Wheeler, P. A., Makshtas, A., Welch, H., Shupe, M. D., Intrieri, J. M., Stamnes, K., Lindsey, R. W., Pielke, R. A., Pegau, W. S., Stanton, T. P., and Grenfeld, T. C.: Surface heat budget of the Arctic Ocean, *B. Am. Meteorol. Soc.*, **83**, 255–275, [https://doi.org/10.1175/1520-0477\(2002\)083<0255:SHBOTA>2.3.CO;2](https://doi.org/10.1175/1520-0477(2002)083<0255:SHBOTA>2.3.CO;2), 2002.
- Walsh, J. E. and Chapman, W. L.: Arctic cloud-radiation-temperature associations in observational data and atmospheric reanalyses, *J. Climate*, **11**, 3030–3045, [https://doi.org/10.1175/1520-0442\(1998\)011<3030:ACRTAI>2.0.CO;2](https://doi.org/10.1175/1520-0442(1998)011<3030:ACRTAI>2.0.CO;2), 1998.
- Wang, W. S., Zender, C. S., and van As, D.: Temporal Characteristics of Cloud Radiative Effects on the Greenland Ice Sheet: Discoveries From Multiyear Automatic Weather Station Measurements, *J. Geophys. Res.*, **123**, 11 348–11 361, <https://doi.org/10.1029/2018JD028540>, 2018.
- Warren, S.: Optical Properties of Snow, *Rev. Geophys. Space Phys.*, **20**, 67–89, 1982.

- Weihls, P., Lenoble, J., Blumthaler, M., Martin, T., Seckmeyer, G., Philipona, R., de la Casiniere, A., Sergent, C., Gröbner, J., Cabot, T., Masserot, D., Pichler, T., Pougatch, E., Rengarajan, G., Schmucki, D., and Simic, S.: Modeling the effect of an inhomogeneous surface albedo on incident UV radiation in mountainous terrain: determination of an effective surface albedo, *Geophys. Res. Lett.*, 28, 3111–3114, 2001.
- 5 Wendisch, M., Pilewskie, P., Jäkel, E., Schmidt, S., Pommier, J., Howard, S., Jonsson, H. H., Guan, H., Schröder, M., and Mayer, B.: Airborne measurements of areal spectral surface albedo over different sea and land surfaces, *J. Geophys. Res.*, 109, Art. No. D08 203, <https://doi.org/doi:10.1029/2003JD004392>, 2004.
- Wendisch, M., Brückner, M., Burrows, J. P., Crewell, S., Dethloff, K., Ebell, K., Lüpkes, C., Macke, A., Notholt, J., Quaas, J., Rinke, A., and Tegen, I.: Understanding causes and effects of rapid warming in the Arctic, *Eos*, 98, <https://doi.org/10.1029/2017EO064803>, 2017.
- 10 Wendisch, M., Macke, A., Ehrlich, A., Lüpkes, C., Mech, M., Chechin, D., Barrientos, C., Bozem, H., Brückner, M., Clemen, H.-C., Crewell, S., Donth, T., Dupuy, R., Ebell, K., Egerer, U., Engelmann, R., Engler, C., Eppers, O., Gehrman, M., Gong, X., Gottschalk, M., Gourbeyre, C., Griesche, H., Hartmann, J., Hartmann, M., Herber, A., Herrmann, H., Heygster, G., Hoor, P., Jafariserajehlou, S., Jäkel, E., Järvinen, E., Jourdan, O., Kästner, U., Kecorius, S., Knudsen, E. M., Köllner, F., Kretzschmar, J., Lelli, L., Leroy, D., Maturilli, M., Mei, L., Mertes, S., Mioche, G., Neuber, R., Nicolaus, M., Nomokonova, T., Notholt, J., Palm, M., van Pinxteren, M., Quaas, J., Richter, P., Ruiz-Donoso, E., Schäfer, M., Schmieder, K., Schnaiter, M., Schneider, J., Schwarzenböck, A., Seifert, P., Shupe, M. D., Siebert, H., Spreen, G., Stapf, J., Stratmann, F., Vogl, T., Welti, A., Wex, H., Wiedensohler, A., Zanatta, M., and Zeppenfeld, S.: The Arctic cloud puzzle: using ACLOUD/PASCAL multi-platform observations to unravel the role of clouds and aerosol particles in Arctic amplification, *B. Am. Meteorol. Soc.*, 100 (5), 841–871, <https://doi.org/10.1175/BAMS-D-18-0072.1>, 2019.